7-1-2011

Substratum interfacial energetic effects on the attachment of marine bacteria

Linnea Ista

Linnea Kathryn Ista
Candidate

Biology
Department

This dissertation is approved, and it is acceptable in quality and form for publication:

Approved by the Dissertation Committee:

Margaret Werner-Washburne , Chairperson

Cristina Takacs-Vesbach

Diana E Northup

Gabriel P. López

SUBSTRATUM INTERFACIAL ENERGETIC EFFECTS ON THE ATTACHMENT OF MARINE BACTERIA

by

LINNEA KATHRYN ISTA

B.S., Biology, The University of Puget Sound, 1985
M.S., Biochemistry, The University of Missouri, 1994

DISSERTATION

Submitted in Partial Fulfillment of the
Requirements for the Degree of

Doctor of Philosophy
Biology

The University of New Mexico
Albuquerque, New Mexico

July, 2011

Acknowledgements

I wish to express my deepest appreciation to Professor Margaret Werner-Washburne, my advisor and committee chair, for all her help and support beginning before I even entered graduate school and continuing through revisions of this dissertation. Maggie is truly inspirational both as a brilliant scientist and as a fine human being; I feel blessed to have her guidance and friendship. From relearning how to imagine, to a new and nearly magical method of editing to looking for the blessing in every situation, Maggie encouraged me both professionally and personally and I hope to never stop learning from her.

My profound appreciation is also extended to Professor Gabriel P. López, co-advisor, mentor, and esteemed boss. When I first entered Gabriel's lab, I was truly a broken bird; his trust in my abilities and creativity soon boosted my confidence and allowed me to expand my horizons, culminating in the attempt at this degree. He has been a shining example to me of how to be a truly amazing scientist while maintaining high ethical standards. Gabriel helped hone the scientific vision within this work. I thank him for the bottom of my heart for allowing me to maintain my full-time position while pursuing this dream. And also for all the times he made me laugh out loud when I was starting to panic.

I want to thank my committee members, Professor Cristina Takacs-Vesbach and Professor Diana Northup for their enthusiastic support and great discussions that guided this work. Both Tina and Diana helped me reopen my vision when the tunneling that seems inevitable with prolonged concentration on a particular subject.

Their ideas not propelled the work herein to places I hadn't imagined, but also provided several avenues to explore as I continue my career. I hope my association with them both continues long beyond graduation.

I wish to thank Professor Andrew Schuler for collaboration on this project, particularly in Chapter 4.

The López lab has been my scientific home for the last 16 years and I wish to thank its current and former members for making it a happy one. I am particularly indebted to Mr. José Cornejo for assistance with much of the contact angle data herein and to both José and to Dr Brett Andrejewski for keeping the ancient gold evaporator running reliably all these years. Special thanks to Dr. Menake Piyasena and Dr. Gautam Gupta for their friendshipand support. My time in the López lab was enriched by the presence of Mr. Phanindhar Shivapooja in the last few years. Phani did everything he could think of in the last few years to make my life and this process smoother and for constant boosts to my confidence.

I also wish to thank my colleagues in the Laboratory of Dr David Whitten, and indeed Dave himself, for their friendship, support and patience as I have been trying to balance work and school, particularly in the last few months. I am especially grateful for the tremendous help given to me by Ms. Jennifer Rice and Ms. Nicolette Estrada in the lab. I want to give a huge thank you to Dr. Thomas Corbitt, who, having recently gone through this process, was always there to say that what I was going through was normal and no matter how dire the situation seemed, I do not, in fact, suck.

I wish to thank Professor Plamen Atanassov and Dr. Carolin Lau for their constant encouragement, and generosity with space, material and equipment.

I hereby acknowledge and proclaim that the members of my “posse” at work: Heather Canavan, Eva Chi, Elizabeth Dirk and Susan Bogus-Halter are responsible for any vestigial sanity that remain once this dissertation is complete. Heather, especially, was always there with a joke, a meal or a beer. They, being engineers also helped tremendously when I experienced gaps in my mathematical education. Hey Ladies! Thank you so much!

To (now Dr) Jamie Reed and Kimberly-Kanigal-Winner, who have gone through this process with me, thanks for your help and friendship while we were all grad students together. It wouldn’t have been nearly the same without you. Thanks especially to Jamie for your tips on how to get the Front Matter together.

My family were an unfailing source of support and encouragement throughout this process. Much love and many thanks to my parents, Vera and Paul Ista for their belief in me, lifting me up when I was down, and rejoicing with me when I was up. Thanks to my brother and sister-in-law, Tim and Jane Ista, for their unflagging positivity. I also wish to thank Scout, arguably the very best dog that ever was a dog, for his unconditional love, making me go for walks and reminding me when it was time to call it a night and head to bed.

To my family of choice, the Potter-Paul family (Valerie, Chris and Liam) and the Small family (Dan, Wendy, Campbell, Kira and Caitlyn) my most profound thanks for being there through this and all the changes of the last several years. You keep

me buoyant and authentic; you remind me that our human connections are what in the end, is important.

I also want to thank Carissa, Jeff, Dylan, Asher , Margaret and Cooper Mettling, friends and the most extraordinary neighbors a person could ever wish for. In addition to literally helping me keep my house together, they made me laugh, plied me with wine, and in general helped me keep my nerdy self in balance.

Finally I would like to thank the Office of Naval Research for its financial support of this project through grants N-000140-81-07-4-1 and N00014-10-1-09007. Additional funding was provided by the Defense Threat Reduction Agency. `

SUBSTRATUM INTERFACIAL ENERGETIC EFFECTS ON THE ATTACHMENT OF MARINE BACTERIA

by

Linnea Kathryn Ista

B.S., BIOLOGY, THE UNIVERSITY OF PUGET SOUND, 1985

M.S., BIOCHEMISTRY, THE UNIVERSITY OF MISSOURI-COLUMBIA, 1994

PH.D., BIOLOGY, THE UNIVERSITY OF NEW MEXICO, 2011

ABSTRACT

Biofilms represent an ancient, ubiquitous and influential form of life on earth. They are interesting both scientifically and because of their impacts on our environment, health and technology. Biofilm formation is initiated by attachment of bacterial cells from an aqueous suspension onto a suitable attachment substratum. While in certain, well studied cases initial attachment and subsequent biofilm formation is mediated by specific ligand-receptor pairs on the bacteria and attachment substratum, in the open environment, including the ocean, it is assumed to be non-specific and mediated by processes similar to those that drive adsorption of colloids at the water-solid interface.

Colloidal principles are studied to determine the molecular and physicochemical interactions involved in the attachment of the model marine bacterium, *Cobetia marina* to model self-assembled monolayer surfaces. In the simplest application of colloidal principles the wettability of attachment substrata, as measured by the advancing contact angle of water (θ_{AW}) on the surface, is frequently

used as an approximation for the surface tension. We demonstrate the applicability of this approach for attachment of *C. marina* and algal zoospores and extend it to the development of a means to control attachment and release of microorganisms by altering and tuning surface θ_{AW}.

In many cases, however, θ_{AW} does not capture all the information necessary to model attachment of bacteria to attachment substrata; SAMs with similar θ_{AW} attach different number of bacteria. More advanced colloidal models of initial bacterial attachment have evolved over the last several decades, with the emergence of the model proposed by van Oss, Chaudhury and Good (VCG) as preeminent. The VCG model enables calculation of interfacial tensions by dividing these into two major interactions thought to be important at biointerfaces: apolar, Lifshitz-van der Waals and polar, Lewis acid-base (including hydrogen bonding) interactions. These interfacial tensions are combined to yield ΔG_{adh}, the free energy associated with attachment of bacteria to a substratum.

We use VCG to model ΔG_{adh} and interfacial tensions as they relate to model bacterial attachment on SAMs that accumulate cells to different degrees. Even with the more complex interactions measured by VCG, surface energy of the attachment substratum alone was insufficient to predict attachment. VCG was then employed to model attachment of *C. marina* to a series of SAMs varying systematically in the number of ethylene glycol residues present in the molecule; an identical series has been previously shown to vary dramatically in the number of cells attached as a function of ethylene glycols present.

Our results indicate that while VCG adequately models the interfacial tension between water and ethylene glycol SAMs in a manner that predicts bacterial attachment, ΔG_{adh} as calculated by VCG neither qualitatively nor quantitatively reflects the attachment data. The VCG model, thus, fails to capture specific information regarding the interactions between the attaching bacteria, water, and the SAM. We show that while hydrogen-bond accepting interactions are very well captured by this model, the ability for SAMs and bacteria to donate hydrogen bonds is not adequately described as the VCG model is currently applied. We also describe ways in which VCG fails to capture two specific biological aspects that may be important in bacterial attachment to surfaces:1.) specific interactions between molecules on the surface and bacteria and 2.) bacterial cell surface heterogeneities that may be important in differential attachment to different substrata.

Table of Contents

Chapter 1: Introduction

Motivation

Biofilms are ubiquitous, form spontaneously, and are the preferred state of microorganisms. They form when microorganisms encounter virtually any surface or are in a mixed-population, non-sterile environment (20). Because bacteria and archea represent most of the living matter in the ecosphere (72), biofilms are likely to be the predominant form of life on earth. Because study of biofilms has, to date, been largely limited to heterotrophic opportunistic pathogens, the extent to which biofilm formation is similar or different among different bacteria is an exciting question and one which we extend into organisms found in the marine environment.

Discovery of fossil stromatolites, dating to 3.5 Gya, led to a number of important, evolutionary inferences about the formation of biofilms. First, these fossils indicate that the formation of multicellular assemblages was an early evolutionary development (31). Second, the first microbes were chemolithotrophs and surface positioning was probably required for cells to be connected to their energy source. Finally these fossils were built in a marine as environment, which should also easily support free living organisms. How and why bacteria first became attached and formed communities within marine environment is an important evolutionary question.

Bacterial attachment

Attachment or primary adhesion is the first step in biofilm formation (Figure 1). Attachment influences all other steps in biofilm formation, triggering a separate developmental process with unique molecular events(31, 53, 64, 65).. We know that initial attachment patterns has a profound influence on the final properties of the mature biofilm (13, 29)., How attachment substratum properties influence ,for example, expression of genes regulating basic biofilm processes including quorum sensing (24, 41), production of cyclic dinucleotides (21), programmed cell death (12) or even swarming(9, 66) still remain to be answered. To address these questions, we need to ask how the substratum affects attachment.

The major goal of this research is to understand the physical interactions involved in bacterial attachment. Both specific and non-specific mechanisms have been found to drive bacterial attachment (31, 32, 38, 40, 64) } and identifying which of these dominates in a given circumstance is important but not always straightforward. Whether attachment is specific or nonspecific may be differentiated by its ability to be modeled by colloidal models of attachment (see below). Nonspecific attachment has been shown to be modeled well using colloidal models whereas specific attachment is not (43, 44) whereas specific attachment is not. For specific attachment, typically the properties of only one part of the cell surface are relevant. Colloidal theory discounts the role of cell surface heterogeneity. A major part of this dissertation addresses the question whether attachment observed on a variety of surfaces is non-specific and therefore modeled effectively by colloidal models.

Specific attachment is promoted by intereactions between a receptor on the bacterial cell and a ligand on the substratum. An example are the well-known interactions between cell surface proteins *Staphylococcus sp.* and the plasma and mammalian cell surface protein, fibronectin, (32) or the mannose binding domains of type I fimbriae in *Escherichia coli* (40). Specific attachment can also be mediated by binding of a bacterial cell surface molecule to a non-specific organic layer called a conditioning film on the substratum. The best example of specific attachment to conditioning films is that of commensal oral streptococci to tooth enamel, mediated by deposits of sialic acids from saliva (51). While nonspecific attachment is thought to dominate in the marine environment, recent evidence suggests that marine bacteria not only respond to both naturally-occurring (37) and laboratory-derived (30) conditioning films but also that they may be the source of these films(14). Because a clear case of specific attachment has not been established for bacteria living in the marine evironment, however, most investigators assume non-specific attachment is occurring.

Colloidal models for understanding bacterial attachment

Colloidal models of initial attachment are frequently employed to understand initial attachment of those bacteria for which specific adhesins do not exist or remain to be discovered. Such models assume non-specific attachment (15, 23) and are particularly attractive because the upper size limit of colloids is the same size as a bacterial cell. Colloidal models can give us information regarding the interfacial interactions that drive attachment. Although relatively straightforward in their application, colloidal models have had limited success and have been predictive only for a few instances (2, 43, 44). Thus, while the colloidal model seems extremely

appropriate to understand bacterial attachment to surfaces, the models we have analyzed so far have significant limitations.

Table 1: Summary of colloidal models applied to bacterial attachment

Model	Date	Description	Limitations	Notes	Refer-ences
Derjaguin, Landau, Verwey and Overbeek (DLVO)	1945	ΔG^{adh} is determined by the interactions between London dispersion (attractive); electrostatic interactions (repulsive).	Ignores hydrogen bonding interactions. Assumes atomistically smooth surfaces. Does not account for conformational changes of biopolymers.	The modified DLVO theory considers Lewis acid and base interactions as described by van Oss (below). Most recent incarnation is QC	(25, 56, 70, 71) }
Baier Curve	1984	Materials with water contact angles > 90° will not attach bacteria	Bacteria do attach to such surfaces.	Still commonly invoked by researchers investigating marine biofouling.	(4)
Equation of State (Neumann)	1983	Inputs into ΔG^{adh} estimated by calculations derived from water contact angles.	Does not accurately estimate surface tension for polar surfaces.		(1)
van Oss Chaudhury Good (VCG)	1988	ΔG^{adh} is a function of both polar and non-polar interactions. Specifically includes hydrogen bonding.	Results highly dependent on selection of contact angle solvents. Only limited correlation between calculated ΔG^{adh} and attachment(Chapter 4)		(68, 69)
Chen/Qi Ratio	2011	Interaction energy estimated by ratio of apolar to hydrogen-bond accepting components of surface tension.	Doesn't model attachment (Chapter 4)	While purportedly derived from DLVO theory, uses VCG calculations.	(42)

A summary of colloidal models for microbial adhesion is found in Table 1 and an exhaustive review of many of these is found in the literature (58). The two models that have influenced our work have been the Equation of State Model of Neuman (EOS) (1) and the Lifshitz-van der Waals/Lewis acid base model of van Oss, Chaudhury and Good (VCG) (1, 68, 69). These models start with their basis a theromodynamic relationship relating the free energy of adhesion, ΔG_{adh}, to the interfacial tensions between the attaching bacterium and the attachment substratum (γ_{BS}), the bacterium and the bulk liquid (γ_{BL}) and the attachment substratum and the bulk liquid (γ_{SL}) (Figure 2):

$$\Delta G_{adh} = \gamma_{BS} - \gamma_{BL} - \gamma_{SL}$$ (1, 69).

Simply put, these models if the interaction between the bacterium and the substratum is more energetically favorable than both the interactions between the bacterium and the bulk liquid **and** the substratum and the liquid, attachment is thermodynamically allowed. These models assert that these interfacial tensions can be derived from the individual surface tensions of the bacterium (γ_{BV}), the substratum (γ_{SV}) and the liquid (γ_{LV}), and, further, that the substratum surface tensions can be experimentally determined using analysis of the interior angle formed when a drop of solvent is placed on the surface (contact angle; θ; Figure 3) (although neither model specifies how γ_{BV} is obtained, the current state of the art is to take contact angles on a mat of bacteria filtered through a membrane(67)). Where these models differ is in the specific equations relating θ to γ_{SV} or γ_{BV} and the number of contact angle (θ) measurements required for each surface.

Our contributions to understanding non-specific attachment

We have studied processes involved in initial attachment of bacteria over the last 15 years, with specific reference to colloidal models. We have brought two major technical advancements to the field. The first of is using logarithmic phase chemostat culture of cells in defined medium, which was an improvement over the use of overnight cultures often grown in rich medium; since most of the cells in the chemostat were in log phase, their physiology was consistent from day to day, allowing for a constistant cell population with similar over several weeks or even months. Biological variations between experiments, was, as far as possible, minimized.

The second advance, the use of self assembled monolayers (SAMs), imparted chemical consistency on a field that had heretofore relied on commercially available substrata with undefined surface chemistry and other variations in surface properties that made assessment of a single parameter, such as $\gamma_{SV'}$ among the samples inseparable from other variables. SAMs are formed by placing clean gold (or silver) surfaces into ethanolic alkanethiol (general structure: $HS(CH_2)_nX$) solutions (6, 7, 55). The thiol moiety forms a thiolate bond with the gold substrate, and the alkane chains of the molecules pack in an orderly fashion, resulting in a surface on which the ω-substitution (X) is expressed in a semicrystalline array as shown in Figure 3. SAMs can be precisely and systematically varied by mixing two (or more) differently terminated alkanethiolates in the forming solution, with the resulting SAM exhibiting both moieties on the surface in some proportion related to their relative mole fractions in the initial solution (5). SAMs have been used

extensively to systematically study the effects of chemistry and molecular topography on microbial attachment (8, 16, 17, 22, 28, 33, 73, 74) as well as on adsorption of proteins and mammalian cells (45-47, 54, 63).

Cobetia marina – a model marine organism

Cobetia marina (ATCC 25374) (Basonym, *Halomonas marina* (Dobson 1996)) (3, 11, 27), a Gram negative bacterium originally thought to be an Actonomycete, has been our model organism of choice for the last 15 years. It was originally isolated as *Arthrobacter marinus*, in a littoral region off of Wood's Hole, MA (19). This assignment of Cobetia marina to the Actinomycetes was due to its cyclic growth pattern of long, Gram negative staining rods in logarithmic phase and short rods (described as coccoid in Cobet's original paper) and the fact that daughter cells were in a 'V' formation often seen in coroyneform bacteria (19). The G+C content of the isolate was 63%, which is also similar to other arthrobacters (19). C. marina was reclassified as *Pseudomonas marina* in a broad survey of aerobic Gram negative marine organisms (10) and as *Deleya marina* in 1983 (11). The genus *Deleya* was incorporated into *Halomonas* in 1996(27), and, based on rRNA sequencing, in 2002, *Halomonas marina* was reclassified as *Cobetia marina* (3).

A number of characteristics made *C. marina*, then named *Deleya marina*, an ideal model organism for studying bacterial attachment (59-62). It is obligately aerobic and heterotrophic, meaning that it is well-defined physiologically (11). It is obligately halophilic making it easier to maintain un-contaminated cultures under chemostat conditions, an important consideration in a laboratory that occasionally employs non-biologist student workers. In its planktonic state it never expresses pili

and only occasionally flagella (59), although we have never observed flagellated or motile cells in all our years of working with it; lacking these appendages, we know that attachment is made directly with the cell surface, and thus, techniques for general estimates of bacterial surface tension outlined above are more likely to be appropriate. Finally, the growth stage can be easily verified because *C. marina* undergoes a distinct morphological change upon transition from logarithmic growth to stationary phase. Rapidly dividing cells are typically rectangle-shaped double rods 4 μm x 1μm, while cells in stationary phase are single short rods 1.5 μm x 1 μm.

An interesting aspect of *C. marina* other marine bacteria (18), is that the bacteria in biofilms appear to play an important role in determining the final organismal composition of the fouling community. Early on, *C. marina* was found to inhibit the settlement of *Bugula neritina* (a bryozoan) and barnacle (*Balanus amphitrite*) larvae (48, 49). The exact nature of this inhibition remains largely uninvestigated, but is thought to be due to chemical cues (18, 48). In contrast, it has been found recently (M.E. Callow, personal communication) that *C. marina* biofilms promote the settlement of *Ulva linza* (sea lettuce) zoospores.

Previous work and context of dissertation research

Using SAMs and *C. marina*, we have investigated the interaction between bacterium and surface, a process that continues in this dissertation. Our first finding was that SAMs of oligo(ethylene glycol) (OEG) resisted attachment of both *C. marina* and *Staphylococcus epidermidis* (33). One observation we made during these studies is that while *C. marina* attached in significantly greater numbers to

hydrophobic than hydrophilic surfaces, *S. epidermidis* attached more readily to more hydrophilic surfaces. This realization lead us back to the EOS (Table one) model of bacterial attachment, where water contact angle (θ_w), is as a direct representative of γ_{SV}. In Chapter 2, we studied attachment of *C. marina* to two component SAMs that varied systematically in their surface chemistry such that an equally spaced range of advancing water contact angles (θ_{AW}) was achieved. The relationship between attachment and $\cos\theta_{AW}$ (which is linearly related to γ_{SV} when using the EOS model) was linear (Chapter 4); this study was a follow up to a study in which we found that the attachment of the zoospores of the macroalga *Ulva linza* (basonym *Enteromorpha linza*) was also dependent on θ_{AW} and similarly showed an increase in attachment with an increase in θ_{AW}.

During this time we were also developing a polymeric system, poly (*N*-isopropyl acrylamide) (PNIPAAm), that we showed is able to reversibly attach and release bacterial cells during a phase transition over a critical solution temperature (34, 36). Although we initially hypothesized that the temperature- dependent attachment and release of bacteria from these surfaces was mechanical, cells attached to collapsed polymer would be forced off the surface when it swelled, we concluded that the effect was surface energetic: *C. marina* , which we knew attached preferentially to hydrophobic surfaces, were only released when they were attached to PNIPAAm that was in a relatively hydrophobic state and the temperature was lowered so that the polymer became relatively hydrophilic; *S. epidermidis*, which had previously attached preferentially to hydrophilic surfaces, was only released when they were attached to PNIPAAm that was in a relatively hydrophilic state and

the temperature was raised that the polymer became relatively hydrophobic (36). When an attempt at grafting PNIPAAm on SAMs (35) demonstrated that we could vary θ_{AW} of thin films of the polymer by varying the composition of the underlying SAM (50), we were a able to examine the effects of γ_{SV} as estimated using $\cos\theta_{AW}$ on the attachment and detachment of *C. marina* and *S. epidermidis*; this work is summarized in Chapter 3.

The previous work used SAMs that were terminated in combinations of methyl and hydroxyl or methyl and carboxylic acid groups; when we added nitrogen containing amine or trimethylamine SAMs to the assay, however, we found that θ_{AW} no longer correlated well with attachment. As seen in Figure 4, amine-containing SAMs attached significantly more cells than carboxylic acid- or hydroxyl terminated SAMs with the same θ_{AW}. Clearly, θ_{AW}, and, therefore, EOS, was not capturing all the interactions involved in attachment.

One of the fundamental flaws of EOS is that was intended to measure only apolar interactions, those dominated by the random dipoles induced by fluctuations in the distribution of electrons over a molecules (52); it does not take into account polar, specifically hydrogen bonding, interactions that are ubiquitous in biological molecular interactions. The model of van Oss Chaudhury and Good (VCG; Table one) explicitly takes hydrogen bonding into account as a specific case of Lewis acid-base (LAB) interactions in addition to apolar interactions, which they describe as Lishitz/van der Waals interactions. The polar, or LAB, component of surface tension (γ_{SV}^{AB}) is itself the result of two non additive components, an electron-donating (hydrogen bond accepting) Lewis basic component (γ_{SV}^{-}) and an electron-accepting

(hydrogen bond donating) Lewis acidic component (γ_{SV}^{+}). Such an analysis is found in Chapter 4, which, relates γ_{SV} and γ_{BV} to attachment of several wastewater bacteria.

Although VCG captures accurately models bacterial attachment in certain cases (43, 44), it is not universally applicable (58). Questions remain as to whether VCG, as currently articulated and implemented, captures all the molecular interactions contributing to ΔG_{adh}. The model has been plagued, since its inception, on the suspicion that the values of ΔG_{adh} obtained are dependent on the properties of the contact angles used as inputs into its equations.

In Chapter 4, VCG was applied to SAMs with very different apolar, Lewis acidic and Lewis basic properties and bacteria that, due to their physiology, were not amenable to chemostat growth with mixed results. VCG and its possible shortcomings cannot be critically evaluated using such a varied system. In Chapter 5, we use VCG to model attachment of chemostat-grown *C. marina* to a series of SAMs with different lengths of oligo(ethylene glycol); these SAMs have been previously demonstrated to systematically vary in their ability to attach proteins (54)and microbes (57). VCG will also be used in Chapter 5 to experimentally test mathematical models of the mechanisms of resistance of some OEG-SAMs to attachment. This work will bring us full circle to our initial work establishing that OEG-SAMs are effective against attachment of bacteria.

The work herein yields important insights into the interfacial energetics at work in initial attachment of bacteria. Subsequent steps of biofilm formation may

also be influenced be interactions at the cell-surface interface. It has been shown, for example, that the chemical composition of SAMs can influence subsequent bacterial surface growth (22). Surface migration is known to play an important role in the development of mature biofilm architecture (9, 26, 39). These influences are most certainly genetically mediated and specific mechanisms underlying them can elucidated by combining systematic chemical modification of the attachment substratum with genomic interrogation of the affected or mediating biological processes; such studies will provide not only insights into ways in which attachment and subsequent biofilm formation can be directed, but will also provide insights into how this ancient process evolved.

Literature cited

1. **Absolom, D. R., F. V. Lamberti, Z. Policova, W. Zingg, C. J. van Oss, and A. W. Neumann.** 1983. Surface thermodynamics of bacterial adhesion. Appl. Environ. Microbiol. **46:**90-97.
2. **Abu-Lail, N. I., and T. A. Camesano.** 2003. Role of lipopolysaccharides in the adhesion, retention, and transport of Escherichia coli JM109. Environmental Science & Technology **37:**2173-2183.
3. **Arahal, D. L., A. M. Castillo, W. Ludwig, K. H. Schliefer, and A. Ventosa.** 2002. Proposal of *Cobetia marina* gen. nov, comb. nov., within the family Halomonadaceae, to include the species *Halomonas marina*. Syst. Appl. Microbiol. **25:**207-211.
4. **Baier, R. E., A. E. Meyer, J. R. Natiella, R. R. Natiella, and J. M. Carter.** 1984. Surface properties determine bioadhesive outcomes - methods and results. J Biomed Mater Res **18:**337-355.
5. **Bain, C. D., J. Evall, and G. M. Whitesides.** 1989. Formation of monolayers by the coabsorption of thiols on gold: variations in the head group, tail group, and solvent. J Am Chem Soc **111:**7155-7164.
6. **Bain, C. D., E. B. Troughton, Y.-T. Tao, J. Evall, and G. M. Whitesides.** 1989. Formation of monolayer films by the spontaneous assembly of organic thiols from solution onto gold. J Am Chem Soc **111:**321-335.
7. **Bain, C. D., and G. M. Whitesides.** 1989. Modeling organic surfaces with self-assembled monolayers. Angew Chem Int Edit **28:**506-512.
8. **Balamurugan, S., L. K. Ista, J. Yan, G. P. Lopez, J. Fick, M. Himmelhaus, and M. Grunze.** 2005. Reversible protein adsorption and bioadhesion on

monolayers terminated with mixtures of oligo(ethylene glycol) and methyl groups J Am Chem Soc **127:**14548-14549.

9. **Barken, K. B., S. J. Pamp, L. Yang, M. Gjermansen, J. L. Bertrand, M. Klausen, M. Givskov, C. B. Whitchurch, J. N. Engel, and T. Tolker-Nielsen.** 2008. Roles of type IV pili, flagellum-mediated motility and extracellular DNA in the formation of mature multicellular structures in *Pseudomonas aeruginosa* biofilms. . Environ Microbiol **10:**2331-2343.
10. **Baumann, L., P. Baumann, M. Mandel, and R. D. Allen.** 1972. Taxonomy of aerobic marine eubacteria. J Bacteriol **110:**402-429.
11. **Baumann, L., R. D. Bowditch, and P. Baumann.** 1983. Description of *Deleya* gen-nov created to accommodate the marine species *Alcaligenes-aestus*, *Alcaligenes-pacificus*, *Alcaligenes-cupidus*, *Alcaligenes-venustus*, and *Pseudomonas-marina*. Int. J. Syst. Bacteriol. **33:**793-802.
12. **Bayles, K. W.** 2007. The biological role of death and lysis in biofilm development. . Nature Rev Microbiol **5:**721-726.
13. **Becker, K.** 1996. Exopolysaccharide production and attachment strength of bacteria and diatoms on substrates with different surface tensions. Microb Ecol **32:**23-33.
14. **Beech, I. B., R. Gubner, V. Zinkevich, L. Hanjangsit, and R. Avci.** 2000. Characterisation of conditioning layers formed by exopolymeric substances of Pseudomonas NCIMB 2021 on surfaces of AISI 316 stainless steel. Biofouling **16:**93-104.
15. **Burton, E. A., K. A. Sirnon, S. Y. Hou, D. C. Ren, and Y. Y. Luk.** 2009. Molecular gradients of bioinertness reveal a mechanistic difference between mammalian cell adhesion and bacterial biofilm formation. Langmuir **25:**1547-1553.
16. **Callow, J. A., M. S. Stanley, R. Wetherbee, and M. E. Callow.** 2000. Cellular and molecular approaches to understanding primary adhesion in Enteromorpha: an overview. Biofouling **16:**141-150.
17. **Callow, M. E., J. A. Callow, L. K. Ista, S. E. Coleman, A. C. Nolasco, and G. P. López.** 2000. Use of self-assembled monolayers of different wettabilities to study surface selection and primary adhesion processes of green algal (Enteromorpha) zoospores. Appl Environ Microbiol **66:**3249-3254.
18. **Clare, A. S.** 1996. Natural product antifoulants: Status and potential. Biofouling **9:**211-229.
19. **Cobet, A. B., C. Wirsen, and G. E. Jones.** 1970. The effect of nickel on a marine bacterium, *Athrobacter marinus* sp. nov. J Gen Microbiol **62:**159-169.
20. **Costerton, J. W., K.-J. Cheng, G. G. Geesey, T. I. Ladd, J. C. Nickel, M. Dasgupta, and T. J. Marrie.** 1987. Bacterial biofilms in nature and disease. Ann Rev Microbiol **41**.
21. **Cotter, P. A., and S. Stibitz.** 2007. c-di-GMP-regulation of virulence and biofilm formation. Curr Opin Microbiol **10:**17-23.
22. **Dalton, H., J. Stein, and P. March.** 2000. A biological assay for detection of heterogeneities in the surface hydrophobicity of polymer coatings exposed to the marine environment. Biofouling **15:**83-94.

23. **Dalton, H. M., and P. E. March.** 1998. Molecular genetics of bacterial attachment and biofouling. Curr Opin Biotechnol **9:**252-255.
24. **de Kievit, T. R.** 2009. Quorum sensing in *Pseudomonas aeruginosa*. Environ Microbiol **11:**279-288.
25. **Derjaguin, B., and L. Landau.** 1993. Theory of the Stability of Strongly Charged Lyophobic Sols and of the Adhesion of Strongly Charged-Particles in Solutions of Electrolytes. Progress in Surface Science **43:**30-59.
26. **Diaz, C., P. L. Schilardi, R. C. Salvarezza, and M. F. L. de Mele.** 2011. Have flagella a preferred orientation during early stages of biofilm formation?: AFM study using patterned substrates. Colloid Surface B **82:**536-542.
27. **Dobson, S. J., and P. D. Franzmann.** 1996. Unification of the genera Deleya (Baumann et al 1983), Halomonas (Vreeland et al 1980), and Halovibrio (Fendrich 1988) and the species Paracoccus halodenitrificans (Robinson and Gibbons 1952) into a single genus, Halomonas, and placement of the genus Zymobacter in the family Halomonadaceae. Int J Syst Bacteriol **46:**550-558.
28. **Finlay, J. A., M. E. Callow, L. K. Ista, G. P. Lopez, and J. A. Callow.** 2002. The influence of surface wettability on the adhesion strength of spores of the green alga *Enteromorpha* and the diatom *Amphora.* Integr Comp Biol **42:**1116-1122.
29. **Geesey, G. G.** 2001. Bacterial behaviour at surfaces. Curr Opin Microbiol **4:**296-300.
30. **Gubner, R., and I. B. Beech.** 2000. Characterisation of conditioning layers formed by exopolymeric substances of *Pseudomonas* NCIMB 2021 on surfaces of AISI 316 stainless steel. Biofouling **16:**93-104.
31. **Hall-Stoodley, L., W. J. Costerton, and P. Stoodley.** 2004. Bacterial biofilms: from the natural environment to infectious diseases. Nature Reviews **2:**95-108.
32. **Henderson, B., S. Nair, J. Pallas, and M. A. Williams.** 2011. Fibronectin: a multidomain host adhesin targeted by bacterial fibronectin-binding proteins FEMS Microb Rev **35:**147-200
33. **Ista, L. K., H. Fan, O. Baca, and G. P. López.** 1996. Attachment of bacteria to model solid surfaces: oligo(ethylene glycol) surfaces inhibit bacterial attachment. FEMS Microb. Lett. **142:**59-63.
34. **Ista, L. K., and G. P. Lopez.** 1998. Lower critical solubility temperature materials as biofouling release agents Journal of Industrial Microbiology and Biotechnology **20:**121-125.
35. **Ista, L. K., S. Mendez, V. H. Perez-Luna, and G. P. Lopez.** 2001. Synthesis of poly(*N*-isopropylacrylamide) on initiator-modified self-assembled monolayers. Langmuir **17:**2552-2555.
36. **Ista, L. K., V. H. Perez-Luna, and G. P. Lopez.** 1999. Surface-grafted, environmentally sensitive polymers for biofilm release. . Appl Environ Microbiol **65:**1603-1609.
37. **Jain, A., and N. B. Bhosle.** 2008. Biochemical composition of the marine conditioning film: implications for bacterial adhesion. Biofouling **25:**13-19.
38. **Jones, G. W., and R. E. Isaacson.** 1983. Proteinaceous bacterial adhesins and their receptors. CRC Crit Rev Microbiol **10:**229-260.

39. **Klausen, M., A. Aaes-Jorgensen, S. Molin, and T. Tolker-Nielsen.** 2003. Involvement of bacterial migration in the development of complex multicellular structures in *Pseudomonas aeruginosa* biofilms. . Molec Microbiol **50:**61-68.
40. **Klemm, P., V. Hancock, and M. A. Schembri.** 2010. Fimbrial adhesins from extraintestinal *Escherichia coli*. Environ Microbiol Rep **2:**628-640.
41. **Labatte, M., H. Zhu, L. Thung, R. Bandara, M. R. Larsen, M. D. P. Wilcox, M. Givskov, S. A. Rice, and S. Kjelleberg.** 2007. Quorum-sensing regulation of adhesion in *Serratia marcescens* MG1 is surface dependent. J Bacteriol **189:**2708-2711.
42. **Liu, C., and Q. Zhao.** 2011. The CQ ratio of surface energy components influences adhesion and removal of fouling bacteria. Biofouling **27:**275-285.
43. **Liu, Y., A. M. Gallardo-Moreno, P. A. Pinzon-Arango, Y. Reynolds, G. Rodriguez, and T. A. Camesano.** 2008. Cranberry changes the physicochemical surface properties of *E. coli* and adhesion with uroepithelial cells. Colloid Surface B **65:**35-42.
44. **Liu, Y. T., J. Strauss, and T. A. Camesano.** 2007. Thermodynamic investigation of *Staphylococcus epidermidis* interactions with protein-coated substrata. Langmuir **23:**7134-7142.
45. **Lopez, G. P., M. W. Albers, S. L. Schreiber, R. Carroll, E. Peralta, and G. M. Whitesides.** 1993. Convenient methods for patterning the adhesion of mammalian cells to surfaces using self-assembled monolayers of alkanethiolates on gold. J Am Chem Soc **115:**5877-5878.
46. **Lopez, G. P., H. A. Biebuyck, R. Harter, A. Kumar, and G. M. Whitesides.** 1993. Fabrication and imaging of 2-dimensional patterns of proteins adsorbed on self-assembled monolayers by scanning electron-microscopy. J Am Chem Soc **115:**10774-10781.
47. **Lopez, G. P., H. A. Biebuyck, and G. Whitesides.** 1993. Scanning electron-microscopy can form images of patterns in self-assembled monolayers. Langmuir **9:**1513-1516.
48. **Maki, J. S., D. Rittschof, and R. Mitchell.** 1992. Inhibition of larval barnacle attachment ot bacterial films: an investigation of physical properties. Microb Ecol **23:**79-106.
49. **Maki, J. S., D. Rittschof, A. R. Schmidt, A. G. Snyder, and R. Mitchell.** 1989. Factors controlling attachment of bryozoan larvae -a comparison of bacterial films and unfilmed surfaces,. Biol Bull **177:**295-302.
50. **Mendez, S., L. K. Ista, and G. P. Lopez.** 2003. Use of stimuli responsive polymers grafted on mixed self-assembled monolayers to tune transitions in surface energy. Langmuir **19:**8115-8116.
51. **Murray, P. A., A. Prakobphol, T. Lee , C. I. Hoover, and S. J. Fisher.** 1992. Adherence of oral Streptococci to salivary glycoproteins. Infec Immun **60:**31-38.
52. **Neumann, A. W., R. J. Good, C. J. Hope, and M. Sejpal.** 1974. Equation-of-state spproach to determine surface tensions of low-energy solids from contact angles. J Colloid Interf Sci **49:**291-304.
53. **O'Toole, G., H. B. Kaplan, and R. Kolter.** 2000. Biofilm formation as microbial development. Annu. Rev. Microbiol. **54**.

54. **Prime, K. L., and G. M. Whitesides.** 1993. Adsorption of proteins onto surfaces containing end-attached oligo(ethylene oxide): a model system using self-assembled monolayers. J Am Chem Soc **115:**10714-10721.
55. **Prime, K. L., and G. M. Whitesides.** 1991. Self-assembled organic monolayers: model systems for studying adsorption of proteins at surfaces. Science **252:**1164-1167.
56. **Rijnaarts, H. H. M., W. Norde, J. Lyklema, and A. J. B. Zehnder.** 1995. The isoelectric point of bacteria as an indicator for the presence of cell-surface polymers that inhibit adhesion. Colloid Surface B **4:**191-197.
57. **Schilp, S., A. Rosenhahn, M. E. Pettitt, J. Bowen, M. E. Callow, J. A. Callow, and M. Grunze.** 2009. Physicochemical properties of (ethylene glycol)-containing self-assembled monolayers relevant for protein and algal cell resistance. Langmuir **25:**10077-10082.
58. **Sharma , P. K., and K. H. Rao.** 2002. Analysis of different approaches for evaluation of surface energy of microbial cells by contact angle goniometry. Adv Colloid Interfac **98:**341-463.
59. **Shea, C., L. J. Lovelace, and H. E. Smith-Somerville.** 1995. *Deleya marina* as a model organism for studies of bacterial colonization and biofilm formation. J Indust Microbiol **15:**290-296.
60. **Shea, C., J. W. Nunley, and H. E. Smith-Sommerville.** 1991. Variable expression of gliding and swimming motility in *Deleya marina.* Can J Microbiol **37:**808-814.
61. **Shea, C., J. W. Nunley, J. C. Williamson, and H. E. Smith-Sommerville.** 1991. Comparison of the adhesion properties of *Deleya-marina* and the exopolysaccharide-defective mutant strain DMR. Appl Environ Microbiol **57:**3107-3113.
62. **Shea, C., and H. E. Smith-Sommerville.** 1994. The effects of phenotype variability on the adhesion properties of *Deleya-marina*. Biofouling **8:**13-25.
63. **Singhvi, R., A. Kumar, G. P. Lopez, G. N. Stephanopoulos, D. I. C. Wang, G. M. Whitesides, and D. E. Ingber.** 1994. Engineering cell shape and function. Science **264:**696-698.
64. **Stoodley, P., K. Sauer, D. G. Davies, and J. W. Costerton.** 2002. Biofilms as complex differentiated communities. Annu Rev Microbiol **56:**187-209.
65. **Straight, P. D., and R. Kolter.** 2009. Interspecies chemical communication in bacterial development. Annu Rev Microbiol **63:**99-118.
66. **Taylor, R. G., and R. D. Welch.** 2008. Chemotaxis as an emergent property of a swarm. J Bacteriol **190:**6811-6816.
67. **Ubbink, J., and P. Schar-Zammaretti.** 2007. Colloidal properties and specific interactions of bacterial surfaces. Curr Opin Colloid Interface Sci **12:**263-270.
68. **van Oss, C. J.** 2006. Interfacial Forces in Aqueous Media, 2nd ed. Taylor and Francis, Boca Raton.
69. **van Oss, C. J., R. J. Good, and M. K. Chaudhury.** 1988. Additive and nonadditive surface-tension components and the interpretation of contact angles. Langmuir **4:**884-891.

70. **Verwey, E. J. W.** 1945. Theory of the Stability of Lyophobic Colloids. Philips Research Reports **1:**33-49.
71. **Verwey, E. J. W.** 1947. Theory of the Stability of Lyophobic Colloids. Journal of Physical and Colloid Chemistry **51:**631-636.
72. **Whitman, W. B., D. C. Coleman, and W. J. Wiebe.** 1998. Prokaryotes: The unseen majority. Proc Natl Acad Sci USA **95:**6578-6583.
73. **Wiencek, K. M., and M. Fletcher.** 1995. Bacterial adhesion to hydroxyl- and methyl-terminated alkanethiol self-assembled monolayers. J Bacteriol **177:**1959-1966.
74. **Wiencek, K. M., and M. Fletcher.** 1997. Effects of substratum wettability and molecular topography on the initial adhesion of bacteria to chemically defined substrata. BIofouling **11:**293-311.

Chapter 2: Effect of Substratum Surface Chemistry and Surface Energy on Attachment of Marine Bacteria and Algal Spores

Linnea K Ista[1], Maureen E Callow[2], John A Finlay[2], Sarah E Coleman[1], Aleece C Nolasco[1], Robin H Simons[1], James A Callow[2] and Gabriel P. López[1].

[1]Department of Chemical and Nuclear Engineering

The University of New Mexico

Albuquerque, NM 87131 USA

[2]School of Biosciences

University of Birmingham

Birmingham B15 2TT UK

My contribution to this work: I handled the exchange of materials and communication between UNM and UB for this work. I also interpreted the x-ray photoelectron spectroscopy data for Figure 2 and performed the *C. marina* attachment data for Figure 3. I did the original patterning for the mixed sample data as shown in Figure 5A and the preliminary work for the generation of mixed SAMs with the range of water contact angles used throughout the paper. Sarah Coleman and Aleece Nolasco were undergraduates who generated most of the SAM samples used in this work under my direct supervision. I also wrote the manuscript and handled the revisions.

Applied and Environmental Microbiology, 2004, **70**(7): 4151-4157.

APPLIED AND ENVIRONMENTAL MICROBIOLOGY, July 2004, p. 4151–4157 Vol. 70, No. 7
0099-2240/04/$08.00+0 DOI: 10.1128/AEM.70.7.4151–4157.2004

Effect of Substratum Surface Chemistry and Surface Energy on Attachment of Marine Bacteria and Algal Spores

Linnea K. Ista,[1] Maureen E. Callow,[2] John A. Finlay,[2] Sarah E. Coleman,[1] Aleece C. Nolasco,[1] Robin H. Simons,[1] James A. Callow,[2] and Gabriel P. Lopez[1]*

Department of Chemical and Nuclear Engineering, The University of New Mexico, Albuquerque, New Mexico 87131,[1] and School of Biosciences, The University of Birmingham, Birmingham B15 2TT, United Kingdom[2]

Received 13 November 2003/Accepted 8 March 2004

Two series of self-assembled monolayers (SAMs) of ω-substituted alkanethiolates on gold were used to systematically examine the effects of varying substratum surface chemistry and energy on the attachment of two model organisms of interest to the study of marine biofouling, the bacterium *Cobetia marina* (formerly *Halomonas marina*) and zoospores of the alga *Ulva linza* (formerly *Enteromorpha linza*). SAMs were formed on gold-coated glass slides from solutions containing mixtures of methyl- and carboxylic acid-terminated alkanethiols and mixtures of methyl- and hydroxyl-terminated alkanethiols. *C. marina* attached in increasing numbers to SAMs with decreasing advancing water contact angles (θ_{AW}), in accordance with equation-of-state models of colloidal attachment. Previous studies of *Ulva* zoospore attachment to a series of mixed methyl- and hydroxyl-terminated SAMs showed a similar correlation between substratum θ_{AW} and zoospore attachment. When the hydrophilic component of the SAMs was changed to carboxylate, however, the profile of attachment of *Ulva* was significantly different, suggesting that a more complex model of interfacial energetics is required.

Upon submersion in a nonsterile aqueous liquid, most surfaces become rapidly colonized by collections of bacteria and other microorganisms. These attached cells, along with extracellular material they produce and other organic compounds adsorbed to the surface, comprise a structure referred to as a biofilm (17). Biofilms are ubiquitous in natural aqueous milieus and are increasingly considered to represent a separate developmental form of microorganisms (29). Similarly, a number of macroorganisms, such as algae, exploit a unicellular form for attachment and colonization of surfaces. Surface coverage by both macro- and microorganisms, therefore, depends initially on the ability of single cells to adsorb and adhere to the attachment substratum.

The tendency (driving force) for a microorganism to attach to a given surface is given by the free energy of adhesion (ΔG^{adh}), which can be expressed by the following equation as a thermodynamic energy balance between the interfacial energies between the substratum, the organism, and the surrounding liquid (1): $\Delta G^{adh} = \gamma_{BS} - \gamma_{BL} - \gamma_{SL}$, where γ_{BS} is the interfacial tension between the organism (e.g., a bacterium) and substratum, γ_{BL} is the interfacial tension between the organism and the liquid, and γ_{SL} is the interfacial tension between the substratum and the liquid.

Experimental determination of the interfacial energy values for the above equation is controversial and has led to three different, yet complementary, models (8). All rely on estimation of interfacial energies by contact angles as indicated by Young's equation (2), which states that γ_{SV} (the vapor interfacial tensions [surface tensions] of the substratum) is related to the contact angle (θ) formed by a drop of liquid on the substratum such that $\gamma_{SV} = \gamma_{SL} + \gamma_{LV}\cos\theta$, where γ_{SL} is the interfacial tension between the surface and the liquid and γ_{LV} is the interfacial tension between the liquid and vapor phases.

The simplest and most elegant of these models invokes an equation of state, of the form $\gamma_{12} = f(\gamma_{13},\gamma_{23})$ (28). Thus, γ_{SL} can be obtained as a function of γ_{SV} and γ_{LV}, γ_{BS} can be obtained as a function of γ_{BV} and γ_{SV}, and γ_{BL} can be obtained as a function of γ_{BV} and γ_{LV}, where γ_{BV} and γ_{LV} are the vapor interfacial tensions (surface tensions) of the bacterium and liquid, respectively. The empirically determined equation of state derived by Absolom et al. (1) leads to the following qualitative prediction: if $\gamma_{LV} < \gamma_{BV}$, bacterial attachment will increase with increasing γ_{SV}; conversely, if $\gamma_{LV} > \gamma_{BV}$, bacterial attachment will increase with decreasing γ_{SV}. Absolom et al. observed not only this relationship but also a linear relationship between γ_{SV} (as calculated from the water contact angle of the substratum) and bacterial attachment under both conditions.

A second model asserts that the contributions of Lifschitz-Van der Waals and polar interactions are the major components of interfacial energies and are most important to thermodynamic balance (8). Experimental systems based on this model require the measurement of contact angle with two liquids, one polar and one nonpolar, in order to estimate the relative interfacial energies. A variation on this model further divides the acid-base component into its electron donor and electron acceptor constituents. This model, called the extended DLVO (Derjaguin-Landau-Verwey-Overbeek) model, puts particular emphasis on electrostatic interactions as the major contribution to surface energy. These two models have also

* Corresponding author. Mailing address: Department of Chemical and Nuclear Engineering, The University of New Mexico, Albuquerque, NM 87131. Phone: (505) 277-4939. Fax: (505) 277-5433. E-mail: gplopez@unm.edu.

been empirically tested and, in certain cases, have been found to be valid under laboratory conditions (7).

The experimental results from these three different models, although predictive in certain cases, do not result in the same estimations of interfacial energy, and thus predict different values for ΔG^{adh}. Systematic determination of the best model for γ_{SV} and the subsequent effect on microbial attachment has been difficult in the past, because the majority of studies have by necessity used either glass or polymeric substrata which can vary enormously in more than one energetic parameter from sample to sample (9). The use of self-assembled monolayers (SAMs) of ω-substituted alkanethiolates on gold has been an effective technique for the systematic investigation of the effect of substratum physicochemistry on protein adsorption (30, 31, 33) as well as on attachment of mammalian cells (15, 16, 27) and microbes (12, 23, 38, 39). The use of mixed monolayers has been particularly useful for the generation of surfaces constant in one parameter (e.g., contact angle or surface roughness) while varying the chemistry by changing the relative concentrations of different thiolates within the monolayer (3, 4). Furthermore, a series of samples can be produced in which one parameter (e.g., contact angle) is held constant while varying the chemical composition by using mixed monolayers with different thiolate components on different samples.

For this set of experiments, we sought to examine attachment by using the most simple of the models, derived from equations of state, which derives its estimations of interfacial energy on the contact angle of water. Using Absolom et al.'s interpretation of the equation of state, computer-generated tables give the value of γ_{SV} when θ and γ_{LV} are known (28), γ_{SV} being linear with regard to cosθ of water. Thus, the relationship between attachment and cosθ reflects the relationship between attachment and γ_{SV}.

In this study, we investigate the integrity of this model by examining the effect of varying the chemical composition of mixed monolayers on microbial attachment while keeping θ_{AW} and, thus, γ_{SV} approximately constant. Two series of mixed monolayers were produced, consisting of methyl- and hydroxyl-terminated and methyl- and carboxylic acid-terminated SAMs with identical, stepped contact angles. The attachment of bacterial cells and algal spores was then tested on each series. We used the gram-negative bacterium *Cobetia marina* (formerly *Halomonas marina* [3]) as a model marine biofouling bacterium (32). This organism was originally isolated from a marine biofilm and has many practical considerations that make it ideal for such studies: it is obligately aerobic, thus ensuring one mode of growth; it requires high salt concentrations, which inhibits contamination while growing in chemostat; and while in log phase, the cells are relatively large and easy to see during assays. Studies of this organism and its exopolysaccharide and motility mutants (32) have yielded a detailed picture of its biofilm developmental cycle, which allows for understanding of results, particularly for long-term experiments, in the context of this cycle. Previous studies have shown that, when grown in minimal medium with limiting carbon source, *C. marina* shows a greater affinity for attachment to hydrophobic surfaces (23, 24). The present study addresses this observation in detail.

We also examined attachment of zoospores of the marine alga *Ulva linza* (formerly *Enteromorpha linza*), an organism ubiquitous in marine biofilms. Dispersal and rapid colonization of substrata by this green fouling alga occurs mainly through the production of vast numbers of motile spores (11). Asexual zoospores are quadriflagellate, naked (i.e., lacking a cell wall), pyriform cells, the spore body being 7 to 10 μm in length. Critical events in the colonization of new substrata involve the swimming spore locating a suitable surface on which to settle (11, 13), followed by permanent adhesion through the rapid secretion and curing of a swollen, hydrophilic gel-like adhesive composed of an *N*-linked, polydisperse glycoprotein (molecular size of 110 kDa under denaturing reducing conditions) that anchors the spore to the substratum (10, 35).

Prior to adhesion, the swimming spore undergoes characteristic presettlement behavior that involves a searching pattern of exploration close to the substratum (13). A number of cues moderate the way in which a spore interacts with the substratum (11), and recent evidence suggests that the swimming spore is able to select suitable surfaces on the basis of surface characteristics, such as topography (14), or on the basis of physicochemical properties, such as contact angle (12). It was previously demonstrated that the number of *Ulva* zoospores settling and attaching increases with increasing contact angle on mixed monolayers containing hydroxyl- and methyl-terminated alkanethiolates (12, 20). In this work, we extend these studies by changing the hydrophilic component of the mixed SAMs to carboxylic acid in order to determine whether the equation of state model is predictive independent of chemistry.

MATERIALS AND METHODS

SAMs. SAMs were prepared at the University of New Mexico (UNM) on gold films evaporated onto glass microscope slides. The glass slides (VWR Scientific) were cleaned by immersion in a solution (piranha etch) prepared by mixing 70% (vol/vol) concentrated H_2SO_4 with 30% H_2O_2 for 20 min to 1 h, thoroughly rinsing the slides in deionized water, and drying them under a stream of nitrogen. Piranha etch is a powerful oxidizer and can react violently when placed in contact with organics and should be stored in containers which prevent pressure buildup. The samples were then placed into the vacuum chamber of a metal evaporator. The system was evacuated to 10^{-7} torr, and 10 Å of chromium followed by 300 Å of gold was deposited on the substrata. The system was then restored to room pressure, and the samples were removed and submerged in 1 mM ethanolic solutions of dodecanethiol (referred to herein as CH_3-thiol and obtained from Aldrich Chemical), 11-mercapto-1-undecanol (OH-thiol; Aldrich Chemical), 12-mercaptodecanoic acid (COOH-thiol; Aldrich Chemical), or mixtures of two of these thiols. The samples were immersed in thiol solution overnight at 4°C, after which they were rinsed in ethanol and dried under a stream of N_2. The resulting surface (i.e., the SAMs of ω-terminated alkanethiolates) will be referred to as CH_3-SAM, OH-SAM, COOH-SAM, or, in the case of mixed monolayers, COOH/CH_3-SAM, OH/CH_3-SAM, or COOH/OH-SAM.

Patterned SAMs were produced by serial electrochemical desorption and reformation of the SAMs as described previously (12, 36). Briefly, a CH_3-SAM was formed on gold. A laser ablation system composed of a Nikon Diaphot inverted microscope, adapted with a computer-controlled, pulsed-nitrogen pumped-dye laser (λ = 390; 15 μJ pulse^{-1}; 20 pulses s^{-1}) was used to cut lines in the gold film to form electrically isolated regions in the film. The UV laser beam was focused through a 10× objective of the microscope and ablated the gold and supported SAMs generating lines of exposed glass approximately 15 μm wide. The slide was then placed in 0.5 M ethanolic KOH, and an anode was connected to one element. A cyclic current was then applied (−1.0 to 1.5 V versus Ag/AgCl; 500 mV s^{-1}) to the element for 6 cycles. Desorption of CH_3-SAM was monitored by cyclic voltammetry to ensure complete removal of the SAM. The exposed gold was then treated with a 10 mM ethanolic solution of the desired ω-substituted alkanethiol for 20 min. A series of elements could thus be addressed sequentially, resulting in a pattern of different SAMs upon a single surface.

Zoospore attachment studies were done at the University of Birmingham (UB), United Kingdom. For transportation, the SAMs were removed from the

thiol solutions, rinsed, and placed into Coplin staining jars containing deionized water which had been deoxygenated in a stream of nitrogen for one hour. The lids of the jars were screwed on and sealed with Teflon tape. The jars were immediately packaged and sent via overnight delivery.

Surface characterization of SAMs. X-ray photoelectron spectroscopy (XPS) was used to determine the surface composition of mixed monolayers. The analysis was conducted on an AXIS-HSi instrument from Kratos Analytical, Inc. (Ramsey, N.Y.) at UNM. An A1 $K\alpha_{1,2}$ monochromatized X-ray source ($h\nu$ = 1,486.7 eV) with an emission power of 225 W was used to stimulate photoelectron emission. The residual pressure in the analysis chamber was $\sim 4 \times 10^{-10}$ torr during spectral acquisition. To minimize X-ray-induced sample damage, the exposure time for SAMs during analysis was limited to <60 min. The samples were loaded into the vacuum chamber less than 30 min after removal from the thiol solutions. Survey scans and high-resolution C_{1s} and O_{1s} spectra were recorded for each sample. The Au_{4f} peak was referenced at 84 eV, which consistently located the main C_{1s} hydrocarbon peak at 284.7 eV. Survey spectra were acquired by using a constant pass energy of 160 eV, whereas high-resolution spectra were acquired by using a pass energy of 80 eV. The spectral envelopes were resolved into Gaussian peaks to fit the spectra.

Contact angles of samples were measured both prior to and after shipment to ensure that the integrity of the samples was maintained in transit. Advancing water contact angles (θ_{AW}) were measured both immediately before packing and immediately before use in the adhesion assays after the following washing treatment: each slide was washed in ethanol, dried in a stream of nitrogen, and then washed in 0.1 M HCl followed by three rinses in deionized water.

Bacterial strain. *C. marina* American Type Culture Collection (Manassas, Va.) strain 25374 (6, 19) was established as a chemostat culture in modified basal medium (200 mM NaCl, 50 mM $MgSO_4 \cdot 7H_2O$, 10 mM KCl, 10 mM $CaCl_2 \cdot 2H_2O$, 19 mM NH_4Cl, 0.33 mM K_2HPO_4, 0.1 mM $FeSO_4 \cdot 7H_2O$, 5 mM Tris-HCl [pH 7.5], and 2 mM glycerol [25]) as described previously (23). The chemostat was maintained at a flow rate of 1.2 ml min^{-1} with constant stirring. The cellular concentration of the subsequent culture was 5×10^7 cells ml^{-1}.

Bacterial attachment studies. SAMs prepared on gold films coated on 60- by 24-mm coverslips were placed into a flow-cell apparatus (23) which was then mounted onto the stage of an optical microscope (Labophot; Nikon) and connected to the outflow of the chemostat. The *C. marina* culture was allowed to flow through the cell at a rate of 1.2 ml min^{-1} for 2 h. Under these experimental conditions, the Reynolds number was $\sim 2 \times 10^{-3}$, indicating laminar flow. The surface shear rate was 664 s^{-1}. Bacterial attachment was monitored through a CCD camera attached to the microscope. The images were fed to a computer by using a Data Translations 3155 frame-grabber card and Image Tool imaging software (available from the University of Texas Health Science Center at San Antonio). At the end of the attachment time, images of 10 fields of view within 10 mm of the horizontal midline of the slide were captured, the number of attached bacteria were counted, and the average for each slide was determined.

Algal material. Fertile plants of *U. linza* were collected from Wembury Beach, United Kingdom (50°18′N, 4°02′W). Zoospores were released and prepared for attachment experiments as described previously (12).

Zoospore adhesion assays. Zoospore suspensions were standardized as described previously (13). The concentration of spores was adjusted to 1×10^6 to 2×10^6 ml^{-1} with natural seawater; the exact concentration is given for individual experiments. Each microscope slide was placed in a compartment of a polystyrene culture dish (Fisher Scientific Co.), and 10 ml of spore suspension was added. After incubation in the dark at 20°C for 60 min, the slides were washed by being passed back and forth 10 times in a beaker of seawater before being fixed in 2% glutaraldehyde in seawater for 10 min, followed by washing as described previously (12). Images of spores were recorded in 10 fields of view at 0.5-mm intervals through the mid-point of the long axis of each of three replicate slides by using a Zeiss epifluorescence microscope via a video camera. Spores were visualized by autofluorescence of chlorophyll. Spore counts were generated from the images by using an algorithm that had been calibrated against manual counts of spore numbers. Data are presented for the mean number of spores adhered at ±95% confidence limits (x = 30).

Zoospore adhesion to SAMs formed from mixtures of COOH- and OH-thiols. Four slides of each SAM were shipped and treated immediately prior to use in the spore adhesion assay as described above. The SAMs that were used were formed with different solution mole fractions of COOH-thiol on a solvent-free basis (χ_{COOH}^{sol}) according to the formula χ_{COOH}^{sol} = (COOH-thiol)/(COOH-thiol + OH_3-thiol). Three replicate slides were used for zoospore adhesion assays; the remaining slide was used to determine the contact angle. Samples were incubated for 1 h in a suspension of 1.0×10^6 ml^{-1} zoospores and were processed as described above for adhesion assays.

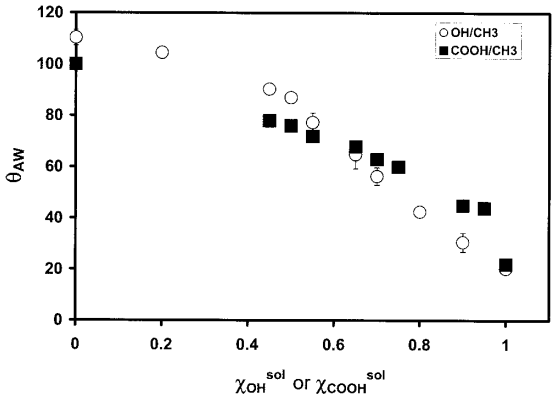

FIG. 1. θ_{AW} of OH/CH_3- and $COOH/CH_3$-SAMs as a function of the mole fraction of the hydrophilic component (X) in the forming solution (χ_X^{sol}). Data are the averages of at least three measurements on three individual samples ± standard errors.

Measurement of spore adhesion to patterned SAMs. Three replicate patterned slides were prepared and incubated as described above. The pattern was arranged in pairs such that OH/CH_3-SAM and $COOH/CH_3$-SAM elements with comparable contact angles were in close proximity on the slide, with contact angle increments of ca. 20° between each pair of elements. A schematic of the patterns is shown in Fig. 5A. The spore concentration was 2×10^6 ml^{-1}. Following incubation and rinsing, three replicates were fixed in 2% glutaraldehyde in seawater and spore counts were taken at 1-mm intervals along the middle of the long axis of each sector.

RESULTS

Surface analysis. Figure 1 shows the contact angle data for OH/CH_3- and $COOH/CH_3$-SAMs in relation to the composition of the mixed thiol solutions from which they were formed. Surface composition data are shown in Fig. 2. For $COOH/CH_3$- and OH/CH_3-SAMs, the surface composition (χ_x^{surf}) was estimated by dividing the area of the O_{1s} peak obtained by XPS by that obtained for the pure (i.e., χ_x^{surf} = 1) COOH- or OH-SAM, respectively. For the COOH/OH-SAMs, the mole fraction of COOH constituents was also estimated using the area of the O_{1s} peaks; however, the area for a pure OH-SAM was first subtracted from the area of the mixed SAMs prior to division.

The values of χ_{COOH}^{sol} used to form $COOH/CH_3$-SAMs for initial zoospore adhesion assays were chosen to yield a series of SAMs for which θ_{AW} increased by increments of roughly 10°. For patterned SAMs used to compare adhesion to $COOH/CH_3$-SAMs and for *C. marina* experiments, ~20° increments were used. θ_{AW} was obtained prior to shipping from UNM and just before use at UB, and the values obtained in both locations were routinely in agreement (±1 to 5°), suggesting that degradation or contamination of the samples during transit was minimized. Subsequent discussion of θ_{AW} will refer to the measurements taken at UNM. For OH/COOH-SAM experiments, the series was produced such that the increments in the surface mole fraction of COOH (χ_{COOH}^{surf}) were 0.2. The measured θ_{AW} for these samples was between 16 and 20°.

The surface roughness of these SAMs is predicted to be on the order of 4 to 5 nm based on atomic force microscopy

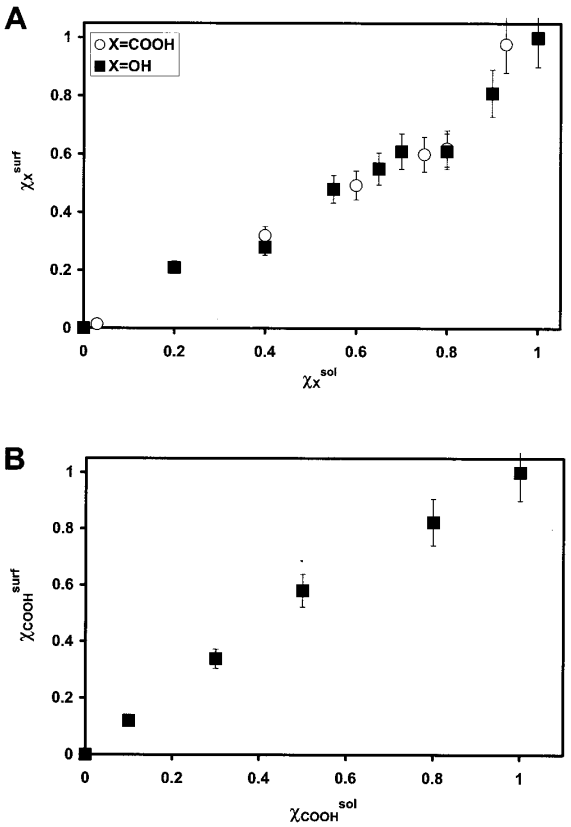

FIG. 2. Composition of mixed SAMs as a function of mole fractions of the forming thiol solutions as estimated by XPS. (A) Surface mole fraction of the hydrophilic component (χ_X^{surf}) as a function of the solution mole fraction of the forming thiol (χ_X^{sol}) for COOH/CH_3- and OH/CH_3-SAMs. (B) Surface mole fraction of COOH-terminated alkanethiolate (χ_{COOH}^{surfl}) as a function of the solution mole fraction of COOH-thiol in the forming solution (χ_{COOH}^{sol}) for COOH/OH-SAMs. Error bars reflect 10% error generally associated with XPS measurements.

studies done with SAMS on similar thicknesses of gold (22), and our own measurements have indicated that surface roughness of SAMs similar to those used in this experiment was <30 nm. As it is known that surface roughnesses of 50 nm or more can produce tangential electrostatic effects on microbial attachment (21), global electrostatic effects are unlikely in the present experiments. However, it is unknown how these could affect smaller, nanometer-sized structures, such as the apical tip of *Ulva* zoospores.

Bacterial attachment. Attachment of *C. marina* to a series of COOH/CH_3- and OH/CH_3-SAMs with 20° increments is shown in Fig. 3. For both series of slides the number of cells increased with decreasing $\cos\theta_{AW}$ and, thus, γ_{SV} (see below) in a linear manner ($R^2 > 0.95$ for both series). Although small differences in the number of cells attached at each contact angle were observed, the profile was nearly identical for both COOH- and OH-containing surfaces.

C. marina grown under these experimental conditions is

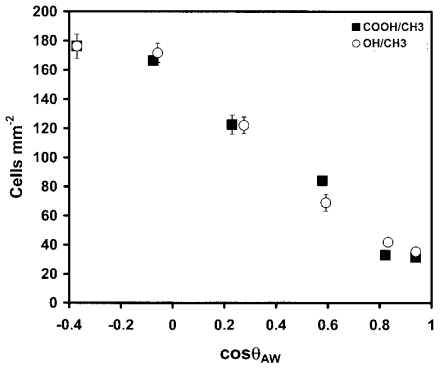

FIG. 3. Attachment of *C. marina* to COOH/CH_3- and OH/CH_3-SAMs as a function of $\cos\theta_{AW}$. Each data point represents the average of at least four experiments. Error bars represent standard errors.

relatively hydrophobic. As part of ongoing strain monitoring in the laboratory, hydrophobic interaction chromatography on octyl-Sepharose (34) is performed regularly on the chemostat to monitor for possible changes in surface characteristics; only those cultures which show ~85% of the cells retained by the hydrophobic column against artificial seawater were used in attachment experiments. Recent studies (data not shown) indicated that approximately 70% of the cells from a suspension in 0.1 M phosphate buffer (pH 7) segregate into the organic phase when mixed with decane.

Zoospore attachment. Attachment of *Ulva* zoospores to a series of COOH/CH_3-SAMs with 10° θ_{AW} is shown in Fig. 4. Data from a previous experiment with OH/CH_3-SAMs are shown in the inset (12). Although the OH/CH_3 series shows approximately linear attachment between $\cos\theta_{AW}$ and spore attachment ($R^2 = 0.89$), that of the COOH/CH_3-SAM series does not ($R^2 = 0.45$). Because these data were obtained from spores collected at different times, we confirmed these results with patterned SAMs containing five pairs of ele-

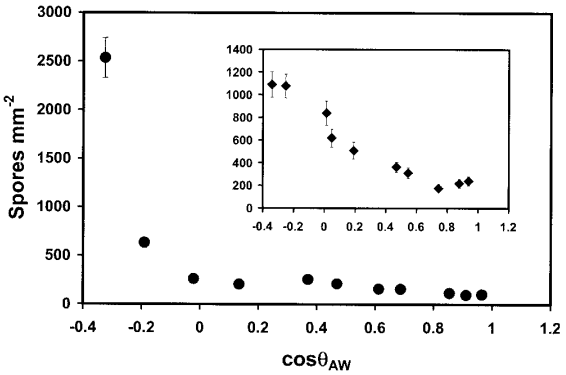

FIG. 4. Attachment of *Ulva* zoospores to COOH/CH_3-SAMs as a function of $\cos\theta_{AW}$. Attachment data for similar experiments performed on OH/CH_3-SAMs (12) is shown in the inset. Attachment was for 1 h. Each point is the mean of 30 fields of view, 10 from each of three replicates. Bars show 95% confidence levels. Spore concentration was 2×10^6 ml^{-1}.

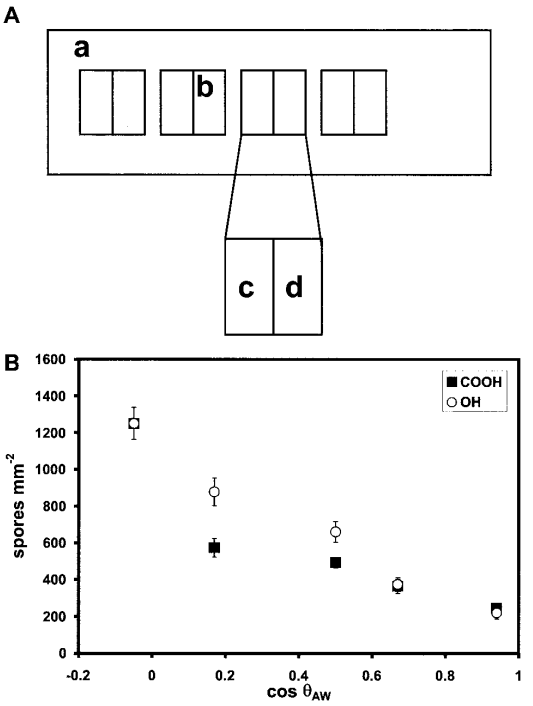

FIG. 5. Attachment of *Ulva* zoospores to $COOH/CH_3$- and OH/CH_3-SAMs with similar $\cos\theta_{AW}$ values. (A) Schematic representation of patterned $COOH/CH_3$- and OH/CH_3-SAMs on a single slide. A gold film supporting a CH_3-SAM was laser etched to produce four divided squares (b), each 10 by 10 mm and containing two electrically isolated elements. Electrochemical desorption of the CH_3-SAM from each element and subsequent exposure to solutions of either $COOH/CH_3$-thiols (c) or OH/CH_3-thiols (d) resulted in a series of adjacent paired SAMs with similar contact angles. (B) Attachment of *Ulva* zoospores as a function of $\cos\theta_{AW}$. Each point is the mean of 30 fields of view, 10 from each of three replicates; bars show 95% confidence limits.

ments (Fig. 5A). Each pair contained one element composed of a $COOH/CH_3$-SAM and one of a OH/CH_3-SAM which had the same ($\pm 1°$) θ_{AW}. Attachment studies were done as described above, and the results are shown in Fig. 5B. Once again, there is a clear divergence between attachment to $COOH/CH_3$- and OH/CH_3-SAMs, with the OH/CH_3 series once again exhibiting a nearly linear relationship between attachment and $\cos\theta_{AW}$ ($R^2 = 0.97$), while that of the $COOH/CH_3$ series was significantly less linear ($R^2 = 0.79$).

To further study the effects of COOH-containing SAMs on zoospore attachment, we also examined COOH/OH-SAMs. The results of these investigations are shown in Fig. 6. Low numbers of zoospores attached to all the COOH/OH-SAMs, irrespective of χ_{COOH}^{surf}. All surfaces were very hydrophilic, with $\cos\theta_{AW}$ being within the range of 0.93 to 0.97.

DISCUSSION

We have generated a matched series of $COOH/CH_3$- and OH/CH_3-SAMs which vary systematically in $\cos\theta_{AW}$ and, thus,

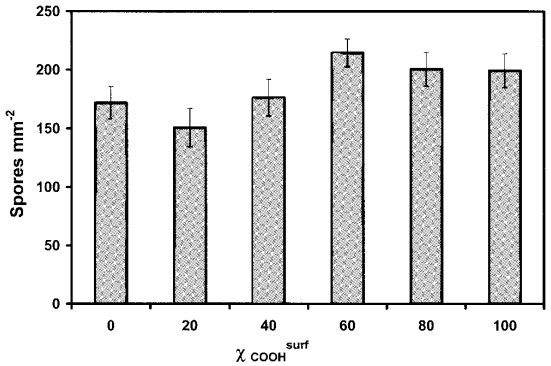

FIG. 6. Attachment of *Ulva* zoospores to $COOH/CH_3$-SAMs. The number of zoospores is plotted versus χ_{COOH}^{surf}. Spore concentration was 10^6 ml^{-1}. Each point is the mean of 30 fields of view, 10 from each of three replicates; error bars show 95% confidence limits.

γ_{SV}, according to equation-of-state models for its estimation (1, 28). Analysis by XPS shows that θ_{AW} varies in accordance with the changes in the relative molar ratios of different alkanethiolates within the SAM (4, 5).

As has been qualitatively observed in previous studies, *C. marina* attached preferentially to hydrophobic surfaces (23, 24). In this study, we have shown a linear correlation between the attachment of this bacterium and decreasing $\cos\theta_{AW}$ and, thus, γ_{SV}, as would be estimated by advancing water contact angles. As the cell surface of *C. marina* is also relatively hydrophobic, these results agree with the predictions of the equation-of-state models of bacterial attachment set forth by Absolom et al. (1). Attachment of *Ulva* zoospores to mixed $COOH/CH_3$-SAMs was positively correlated with decreasing $\cos\theta_{AW}$. However, a dramatic response was observed only below a $\cos\theta_{AW}$ of 0, and the relationship between attachment and $\cos\theta_{AW}$ was nonlinear. The difference was especially apparent on patterned SAMs where direct comparison between attachment on OH- and COOH-containing SAMs of the same $\cos\theta_{AW}$ was possible. This contrasts with the response to zoospore attachment on OH/CH_3-SAMs, where the relationship between $\cos\theta_{AW}$ and attachment was linear (Fig. 4, inset) (12). These results also differ from those obtained for *C. marina* in which the chemistry of the hydrophilic component of the SAMs did not alter the attachment profile. The global cell hydrophobicity of *Ulva* could not be reliably measured. Lacking a cell wall, the zoospore would be seriously disrupted by attempted partition into organic solvents; hydrophobic interaction chromatography uses what is essentially a redundant measurement of attachment to a solid and which is not determined by global cellular surface energy but rather by the sum of energies in a step-by-step process.

It is known that carboxylic acid-terminated SAMs change their surface energy in response to the pH of the surrounding medium (18, 26, 40). These SAMs can be titrated, with the range and position of the pH-dependent change in θ_{AW} varying with the surface concentration of COOH-containing thiolates. It is possible that, under our experimental conditions, the difference in attachment of *Ulva* zoospores on the OH/CH_3- and

$COOH/CH_3$-SAMs might be attributable to a titration effect as the pH of the test medium (i.e., seawater) might be predicted to more strongly affect contact angles of SAMs with higher χ_{COOH}^{surf} values (5). If this was indeed the case, attachment to the surfaces should also be titratable. We therefore tested the effect of pH on attachment of *Ulva* zoospores to $COOH/CH_3$-SAMs with χ_{COOH}^{surf} of 0, 0.25, 0.5, and 0.75 at pH 7.8 and 9.5. This set was chosen so that their titration curves spanned the range of pHs used (5); thus, we could expect different attachment profiles in response to pHs for different SAMs. The results of these experiments were inconclusive. While there were changes associated with attachment to the COOH-containing SAMs at different pHs, there were no obvious trends. Moreover, attachment to SAMs with χ_{COOH}^{surf} of 0 (i.e., a pure CH_3-SAM) was also influenced by pH. Because CH_3-SAMs should not change their surface ionization or contact angle in response to pH, we concluded that different pHs affected not only the COOH-containing SAMs but also the surface charge and/or physiology of the zoospores. The effect could be on one of several presettlement processes of the zoospores, including motility, sensing, or secretion and/or polymerization of the adhesive.

As the equation-of-state model fell short of quantitatively modeling the attachment of *Ulva* to both kinds of surface, the suitability of the other models must be considered. Because the difference in attachment occurred on surfaces containing an ionizable group, one must consider the effects of electrostatic interactions on the attachment of *Ulva* zoospores to the surface. It should be noted that the molarity of artificial or natural seawater (ca. 250 mM) is sufficiently high to compress the double layer and to interrupt possible electrostatic repulsion (21). The potential for surface charge also requires that one consider the effect of Lewis acid-base interactions, which have been postulated to be the main driving force in microbial attachment (8, 37). Investigations are presently under way to examine this parameter of microbial attachment and will be presented in a subsequent report.

Our evaluation of the attachment of *Ulva* zoospores was obtained after washing and fixing of the slides, i.e., after the settled cells had undergone secondary, irreversible attachment. Successful attachment in this organism is the result of several steps, each of which involves cellular structures whose physicochemistry would be expected to exert a different influence during different times or processes in attachment (11, 13). It was previously shown that selection of the attachment site is affected by surface energy (12, 20), but the effect of surface energy is very likely influential at other specific points in the process of attachment as well. In this study, after settlement and secondary attachment, *Ulva* zoospores appeared to be less strongly adhered to $COOH/CH_3$- than to OH/CH_3-SAMs (data not shown), suggesting a direct effect of the physicochemical properties of the glycoprotein adhesive. We are presently investigating the effects of surface energy and chemistry on the spreading and firmness of attachment of the adhesive. Another possibility suggests itself when the spatial arrangement of the zoospores on various SAMs is considered. *Ulva* zoospores often settle gregariously (i.e., in groups) (13), and it has been observed that on OH/CH_3-SAMs, an increase in the size of spore groups (group was defined as adjacent, touching zoospores) correlated with an increase in the number of spores settled as surface energy decreased (12, 20). On $COOH/CH_3$-SAMs, however, a less marked effect was seen in regard to the size of attached groups versus $\cos\theta_{AW}$ values. For this series of SAMs, 80% of the spores attached to all surfaces with $\cos\theta_{AW} \geq 0$ were present in groups of no more than three spores. Larger spore groups (group sizes of up to 15 spores per group) were found only on the SAMs with $\cos\theta_{AW} < 0°$. Significantly, these were also the samples on which a marked increase in the total number of attaching spores was observed. It is possible, therefore, that the lack of attachment to $COOH/CH_3$-SAMs with higher surface energy may be due to interference with mechanisms promoting gregarious settlement, such as cell-to-cell signaling.

Using SAMs, we were able to systematically investigate the accuracy of surface energy estimations based on equations of state for modeling the attachment of two quite different microorganisms, both of which use a unicellular means of substratum colonization. We have found that while estimations of surface energy by this approach would, indeed, accurately predict the pattern attachment of *C. marina* to the model solid surfaces under study, they were less accurate for attachment of *Ulva* zoospores. The exploration of other, more complex models must therefore be undertaken in order to generate a global model for microbial attachment, and such investigations are planned in future studies. Systematic studies of physicochemical properties such as these are important for understanding microbial attachment processes and may lead to the development of materials that resist or rapidly release microorganisms in order to control biofilm formation on submerged materials.

ACKNOWLEDGMENTS

This work was supported through Office of Naval Research grants N00014-95-0901 and N0014-02-1-0377 to G.P.L. at UNM and grants N00014-95-0901 and N00014-02-1-0521 to M.E.C. and J.A.C. at UB.

We also thank Víctor Pérez-Luna and Lee Perry for help in obtaining and interpreting the XPS spectra and Dimiter Petsev for helpful discussions.

REFERENCES

1. **Absolom, D. R., F. V. Lamberti, Z. Policova, W. Zingg, C. J. van Oss, and A. W. Neumann.** 1983. Surface thermodynamics of bacterial adhesion. Appl. Environ. Microbiol. **46:**90–97.
2. **Adamson, A. W.** 1990. The solid-liquid interface-contact angle, p. 379–420. Physical chemistry of surfaces, 5th ed. Wiley and Sons, New York, N.Y.
3. **Bain, C. D., J. Evall, and G. M. Whitesides.** 1989. Formation of monolayers by the coabsorption of thiols on gold: variations in the head group, tail group, and solvent. J. Am. Chem. Soc. **111:**7155–7164.
4. **Bain, C. D., and G. M. Whitesides.** 1988. Formation of two-component surfaces by the spontaneous assembly of monolayers on gold from solutions containing mixtures of organic thiols. J. Am. Chem. Soc. **110:**6560–6561.
5. **Bain, C. D., and G. M. Whitesides.** 1989. A study by contact angle of acid-base behavior of monolayers containing ω-mercaptocarboxylic acids adsorbed on gold: an example of reactive spreading. Langmuir **5:**1370–1378.
6. **Baumann, L., R. D. Bowditch, and P. Baumann.** 1983. Description of *Deleya* gen. nov. created to accommodate the marine species of *Alcaligenes aestus, A. pacificus, A. cupidis, A. venustus,* and *Pseudomonas marina*. Int. J. Syst. Bacteriol. **33:**793–802.
7. **Bellon-Fontaine, M.-N., J. Rault, and C. J. van Oss.** 1996. Microbial adhesion to solvents: a novel method to determine the electron-donor/electron-acceptor or Lewis acid-base properties of microbial cells. Colloids Surf. B **7:**47–53.
8. **Bos, R., H. C. van der Mei, and H. J. Busscher.** 1999. Physico-chemistry of initial microbial adhesive interactions—its mechanisms and methods of study. FEMS Microbiol. Rev. **23:**179–230.
9. **Busscher, H. J., J. Sjollema, and H. C. van der Mei.** 1990. Relative importance of surface free energy as a measure of hydrophobicity in bacterial adhesion to solid surfaces, p. ●●●. *In* R. J. Doyle and M. Rosenberg (ed.), Microbial cell surface hydrophobicity. American Society for Microbiology, Washington, D.C.

10. **Callow, J. A., M. S. Stanley, R. Wetherbee, and M. E. Callow.** 2000. Cellular and molecular approaches to understanding primary adhesion in *Enteromorpha*. Biofouling **14:**141–150.
11. **Callow, M. E., and J. A. Callow.** 2000. Substratum location and zoospore behaviour in the fouling alga, *Enteromorpha*. Biofouling **15:**49–56.
12. **Callow, M. E., J. A. Callow, L. K. Ista, S. E. Coleman, A. C. Nolasco, and G. P. Lopez.** 2000. The use of self-assembled monolayers of different wettabilities to study surface selection and primary adhesion processes of green algal (*Enteromorpha*) zoospores. Appl. Environ. Microbiol. **66:**3249–3254.
13. **Callow, M. E., J. A. Callow, J. D. Pickett-Heaps, and R. Wetherbee.** 1997. Primary adhesion of *Enteromorpha* (Chlorophyta, Ulvales) propagules: quantitative settlement studies and video microscopy. J. Phycol. **33:**938–947.
14. **Callow, M. E., A. R. Jennings, A. B. Brennan, C. E. Seegert, S. Gibson, L. Wilson, A. Feinberg, R. Baney, and J. A. Callow.** 2002. Microtopographic cues for settlement of zoospores of the green fouling alga *Enteromorpha*. Biofouling **18:**237–245.
15. **Cooper, E., L. Parker, C. A. Scotchford, S. Downes, G. J. Leggett, and T. L. Parker.** 2000. The effect of alkyl chain length and terminal group chemistry on the attachment and growth of murine 3T3 fibroblasts and human osteoblasts on self-assembled monolayers of alkanethiols on gold. J. Mater. Chem. **10:**133–139.
16. **Cooper, E., R. Wiggs, D. A. Hutt, L. Parker, G. J. Leggett, and T. L. Parker.** 1997. Rates of attachment of fibroblasts to self-assembled monolayers formed by the adsorption of alkylthiols onto gold. J. Mater. Chem. **7:**435–441.
17. **Costerton, J. W., K. J. Cheng, G. G. Geesey, T. I. Ladd, J. C. Nickel, M. Dasgupta, and T. J. Marrie.** 1987. Bacterial biofilms in nature and disease. Annu. Rev. Microbiol. **41:**435–464.
18. **Creager, S. E., and J. E. Clarke.** 1994. Contact-angle titrations of mixed ω-mercaptoalkanoic acid/alkanethiol monolayers on gold. Reactive vs. nonreactive spreading and chain length effects on surface pK_a values. Langmuir **10:**3675–3684.
19. **Dobson, S. J., and P. D. Franzmann.** 1996. Unification of the genera *Deleya* (Baumann, et al. 1983), *Halomonas* (Vreeland et al. 1980), and *Halovibrio* (Robinson and Gibbons, 1952) into a single genus, *Halomonas*, and the placement of the genus *Zymobacter* in the family *Halomonadaceae*. Int. J. Syst. Bacteriol. **46:**550–558.
20. **Finlay, J. A., M. E. Callow, L. K. Ista, G. P. Lopez, and J. A. Callow.** 2002. The influence of surface wettability on the adhesion strength of spores of the green alga *Enteromorpha* and the diatom *Amphora*. Integr. Comp. Biol. **42:**1116–1122.
21. **Hermansson, M.** 1999. The DLVO theory in microbial adhesion. Colloids and Surfaces Part B: Biointerfaces **14:**105–119.
22. **Huang, Y.-W., and V. K. Gupta.** 2001. Effects of physical heterogeneity on adsorption of poly(ethylene glycol) at a solid-liquid surface. Macromolecules **34:**3757–3764.
23. **Ista, L. K., H. Fan, O. Baca, and G. P. López.** 1996. Attachment of bacteria to model solid surfaces: oligo(ethylene glycol) surfaces inhibit bacterial attachment. FEMS Microb. Lett. **142:**59–63.
24. **Ista, L. K., V. H. Perez-Luna, and G. P. López.** 1999. Surface-grafted, environmentally responsive polymers for biofilm release. Appl. Environ. Microbiol. **65:**1603–1609.
25. **Kersters, K.** 1992. The genus *Deleya*, p. 3189–3197. *In* A. Balows, H. G. Trüper, M. Dworkin, W. Harder, and K. H. Schliefer (ed.), The prokaryotes, 2nd ed., vol. 4. Springer-Verlag, New York, N.Y.
26. **Lee, T. R., R. I. Carey, H. A. Biebuyeck, and G. M. Whitesides.** 1994. The wetting of monolayer films exposing acids and bases. Langmuir **10:**741–749.
27. **López, G. P., M. W. Albers, S. L. Schreiber, R. Carroll, E. Peralta, and G. M. Whitesides.** 1993. Convenient methods for patterning the adhesion of mammalian-cells to surfaces using self-assembled monolayers of alkanethiolates on gold. J. Am. Chem. Soc. **115:**5877–5878.
28. **Neumann, A. W., D. R. Absolom, D. W. Francis, and C. J. van Oss.** 1980. Conversion tables of contact angles to surface tension. Sep. Purif. Methods **9:**69–163.
29. **O'Toole, G., H. B. Kaplan, and R. Kolter.** 2000. Biofilm formation as bacterial development. Annu. Rev. Microbiol. **54:**49–79.
30. **Prime, K. L., and G. M. Whitesides.** 1991. Self-assembled organic monolayers: model systems for studying adsorption of proteins at surfaces. Science **252:**1164–1167.
31. **Roberts, C., C. S. Chen, M. Mrksich, V. Martichonok, D. E. Ingber, and G. M. Whitesides.** 1998. Using mixed self-assembled monolayers presenting RGD and (EG_3)OH groups to characterize long-term attachment of bovine capillary endothelium cells to surfaces. J. Am. Chem. Soc. **120:**6548–6555.
32. **Shea, C., L. J. Lovelace, and H. E. Smith-Somerville.** 1995. Deleya marina as a model organism for studies of bacterial colonization and biofilm formation. J. Indust. Microbiol. **15:**290–296.
33. **Sigal, G. B., M. Mrksich, and G. M. Whitesides.** 1998. Effect of surface wettability on the adsorption of proteins and detergents. J. Am. Chem. Soc. **120:**3464–3473.
34. **Sorongon, M. L., R. A. Bloodgood, and R. P. Burchard.** 1991. Hydrophobicity, adhesion, and surface-exposed proteins of gliding bacteria. Appl. Environ. Microbiol. **57:**3193–3199.
35. **Stanley, M. S., M. E. Callow, and J. A. Callow.** 1999. Monoclonal antibodies to adhesive cell coat glycoproteins secreted by zoospores of the green alga *Enteromorpha*. Planta **210:**61–71.
36. **Tender, L. M., R. L. Worley, H. Y. Fan, and G. P. López.** 1996. Electrochemical patterning of self-assembled monolayers onto microscopic arrays of gold electrodes fabricated by laser-ablation. Langmuir **12:**5515–5518.
37. **van Oss, C. J.** 1997. Hydrophobicity and hydrophilicity of biosurfaces. Curr. Opin. Colloid Interface Sci. **2:**503–512.
38. **Weincek, K. M., and M. Fletcher.** 1995. Bacterial adhesion to hydroxyl- and methyl-terminated alkanethiol self-assembled monolayers. J. Bacteriol. **177:**1959–1966.
39. **Weincek, K. M., and M. Fletcher.** 1997. Effects of substratum wettability and molecular topography on the initial adhesion of bacteria to chemically defined substrata. Biofouling **11:**293–311.
40. **Whitesides, G. M., H. A. Biebuyeck, J. P. Folkers, and K. L. Prime.** 1991. Acid-base interactions in wetting. J. Adhesion Sci. Technol. **5:**57–69.

Chapter 3: Attachment and Detachment of Bacteria on Surfaces with Tunable and Switchable Wettability

Linnea K Ista[1,2], Sergio Mendez[2,3], and Gabriel P López[2,3]

[1] Department of Biology, [2] Center for Biomedical Engineering and [3]Department of Chemical and Nuclear Engineering

The University of New Mexico

Albuquerque, NM 87131

My contribution to this work: I was the first to observe the "tunable" phenomenon during the initial work on generating PNIPAAm from SAMs. I made many of the samples used in this study, obtained the contact angles and performed the attachment studies. The data interpretation in this work is also mine. I also wrote the manuscript and revisions.

Biofouling, 2010, **26**(1):111-118

Reprinted with the permission of Taylor and Francis

Biofouling
Vol. 26, No. 1, January 2010, 111–118

Taylor & Francis
Taylor & Francis Group

Attachment and detachment of bacteria on surfaces with tunable and switchable wettability

Linnea K. Ista[a,b], Sergio Mendez[a,c]† and Gabriel P. Lopez[a,c]*

[a]*Center for Biomedical Engineering, The University of New Mexico Albuquerque, NM 87131, USA;* [b]*Department of Biology, The University of New Mexico Albuquerque, NM 87131, USA;* [c]*Department of Chemical and Nuclear Engineering, The University of New Mexico Albuquerque, NM 87131, USA*

(*Received 8 June 2009; final version received 26 September 2009*)

Controlling accumulations of unwanted biofilms requires an understanding of the mechanisms that organisms use to interact with submerged substrata. While the substratum properties influencing biofilm formation are well studied, those that may lead to cellular or biofilm detachment are not. Surface-grafted stimuli-responsive polymers, such as poly (*N*-isopropylacrylamide) (PNIPAAm) release attached cells upon induction of environmentally-triggered phase changes. Altering the physicochemical characteristics of such polymeric systems for systematically studying release, however, can alter the phase transition. The physico-chemical changes of thin films of PNIPAAm grafted from initiator-modified self-assembled monolayers (SAMs) of ω-substituted alkanethiolates on gold can be altered by changing the composition of the underlying SAM, without affecting the overlying polymer. This work demonstrates that the ability to tune such changes in substratum physico-chemistry allows systematic study of attachment and release of bacteria over a large range of water contact angles. Such surfaces show great promise for studying a variety of interactions at the biointerface. Understanding of the source of this tunability will require further studies into the heterogeneity of such films and further investigation of interactions beyond those of water wettability.

Keywords: fouling release; poly (*N*-isopropylacrylamide); *Cobetia marina*; *Staphylococcus epidermidis*; self-assembled monolayers

Introduction

Biofilms are ubiquitous and ancient, if sometimes unwanted, form of microbial life. The basic biological outline of biofilm development has been established and elaborated (O'Toole et al. 2000; Stoodley et al. 2002; Hall-Stoodley et al. 2004). The interfacial interactions between the cells and the supporting substrata are, beyond the points of primary and secondary attachment, less well understood. Removal of unwanted biofilms, or biofouling, requires interruption of the association between the cells and substrata and, therefore, also requires a better understanding of the substratum properties that are important in the maintenance of a biofilm.

Hydrophobicity appears to play a role in maintaining cellular attachment. Prior studies have shown that, although some cells may initially attach well to hydrophobic surface, they are easily removed upon application of low shear forces (Ista et al. 2004). Indeed, hydrophobic and superhydrophobic fouling-release surfaces show great promise for control of biofouling (Yebra et al. 2004; Genzer and Efimenko 2006; Genzer and Marmur 2008). One limitation of low energy fouling-release surfaces is that they often require large shear stresses (Yebra et al. 2004).

A means by which fouling-release can be achieved at relatively low shear stress is by changing the wettability of the surface on which the biofilm is maintained. Environmentally responsive polymers undergo sharp, reversible solubility phase transitions in water as a result of a small change in the environment (eg pH, temperature, redox potential) (Mano 2008). When grafted to a surface, this results in a change in surface wettability (Ista et al. 1999, 2001).

The ability of the temperature responsive polymer, poly (*N*-isopropylacrylamide) (PNIPAAm) to reversibly attach and release bacteria has been demonstrated (Ista et al. 1999, 2001; Cunliffe et al. 2003). These materials have been shown to release not only newly attached bacteria (ie at 2 h) but also fully developed biofilms (ie at 72 h) (Ista et al. 1999).

For release to occur, however, the surface transition must be from one favored for attachment to one disfavored. For example, *Cobetia marina*, which attaches in greater numbers to surfaces with a higher water contact angle (Ista et al. 1996, 2004), attaches

*Corresponding author. Email: gplopez@unm.edu
†Present address: Department of Chemical Engineering, California State University at Long Beach, 1250 Bellflower Blvd, Long Beach, California 90840, USA.

ISSN 0892-7014 print/ISSN 1029-2454 online

DOI: 10.1080/08927010903383455
http://www.informaworld.com

well to PNIPAAm above 32°C, the transition temperature (T_t) of PNIPAAm; when rinsed with solutions below 32°C, *C. marina* is released from the surface (Ista et al. 1999, 2001). The reverse, ie attaching *C. marina* below T_t and rinsing above 32°C, results in no significant release of cells from the PNIPAAm surface (Ista et al. 1999). In contrast, *Staphylococcus epidermidis*, which attaches in greater numbers to surfaces with low water contact angles, attaches and releases reversibly from surface-grafted PNIPAAm only when attached below T_t and rinsed above T_t (Ista et al. 1999). Thus for release to occur, an organism must attach to the surface at a favorable wettability and go through the T_t such that the surface wettability becomes less favorable.

Understanding how and why this process occurs requires systematic investigation over a range of water contact angles. To date, the ability to systematically change the advancing water contact angles (θ_{AW}) of the surfaces has been limited; a change in solubility, and thus, surface contact angle, is achieved by copolymerization of PNIPAAm with other *N*-acyl substituted acrylamides to introduce more hydrophobic or hydrophilic groups (Priest et al. 1987). This process has been exploited in examination of copolymer composition and state of hydrophobicity on attachment of *Salmonella typhimurium* and *Bacillus cereus* (Cunliffe et al. 2003). Although this method produces surfaces that change in θ_{AW}, copolymerization also changes T_t, adding an unintended complexity to data interpretation. While optimizing techniques for grafting PNIPAAm from self-assembled monolayers (SAMs) of ω-substituted alkanethiolates on gold (Ista et al. 2001), it was observed that the θ_{AW} of these surfaces, both above and below T_t, of very thin layers of PNIPAAm was directly related to the composition of the underlying SAM (Mendez et al. 2003). In this article, such surfaces were used to systematically investigate the effect of θ_{AW} and the change in θ_{AW} over the transition ($\Delta\theta_{AW}$) on the attachment and release of *C. marina* and *S. epidermidis*.

Materials and methods

Attachment was studied on two different types of surfaces. The first of these was a series of SAMs without polymer modification. These experiments were done in a flow cell to measure the general response of *S. epidermidis* to changes in surface hydrophobicity. Although it had been observed that *S. epidermidis* attached more readily to hydrophilic than hydrophobic surfaces (Ista et al. 1996, 1999), the effect of systematically changing surface wettability on attachment of this organism had not been examined, as it had for *C. marina* (Ista et al. 2004).

In order to examine attachment and detachment from tunable PNIPAAm surfaces, however, a static immersion method was used. Both unpatterned and patterned surfaces were used for these studies, the latter to increase throughput of the experiments. The apparatus allowed only two slides to be modified at a time, thus patterning the SAMs before modification allowed for generation of several tunable patches on one surface. The patterned slides were examined for similar changes in water contact angle and, when it was found to be the same, these data were combined with those from unpatterned SAMs.

Culture conditions

All media and buffers were prepared in de-ionized water (Barnstead-Thermolyne RoPure/Nanopure system). The final resistivity of the processed water was >18 MΩ cm^{-1}. Marine Broth 2216 (MB, Difco) was prepared according to the manufacturer's instructions. Marine Agar (MA) was prepared by the addition of 1.5% Bacto agar (Difco) to MB. Artificial seawater (ASW) contains 400 mM NaCl, 100 mM $MgSO_4$, 20 mM KCl, 10 mM $CaCl_2$. (Kersters 1992) Modified basic marine medium plus glycerol (MBMMG) contained 0.5 × ASW plus 19 mM NH_4Cl, 0.33 mM K_2HPO_4, 0.1 mM $FeSO_4 \cdot 7H_2O$, 5 mM Trishydroxyaminomethane hydrochloride (pH 7), and 2 mM glycerol (Kersters 1992; Ista et al. 1999).

Nutrient Broth (NB, Difco), was prepared according to the manufacturer's directions. Nutrient agar (NA) was made by the addition of 1.5% Bacto agar to NB. *Staphylococcus* basal medium plus glycerol (SBMG) contained 6 mM $(NH_4)SO_4$, 0.5 mM $MgSO_4 \cdot 7H_2O$, 13.5 mM KCl, 28 mM KH_2PO_4, 72 mM Na_2HPO_4, 1 μg ml^{-1} thiamin; 0.5 μg ml^{-1} biotin; 0.5% Bacto-Peptamin (Difco), and 1 mM glycerol (Ista et al. 1996). Dulbecco's phosphate buffered saline (PBS; Sigma Chemical) was prepared according to the manufacturer's instructions.

Bacterial strains

Cobetia marina (basonym, *Halomonas marina*) (Baumann et al. 1972, 1983; Arahal et al. 2002) ATCC 25374 was revived from the original lyophilate and stored as frozen stock aliquots in MB + 20% glycerol at −70°C. Experimental stock cultures were maintained on MA slants and were stored at 4°C for up to 2 weeks. Prior to inoculation into a chemostat, a single colony from a MB slant was inoculated into 50 ml of MB and grown overnight with shaking at 25°C. A chemostat culture was established by inoculating 3 ml of the overnight culture into MBMMG. The chemostat was maintained at a flow rate of 1 ml min^{-1} (dilution rate,

0.16 h^{-1}) with constant stirring. The concentration of the chemostat culture was $\sim 10^7$ cells ml^{-1}.

S. epidermidis ATCC 14990 was revived in NB from the original lyophilate. Aliquots were stored in NB + 20% glycerol at −70°C. Experimental stock cultures were maintained on NA slants and were stored at 4°C for up to 2 weeks. Prior to inoculation into a chemostat, a single colony was transferred into 50 ml of NB and grown overnight at 37°C with shaking. Five milliliters of this culture were inoculated into 500 SBMG. The flow rate was 1.5 ml min^{-1}, and the dilution rate was 0.16 h^{-1}. The bacterial concentration was $\sim 5 \times 10^7$ cells ml^{-1}.

Self-assembled monolayers

SAMs were prepared on gold films evaporated onto glass microscope slides or coverslips (Bain et al. 1989). The glass supports (VWR Scientific) were cleaned by immersion in a solution prepared by mixing 70% v/v concentrated H_2SO_4 with 30% commercial H_2O_2 (piranha etch) for 20 min to 1 h, thoroughly rinsed in deionized H_2O, and dried under a stream of nitrogen. (Caution: Piranha solution is a powerful oxidizer that can react violently when placed in contact with organics, and should be stored in containers that prevent pressure build-up.) The cleaned samples were placed into the vacuum chamber of a metal evaporator. The system was evacuated to a pressure of 10^{-6} torr. Ten Angstroms of chromium and 300 Å of gold were deposited sequentially on the substrata. Following metallic deposition, the samples were placed into 1 M ethanolic solutions of dodecanethiol (CH_3-thiol, from Aldrich, 96% purity), 12-mercaptodecanol (OH-thiol, from Aldrich, purity 97%) or 12-mercaptododecanoic acid (COOH-thiol, from Aldrich Chemical, purity 95%) or a mixture of two of these alkanethiols. The samples remained in thiol solution overnight at 4°C. Before use, they were rinsed in ethanol and dried under a stream of N_2. The resulting surfaces (ie the SAMs of ω-terminated alkanethiolates) will be referred to as CH_3-SAM, OH-SAM, COOH-SAM, or, in the case of mixtures, COOH/CH_3-SAM or OH/CH_3-SAM.

Patterned SAMs were generated according to a modification of a standard procedure (Tender et al. 1996). A coated copper wire was soldered to the gold of a CH_3-SAM. The region to be ablated was defined by a glass chimney (s-joint) and an o-ring, creating a circular area with radius of 1 cm. The chimney was filled with 0.5 M ethanolic KOH. The cathode was attached to the soldered wire and platinum electrodes for the anode and reference electrode of a potentiostat were inserted into the chimney. A cyclic current was then applied (−1.0 to −1.5 V *vs* Ag/AgCl; 500 mV s^{-1}) to the element for six cycles. Desorption of CH_3-SAM was monitored by cyclic voltammetry. The exposed gold was rinsed with ethanol and deionized water and treated with a 10 mM ethanolic solution of the desired ω-substituted alkanethiol for 20 min. A series of elements could thus be addressed sequentially, resulting in a pattern of several different SAMs upon a single surface. For subsequent PNIPAAm modification, five elements were patterned with varying solution mole fractions of CH_3- and COOH-thiols.

Surface grafting of PNIPAAm was done as described previously (Ista et al. 2001; Mendez et al. 2003). Briefly, COOH-moieties on SAMs were activated by incubation in 10 mM aqueous 2-ethyl-5-phenylisoxazolium-3′-sulfonate (Woodward's reagent K, Aldrich) for 30 min. They were then rinsed with deionized H_2O and placed into a 200 mM aqueous solution of the free-radical initiator, 2,2′azobis(2-amidinopropane) hydrochloride (ABAH, DuPont), and allowed to react for 2 h at room temperature. The initiator-derivatized samples were rinsed in deionized H_2O, dried with liquid nitrogen, and used immediately for polymerization. Recrystallized NIPAAm was dissolved in deionized-H_2O at ∼25% w/v. Initiator-derivatized samples were added and the whole degassed by freeze-thaw three times. The sealed reaction vessel was placed in a preheated water bath. Polymerization was typically carried out for 3 h at 65°C, a time previously determined to yield samples with ellipsometric thickness ≤250 Å, which is required for the tunable phenomenon to occur (Mendez et al. 2003). The NIPAAm solution was removed and the samples washed exhaustively in deionized H_2O. Samples were stored in deionized H_2O at 4°C until analysis. Surface characterization of these samples is described elsewhere (Mendez et al. 2003). Water contact angles were measured below and above T_t as described previously (Ista et al. 1999).

Attachment and detachment of bacteria from tunable surfaces

Attachment and detachment of bacteria on surface grafted tunable PNIPAAm were assessed using either 5×10^6 cells ml^{-1} *C. marina* in ASW or 10^7 cells ml^{-1} *S. epidermidis* in PBS. Prior to introduction of the PNIPAAm surfaces, the cell suspensions were pre-equilibrated at 37°C (*C. marina*) or 25°C (*S. epidermidis*) in glass Petri dishes. PNIPAAm surfaces were placed on the bottom of the Petri dish, test surface up, and incubated in these bacterial suspensions (at the pre-equilibration temperature) for 2 h unstirred. They were then rinsed with deionized H_2O at the equilibration temperature and dried under

a stream of dry N_2. This drying step was found to be necessary in a previous study (Ista et al. 1999) to prevent the artificial detachment of cells due to the release of cells as the surface water came to room temperature.

Phase contrast images of 10 randomly chosen fields of view were captured through a 60× objective (Nikon Labophot) and a digital CCD Camera using Image Tool software. Details of image capture and subsequent analyses have been described elsewhere (Ista et al. 1999). These images provided the estimations of the density of initially attached cells. Cells were detached under shear (estimated shear rate 0.04 Pa) with 60 ml of either 4°C ASW (for *C. marina*) or 37°C PBS (for *S. epidermidis*) delivered from a syringe, rinsed in d-H_2O, and recounted. Each tunable PNIPAAm surface was examined in triplicate, both as a single component sample, and as part of a patterned surface.

Attachment of S. epidermidis *to SAMs*

SAMs prepared on 30 nm gold films coated on 60 × 24 mm coverslips were placed into a flow-cell apparatus (Ista et al. 1996) which was mounted onto the stage of an optical microscope (Diaphot, Nikon) and connected to the outflow of the chemostat. The *S. epidermidis* culture was allowed to flow through the cell at a rate of 1.0 ml min^{-1} for 2 h (shear rate 664 s^{-1}).

Bacterial attachment was monitored through a CCD camera attached to the microscope. The images were fed to a computer using a Data Translations 3155 frame grabber card and Image Tool imaging software. At the end of the attachment time, images of 10 fields of view within 10 mm of the horizontal midline of the slide were captured, the number of attached bacteria counted and the average for each slide determined. At least five replicates were performed for each type of SAM.

Results

Chemical analysis of the SAMs and grafted PNIPAAm used in this study have been described previously (Ista et al. 2001), as was an introduction to the chemistry of tunable PNIPAAm (Mendez et al. 2003). Figure 1 demonstrates how the surface mole fraction of COOH-thiolate ($\chi_{COOH}{}^{surf}$) and advancing water contact angle (θ_{AW}) of the underlying COOH/CH_3 SAM affect the θ_{AW} of films of tunable PNIPAAm taken above and below the polymer T_t. The value of $\chi_{COOH}{}^{surf}$ was estimated using the relative ratios of the oxygen 1s peaks as described previously (Mendez et al. 2003; Ista et al. 2004) for similar self-assembled monolayers. The data in Figure 1 are the combined results of all samples tested for bacterial attachment. Although the absolute value of θ_{AW} measured above and below 32°C changed with the composition of the underlying SAM, the relative difference between the upper and lower θ_{AW} was 13 ± 2°C, similar to values observed for other relatively smooth grafted PNIPAAm surfaces (Ista et al. 1996, 1999). The θ_{AW} of the COOH/CH_3 SAM and the resultant PNIPAAm layer correlate at both 45°C ($R^2 = 0.98$) and 25°C ($R^2 = 0.96$).

Previous studies demonstrated that bacterial release from PNIPAAm occurs when the θ_{AW} is changed from one that favors bacterial attachment to one that disfavors attachment (Ista et al. 1999, 2001). As a first step toward quantifying the effect of $\Delta\theta_{AW}$ on bacterial detachment, it is necessary to quantify the effect of hydrophobicity on bacterial attachment. In a previous study (Ista et al. 2004), the attachment of *C. marina* to two sets of SAMs with differing chemistry was examined, and it was shown that attachment increased linearly as a function of $\cos(\theta_{AW})$.

The effect of the θ_{AW} of mixed COOH/$CH_3{}^-$ and OH/$CH_3{}^-$ SAMs on *C. marina* was previously determined (Ista et al. 2004) and is reproduced in Figure 2A. Attachment of *S. epidermidis* to the same series of mixed SAMs was quantified in the current study and the results are summarized in Figure 2B. Both data sets for *S. epidermidis* show a linear, but inverse relationship between attachment and the θ_{AW}, although the dependence of the relationship between the θ_{AW} and the attachment of cells was less strong on OH-containing SAMs ($R^2 = 0.81$) than on COOH-containing SAMs ($R^2 = 0.99$). In addition, although *S. epidermidis* attachment increased with decreasing θ_{AW}; a significant difference was observed between the slopes of COOH- and OH-containing SAMs.

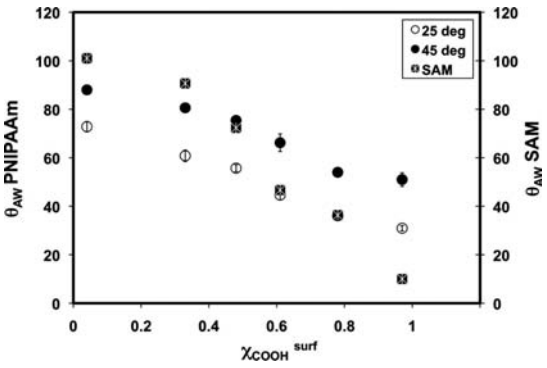

Figure 1. Contact angle of COOH-CH_3-SAMs at room temperature and grafted PNIPAAm at 25 and 45°C as a function mole fraction of COOH-thiolate ($\chi_{COOH}{}^{surf}$) in the underlying SAM.

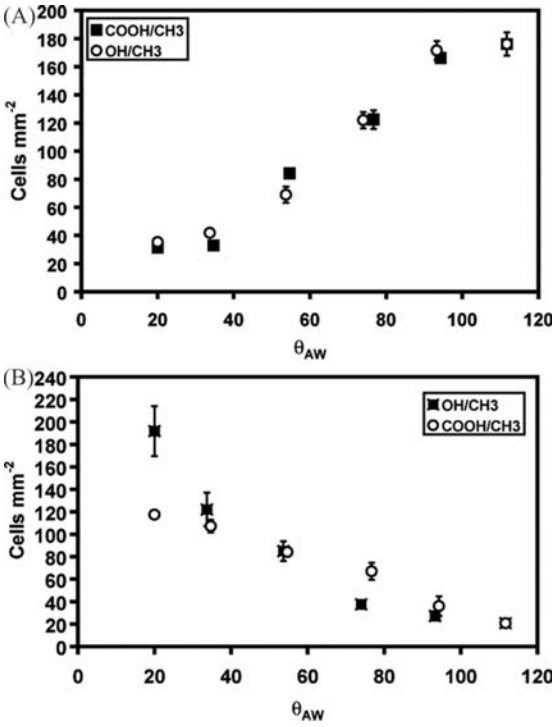

Figure 2. Attachment of (A) *C. marina* (Ista et al. 2004) and (B) *S. epidermidis* as a function of θ_{AW} on mixed monolayer SAMs.

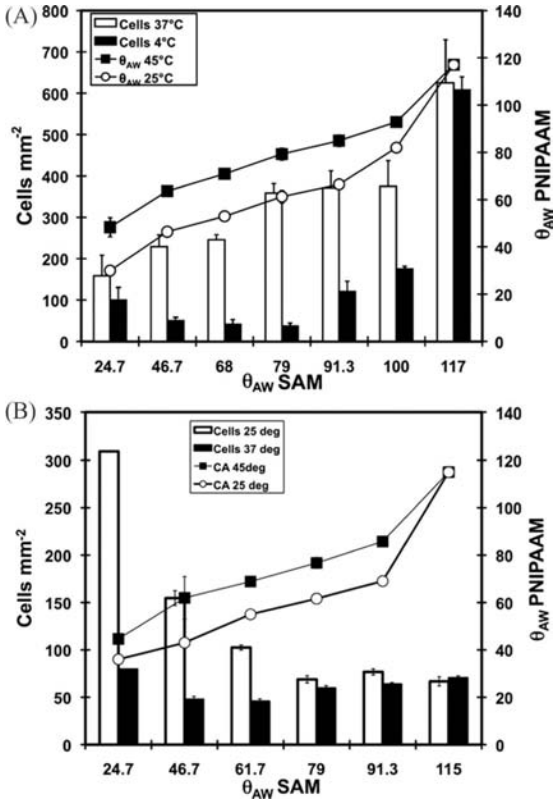

Figure 3. Summary plots of the numbers of cells attached initially and after transition through T_t on (A) *S. epidermidis* and (B) *C. marina* to tunable PNIPAAm.

Figure 3 summarizes the number of cells attached initially and after transition through T_t for *C. marina* (Figure 3A) and *S. epidermidis* (Figure 3B) on tunable PNIPAAm surfaces as a function of θ_{AW} of the underlying $COOH/CH_3$ SAM. These data are coplotted with the θ_{AW} of the polymer above and below T_t. Attachment and release from all tunable surfaces showed the same general trends as observed for both organisms in previous studies with grafted PNIPAAm surfaces (Ista et al. 1999, 2001).

As was the case for pure SAMs (Ista et al. 2004), attachment of *C. marina* to tunable PNIPAAm at 37°C varied positively as a function of the θ_{AW} of PNIPAAm above the T_t and attached more readily to surfaces that were readily hydrophobic. There was a linear relationship between $\cos\theta_{AW}$ and attachment ($R^2 = 0.93$). Attachment of *S. epidermidis* to tunable PNIPAAm below T_t decreased with increasing θ_{AW}, as it did to mixed SAMs, and attached more readily to relatively hydrophilic surfaces. Attachment also varied linearly, albeit negatively, with $\cos\theta_{AW}$ ($R^2 = 0.74$).

The detachment of bacteria as a function of the θ_{AW} of the substratum at the detachment temperature is shown in Figure 4. Detachment of *C. marina* (Figure 4A) from tunable PNIPAAm showed no discernable pattern, but was greatest (89 $\pm$ 1.5%) on PNIPAAm, whose θ_{AW} decreased from 80° to ~61° upon rinsing with 4°C ASW. This value correlates with PNIPAAm grown from a SAM with an intermediate χ_{COOH}^{surf}. Detachment of *S. epidermidis* (B) from tunable PNIPAAm roughly correlated with the θ_{AW} and was greatest (74% $\pm$ 4%) from PNIPAAm as rinsing in 37°C changed the θ_{AW} of the tunable PNIAAm 31° to 51°; this was the PNIPAAm grown on the highest χ_{COOH}^{surf} (0.97). No dependence was observed for organisms on either the change in the θ_{AW} or change in the $\cos\theta_{AW}$.

Discussion

As shown in Figure 1, a series of tunable, surface-grafted PNIPAAm surfaces has been produced, that vary in θ_{AW} at both 25 and 45°C as a function of the chemical composition and the θ_{AW} of the underlying SAM. The nature of the tunable phenomenon is not known, but it has been demonstrated previously that it occurs only when the dry ellipsometric thickness of the

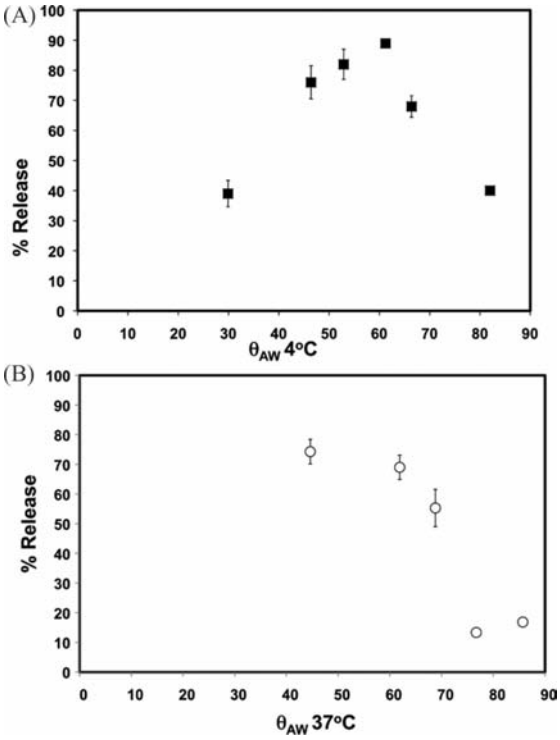

Figure 4. Percentage of (A) *C. marina* (B). *S. epidermidis* removed as a function of θ_{AW} of the surface at the release temperature.

samples is below 25 nm (Mendez et al. 2003), suggesting some influence of the underlying SAM. Possibilities presented previously include heterogeneity of the film covering.

The relationship between the structure of the grafted PNIPAAm and the underlying SAM is, at this point, unclear. It is hypothesized that, as the amount of COOH on the surface increases, so does the subsequent amount of initiator. A previous study (Mendez et al. 2003) suggested that approximately 1/3 of the COOH moieties present on a surface were modified with initiator. This should mean that, as more COOH is present, the number of PNIPAAm chains should also increase. The surface density of the initiator, however, may also have an effect on the polymer length, as more initiator means more solution free radicals, and, hence, more opportunity for early chain termination during polymerization. Since the tunable phenomenon only happens when the dry ellipsometric thickness of the polymer is <25 nm, however, it is fairly certain that none of the samples described herein constitutes polymer brushes.

Data are presented on the attachment of *S. epidermidis* to SAMs of systematically increasing θ_{AW} and demonstrate that, although the attachment of these cells varied in a negative linear fashion with $\cos\theta_{AW}$, there was a dependence on the composition of the hydrophilic component of the mixed SAMs, suggesting that factors other than hydrophobicity alone are playing a role in attachment of this organism. Previously, a similar dependence on the hydrophilic component of similar SAMs was observed on the attachment of zoospores of *Ulva linza* (Ista et al. 2004). This observation supports the assertion made by some in the biofilm community that parameters beyond hydrophobicity should be considered, including hydrogen bonding, Lewis acid-base and/or electrostatic interactions (Sharma and Rao 2002; Palmer et al. 2007).

Attachment of cells to tunable surfaces showed trends similar to those observed in this and previous studies (Ista et al. 1996). *S. epidermidis* attached most to surfaces that are relatively hydrophilic, whereas *C. marina* attached to those surfaces that are relatively hydrophobic. Attachment of *S. epidermidis* to tunable PNIPAAm showed a weak correlation ($R^2 = 0.74$) to the θ_{AW} of samples at the attachment temperature (25°C) and a similarly weak ($R^2 = 0.74$) correlation to $\cos\theta_{AW}$. In contrast, attachment of *C. marina* to tunable PNIPAAm at 37°C, correlated with both the θ_{AW} and $\cos\theta_{AW}$ ($R^2 = 0.93$ for both). In addition, the trendlines for attachment to both SAMs and tunable PNIPAAm as a function of $\cos\theta_{AW}$ were parallel, even though the flow regimes were quite different between static immersion and flow cell studies. These observations are not surprising, given the expected conformation of PNIPAAm above and below T_t. Above 32°C, the polymer will be hydrated and extended (Balamurugan et al. 2003), thus having more exposure and influence on attaching cells than when the polymer is below T_t, when the polymer is collapsed and the effect of the underlying COOH/CH_3^- SAM can be more pronounced.

Upon transition through T_t, both *S. epidermidis* and *C. marina* were removed from tunable surfaces. The number of remaining *S. epidermidis* cells correlated with the wettability of the tunable PNIPAAm after the transition. In contrast, *C. marina* showed no such dependence, showing instead a weak correlation with the $\Delta\cos\theta_{AW}$ through the transition. The best release was obtained at intermediate, but slightly hydrophobic values of θ_{AW}. This observation again underscores that attachment at 37°C, when the grafted PNIPAAm is collapsed, was driven mainly by interactions with the underlying SAM.

Just as observed for the attachment of *S. epidermidis* to SAMs, there was no strong dependence of release of *C. marina* as a function of the θ_{AW} of the tunable PNIPAAm surface and only a moderate

statistical correlation ($R^2 = 0.78$) for *S. epidermidis*. Furthermore, the patterns for the two bacteria were quite dissimilar. Clearly, a change in hydrophobicity of the surfaces alone cannot account for either of these results. Recent studies suggest that the attachment of bacteria to surfaces can be accurately modeled by also considering the contributions of Lewis-acid/base interactions to the surface energy of the attachment substratum (Bellon-Fontaine et al. 1996; Liu et al. 2007). This is of particular importance in the present system because both COO^- and PNIPAAm itself should be expected to undergo such interactions, particularly in the form of hydrogen bonding. Indeed, recent studies suggest a particular role for carboxyl group hydrogen bonding in the T_t behavior of PNIPAAm (Ahmed et al. 2009). It is important to note that the bacteria will encounter very different hydrogen bonding milieus on PNIPAAm above and below the T_t. Above T_t, the carboxyl groups hydrogen-bond with water and, presumably, are free to enter into such bonds with attaching bacteria (Ahmed et al. 2009). On the other hand, on a collapsed PNIPAAm surface, these bonds are unavailable to water or other compounds. This observation increases the complexity of understanding PNIPAAm/bacterial interactions.

These results demonstrate the utility of tunable PNIPAAm for examination of dynamic attachment and detachment of bacteria, on surfaces with a stable T_t, systematically varying the surface water wettability (and perhaps other properties). The results from the *C. marina* data suggest that tunable PNIPAAm provides a means by which cells can be removed at different points in biofilm development in order to assay physiological changes in attached (or attaching cells). One caveat to this observation may be that this system will only work for those strains of bacteria that favor attachment to hydrophobic surfaces. It would be interesting, however, to see whether the strong dependence on the composition of the underlying SAM for attachment could be used for those cells that attach better in response to hydrophilic surfaces. SAMs with a hydrophilic diluent for the COOH moieties might promote attachment in large enough numbers to compensate for the small number of cells released by going from a disfavored state to a favored state of interfacial energy. It is also possible that cells could be driven off from such SAMs due to the mechanical action of the expanding PNIPAAm, although thin layers of PNIPAAm grafted to other surfaces showed no such mechanically-driven release (Ista et al. 1999). A combination of PNIPAAm made tunable by both the grafting technique and copolymerization might well be the best means for similar studies with hydrophilic organisms.

Acknowledgement

The authors thank the Office of Naval Research for supporting this project through grants N00014-08-1-0741 and N00014-05-1-0743.

References

Ahmed Z, Gooding EA, Pimenov KV, Wang LL, Asher SA. 2009. UV resonance Raman determination of molecular mechanism of poly(*N*-isopropylacrylamide) volume phase transition. J Phys Chem B 113:4248–4256.

Arahal DL, Castillo AM, Ludwig W, Schliefer KH, Ventosa A. 2002. Proposal of *Cobetia marina* gen. nov, comb. nov., within the family Halomonadaceae, to include the species *Halomonas marina*. Syst Appl Microbiol 25:207–211.

Bain CD, Troughton EB, Tao Y-T, Evall J, Whitesides GM. 1989. Formation of monolayer films by the spontaneous assembly of organic thiols from solution onto gold. J Am Chem Soc 111:321–335.

Balamurugan S, Mendez S, Balamurugan SS, O'Brien MJ, Lopez GP. 2003. Thermal response of poly(*N*-isopropylacrylamide) brushes probed by surface plasmon resonance. Langmuir 19:2545–2549.

Baumann L, Bowditch RD, Baumann P. 1983. Description of *Deleya* gen. nov. created to accommodate the marine species of *Alcaligenes aestus, A. pacificus, A. cupidis, A.venustus*, and *Pseudomonas marina*. Int J Syst Bacteriol 33:793–802.

Baumann L, Baumann P, Mandel M, Allen RD. 1972. Taxonomy of aerobic marine eubacteria. J Bacteriol 110:402–429.

Bellon-Fontaine M-N, Rault J, van Oss CJ. 1996. Microbial adhesion to solvents: a novel method to determine the electon–donor/electron-acceptor or Lewis acid–base properties of microbial cells. Colloids Surf B: Biointerfaces 7:47–53.

Cunliffe D, de las Heras Alarcon C, Peters V, Smith JR, Alexander A. 2003. Thermoresponsive surface-grafted poly(*N*-isopropylacrylamide) copolymers:effect of phase transitions on protein and bacterial attachment. Langmuir 19:2888–2899.

Genzer J, Efimenko K. 2006. Recent developments in superhydrophobic surfaces and their relevance to marine fouling: a review. Biofouling 22:339–360.

Genzer J, Marmur A. 2008. Biological and synthetic self-cleaning surfaces. Mater Res Soc (MRS) Bull 33:742–746.

Hall-Stoodley L, Costerton JW, Stoodley P. 2004. Bacterial biofilms: from the natural environment to infectious diseases. Nat Rev Microbiol 2:95–108.

Ista LK, Pérez-Luna VH, López GP. 1999. Surface-grafted, enivironmentally responsive polymers for biofilm release. Appl Environ Microbiol 65:1603–1609.

Ista LK, Fan H, Baca O, López GP. 1996. Attachment of bacteria to model solid surfaces: oligo(ethylene glycol) surfaces inhibit bacterial attachment. FEMS Microb Lett 142:59–63.

Ista LK, Mendez S, Perez-Luna VH, Lopez GP. 2001. Synthesis of poly(*N*-isopropylacrylamide) on initiator-modified self-assembled monolayers. Langmuir 17:2552–2555.

Ista LK, Callow ME, Finlay JA, Coleman SE, Nolasco AC, Callow JA, Lopez GP. 2004. Effect of substratum surface chemistry and surface energy on attachment of marine bacteria and algal spores. Appl Environ Microbiol 70:4151–4157.

Kersters K. 1992. The genus *Deleya*. In: Balows A, Trüper HG, Dworkin M, Harder W, Schliefer KH, editors. The prokaryotes. New York: Springer-Verlag. p. 3189–3197.

Liu YT, Strauss J, Camesano TA. 2007. Thermodynamic investigation of *Staphylococcus epidermidis* interactions with protein-coated substrata. Langmuir 23:7134–7142.

Mano JF. 2008. Stimuli-responsive polymeric systems for biomedical applications. Adv Engineer Mater 10:515–527.

Mendez S, Ista LK, Lopez GP. 2003. Tuning wettability with smart polymers grafted on mixed self-assembled monolayers. Langmuir 19:8115–8116.

O'Toole G, Kaplan HB, Kolter R. 2000. Biofilm formation as bacterial development. Ann Rev Microbiol 54:49–79.

Palmer J, Flint S, Brooks J. 2007. Bacterial cell attachment, the beginning of a biofilm. J Ind Microbiol Biotechnol 34:577–588.

Priest JH, Murray SA, Nelson RJ, Hoffman AS. 1987. Lower critical solution temperatures of aqueous copolymers of *N*-isopropylacrylamide and other *N*-substituted acrylamides. ACS Symposium Series 350:255–264.

Sharma PK, Rao KH. 2002. Analysis of different approaches for evaluation of surface energy of microbial cells by contact angle goniometry. Adv Coll Interface Sci 98:341–463.

Stoodley P, Sauer K, Davies DG, Costerton JW. 2002. Biofilms as complex differentiated communities. Ann Rev Microbiol 56:185–209.

Tender LM, Worley RL, Fan HY, López GP. 1996. Electrochemical patterning of self-assembled monolayers onto microscopic arrays of gold electrodes fabricated by laser-ablation. Langmuir 12:5515–5518.

Yebra DM, Kiil S, Dam-Johansen K. 2004. Antifouling technology – past, present and future steps towards efficient and environmentally friendly antifouling coatings. Prog Org Coat 50:75–104.

Chapter 4: Experimental and Theoretical Examination of Surface Energy and Adhesion of Nitrifying and Heterotrophic Bacteria using Self Assembled Monolayers

Mohiuddin Md Taimur Khan[1], Linnea K Ista [2,3], Gabriel P López[3,4] and Andrew J. Schuler[1]

[1]Department of Civil Engineering

[2]Department of Biology

[3]Center for Biomedical Engineering

The Univestiry of New Mexico

Albuquerque, NM 87131

[4]Department of Biomedical Engineering

Duke University,

Durham, NC 27708

My contribution to this work: I designed the experiments and promoted the use of the van Oss Chaudhury and Good model to interpret. I showed Dr. Khan how to make and characterize the SAMs used in this experiment and also shared my flow cell design with him. We were meant to be co-first authors on this paper, but ES&T does not allow this designation.

Environimental Science and Technology, 2011, **54**: 1055-1060

Environ. Sci. Technol. **2011,** *45,* 1055–1060

Experimental and Theoretical Examination of Surface Energy and Adhesion of Nitrifying and Heterotrophic Bacteria Using Self-Assembled Monolayers

MOHIUDDIN MD. TAIMUR KHAN,[†,‡] LINNEA K. ISTA,[§,∥] GABRIEL P. LOPEZ,[§,⊥] AND ANDREW J. SCHULER*[,†]

Department of Civil Engineering, MSC01 1070, University of New Mexico, Albuquerque, New Mexico 87131-0001; Center for Molecular Discovery and Translational Technology, MSC08 4640, University of New Mexico, Albuquerque, New Mexico 87131-0001; Center for Biomedical Engineering, University of New Mexico, Albuquerque, New Mexico 87131-0001; Department of Biology, University of New Mexico, Albuquerque, New Mexico 87131-0001; and Department of Biomedical Engineering, Pratt School of Engineering, P.O. Box 90281, Duke University, Durham, North Carolina 27708-0281

Received April 28, 2010. Revised manuscript received November 7, 2010. Accepted November 18, 2010.

Biofilm-based systems, including integrated fixed-film activated sludge and moving bed bioreactors, are becoming increasingly popular for wastewater treatment, often with the goal of improving nitrification through the enrichment of ammonia and nitrite oxidizing bacteria. We have previously demonstrated the utility of self-assembled monolayers (SAMs) as tools for studying the initial attachment of bacteria to substrata systematically varying in physicochemical properties. In this work, we expanded these studies to bacteria of importance in wastewater treatment systems and we demonstrated attachment rates were better correlated with surface energy than with wettability (water contact angle). Toward the long-term goal of improving wastewater treatment performance through the strategic design of attachment substrata, the attachment rates of two autotrophic ammonia-oxidizing bacteria (*Nitrosomonas europaea* and *Nitrosospira multiformis*) and a heterotroph (*Escherichia coli*) were evaluated using SAMs with a range of wettabilities, surface energies, and functional properties (methyl, hydroxyl, carboxyl, trimethylamine, and amine terminated). Cell attachment rates were somewhat correlated with the water contact angles of the SAMs with polar terminal groups (hydroxyl, carboxyl, trimethylamine, and amine). Including all SAM surfaces, a better correlation was found for all bacteria between attachment rates and surface free energy, as determined using the Lewis Acid−Base approach. The ammonia-oxidizers had higher adhesion rates on the SAMs with higher surface energies than did the heterotroph. This work demonstrated the successful application of SAMs to determine the attachment surface preferences of bacteria important to wastewater treatment, and it provides guidance for a new area of research aimed at improving treatment performance through rational attachment surface design.

Introduction

Activated sludge, a routinely used biotechnology for domestic wastewater treatment, consists of suspended (planktonic) growth bioreactors, followed by sedimentation tanks and recycling of settled biomass to maintain high rates of biological activity in the bioreactors (*1*). Activated sludge systems commonly include nitrification, in which ammonia removal is achieved by oxidation to nitrite and then to nitrate by ammonia oxidizing bacteria (AOB) and nitrite oxidizing bacteria (NOB), respectively. Because these autotrophs are slow growing relative to the heterotrophic bacteria primarily responsible for organic carbon removal, maintaining their activity often dictates operational parameters such as the solids residence time in activated sludge systems (*2*−*5*).

Biofilm-based systems are becoming increasingly popular for domestic wastewater treatment, including integrated fixed-film activated sludge (IFAS) systems (*6*). IFAS systems are characterized by the addition of suspended or fixed-in-place plastic media to activated sludge bioreactors, which provide surfaces for biofilm growth. They have been demonstrated to enrich for nitrifying bacteria populations in the attached (biofilm) phase, which is presumably linked to long biofilm solids residence time relative to suspended biomass (*7*). It has been demonstrated that AOB pure cultures grown in biofilms have higher affinity for ammonium and show quicker recovery after ammonium starvation than that of planktonic cells (*8, 9*). Moving bed bioreactors (MBBRs) are similar to IFAS, but they do not include a suspended biomass phase.

The initial cell attachment to a surface (the initial stage of biofilm formation (*10*)) can play a determining role in later phase biofilm characteristics (*11, 12*). The physicochemical properties of bacterial cells and attachment surfaces strongly influence initial cell adhesion rates (*13*−*17*). There has been little published research addressing attachment surface chemistry effects on biofilms relevant to nitrification in wastewater treatment. It has been demonstrated that a relatively hydrophilic attachment surface (cellulose cross-linked with polyacrylpolyamide epichlorohydrine) provided higher rates of nitrification per volume than did more hydrophobic attachment surfaces (such as rubber) after the surfaces were cultured with nitrifying bacteria (*18*). However, surface area/volume ratios were not reported and may have affected results.

Bacterial adhesion is dependent on nonspecific and specific interactions. Nonspecific interactions include Lifshitz-van der Waals (apolar) forces, Lewis acid−base (polar) interactions, and electrostatic interactions (*19*). Specific interactions exist between ligand−receptor pairs and are usually stronger than nonspecific interactions across small distances, but nonspecific interactions can control whether bacteria come close enough to a surface for the specific interactions to become operative (*16, 20*). Surface energy includes the combined contributions of Lifshitz-van der Waals and polar Lewis acid−base forces.

Self-assembled monolayers (SAMs) of ω-substituted alkanethiolates on gold have proven to be useful tools in the

* Corresponding author phone: (505) 277-4556; fax: (505) 277-1988; e-mail: schuler@unm.edu.
† Department of Civil Engineering, University of New Mexico.
‡ Center for Molecular Discovery and Translational Technology, University of New Mexico.
§ Center for Biomedical Engineering, University of New Mexico.
∥ Department of Biology, University of New Mexico.
⊥ Department of Biomedical Engineering, Pratt School of Engineering.

10.1021/es101389u
Published on Web 12/28/2010

systematic study of microbial attachment (*21*−*23*). Such SAMs, depicted in Figure S1of the Supporting Information, SI, result in model surfaces that exhibit well-defined surface chemistry, elastic modulus and low surface roughness (*24, 25*). Selection of different ω-terminal functional groups, either singly or as a mixture, has been used extensively to produce surfaces that vary systematically in wettability and surface energy (*15, 16, 22, 23*).

It was hypothesized that surface chemistry affects the adhesion of key species for nitrification in wastewater. The objectives of this work were to determine whether surface energy is an important factor governing attachment of nitrifying bacteria of interest in wastewater treatment, and to determine whether use of high or low surface energy surfaces has the potential to select for nitrifying bacteria over heterotrophs. The approach was to study the attachment of pure bacterial strains of interest to chemically well-defined surfaces using SAMs. The potential long-term application of this research is to develop new media for use in IFAS and MBBR systems to improve rates of nitrification, and potentially other process functions.

Experimental Methods

Bacterial Strains and Cultures. The Gram-negative autotrophic AOB *Nitrosomonas europaea* (ATCC 25978) and *Nitrosospira multiformis* (ATCC 25196), and the Gram-negative heterotroph *Escherichia coli* (environmental isolate obtained from the Department of Microbiology, Montana State University (*26*)) were used in this work. *N. europaea* and *N. multiformis* were cultured to late log phase in ATCC 2265 and ATCC 929 media, respectively, per instructions provided with the stock cultures. *E. coli* was grown on Luria−Bertani (LB) agar (Fisher Scientific, Palatine, IL) at 37 °C for 20 h. Single colonies from the LB agar streak plates were transferred to a 50-mL culture tubes containing approximately 10-mL of LB broth (Fisher Scientific, Palatine, IL). The cultures in LB broth were incubated on a shaker at 180 rpm and 37 °C for 18 h and were grown to late log phase at a concentration of $\sim 10^9$ CFU/mL measured by serial dilution plate counting on LB agar plates. The AOB cell numbers per unit volume were enumerated using a hemocytometer (Double Neubauer, Hausser Scientific) and digital microscopy (DP7, Olympus America, Inc., PA). All cultures were diluted to $\sim 10^3$ cells/mL in their respective growth media for use in the attachment experiments. The pH of all cultures was 7.5−8.0.

SAM Surfaces. SAM surfaces were prepared as previously described (*17, 25, 27*). Briefly, glass microscope coverslips (24 × 60 mm, #1, VWR, USA) were cleaned by immersion in 70% (v/v) concentrated H_2SO_4 with 30% industrial grade H_2O_2 (piranha solution) for 2 h. The cleaned samples were placed into the vacuum chamber of a metal evaporator. The system was evacuated to a pressure of 10^{-6} Torr. A 30-Å portion of chromium and 300 Å of gold were deposited sequentially on the substrata. Following metallic deposition, the samples were placed into an ethanol solution containing 1 mM $HS(CH_2)_{11}CH_3$ (referred to hereafter as CH_3-thiol; Aldrich Chemical, USA); $HS(CH_2)_{10}COOH$ (COOH-thiol; Aldrich Chemical, USA); $HS(CH_2)_{11}OH$ (OH-thiol; Aldrich Chemical, USA); $HS(CH_2)_{11}NH_3Cl^-$ (amine or NH_2-thiol; Asemblon, Inc., USA); and $HS(CH_2)_{11}NMe_3$ (trimethyl amine or NMe_3-thiol; ProChimia Surfaces Sp., Poland). The COOH, NH_2, and NMe_3 SAMs were submersed in a glass vial containing pure ethanol (200 proof HPLC/spectrophotometric grade, Sigma-Aldrich, USA) and sonicated for 1.5 min in a water bath according to protocols recommended by the supplier (Asemblon, Inc., USA). The pH of the ethanolic solution during sonication was adjusted to 2 for the COOH-SAM and it was 12 for the NH_2 and NMe_3-SAMs. All SAMs were rinsed in ethanol and dried under a stream of N_2 gas prior to installation in the flow cell. The COOH and OH SAMs are considered to be negatively charged (*28, 29*), the NH_2 and NMe_3 SAMs positively charged (*28*), and the CH_3 SAM has no charge (*28*).

Flow Cell and Attachment Experiments. Flow cell studies were conducted using methods and apparatus described previously (*22, 27*). The flow cell is shown in Figure S2 of the SI. After each SAM was placed in the flow cell, a diluted suspension of bacterial culture was pumped continuously through the cell at 1 mL/min for 120 min maintaining the hydraulic residence time (HRT) at 0.1 min. The culture was kept at room temperature (20−25 °C) and was well mixed by a stirrer during injection into the flow cell. Images were obtained in situ using phase contrast microscopy at 400× magnification with a digital camera (DP7, Olympus America, Inc., PA). The microscope transmission light was on only while capturing images at 20 min intervals during each experiment. Four to six images at randomly selected locations were captured for cell counting using Microsuite software (Olympus), which was determined to be sufficient to provide statistically significant differences between samples. This procedure was repeated for the five SAM surfaces and for each of the three bacterial strains.

Contact Angle Measurements. The contact angles for bacteria and substrates were determined for three probe liquids with a range of polarities, including ultrapure water, diiodomethane (99%, Sigma-Aldrich, USA), and formamide (>99.5%, Sigma-Aldrich, USA). Measurements were made at room temperature and ambient humidity using the sessile drop technique with a goniometer (Ramé-Hart Instrument Co., Model No. 400-22-300 with DROPimage Standard, NJ) (*30*). The deposition of 1.5 μL droplets on each substrate was recorded in a video and analyzed to obtain the contact angles. Each measurement was made on at least 5 droplets at different locations on each SAM surface for each of the three liquids.

Contact angles for bacteria were measured by the method described by Liu et al. (*31*). Pure cultures of *E. coli* (3 mL) at $\sim 10^9$ CFU/mL; *N. europaea* (5 mL) at $\sim 10^6$ cells/mL and *N. multiformis* (5 mL) at $\sim 10^6$ cells/mL (after washing) were filtered onto separate 25 mm diameter, 0.45 μm pore cellulose acetate membrane filters (GE Osmonics, MN) using negative pressure so that (5 to 10) × 10^6 cells were evenly deposited on each filter, which was reported to provide a layer of bacteria approximately 50 to 90 cells thick covering the filter membrane (*31*). The appropriate drying time for evaporation of the loosely held moisture associated with the bacteria, without dehydrating the cells themselves, was determined by measuring the water contact angle as a function of time (*31*), whereby the time required for the contact angle measurements to reach a plateau was interpreted to indicate the time for removal of exterior moisture. On the basis of these measurements, drying times of 40, 30, and 32 min for *E. coli*, *N. europaea*, and *N. multiformis*, respectively, were used for contact angle measurements. Each measurement was made on at least 5 droplets at different locations on each bacterial surface for each of the three probe liquids, which was used to calculate standard deviations. These measurements were repeated on two of each bacterial and SAM surfaces.

Surface Energy Calculations. The surface energy of each SAM and bacterial surface was calculated from the measured contact angles using the approach developed previously by van Oss and co-workers (*19, 32, 33*), and summarized by Liu et al. (*31*). Briefly, the total surface energy (γ^{total}) was calculated as the sum of the apolar (or Lifshitz-van der Waals; LW), and the polar (or Lewis acid−base; AB) components of the surface energy:

$$\gamma^{total} = \gamma^{LW} + \gamma^{AB} \quad (1)$$

The acid−base component of the surface energy (γ^{AB}) is the geometric mean of the electron-donor (γ^-) and electron-acceptor (γ^+) parameters for the applied probe liquid or the substrata, given by the following:

$$\gamma^{AB} = 2 \cdot \sqrt{\gamma^+ \cdot \gamma^-} \quad (2)$$

The relationships between the three components of the surface energy (i.e., γ^{LW}, γ^+, and γ^-) of a solid surface and the known surface energy components of the probe liquids can be calculated using the Young−Dupré equation:

$$\gamma_L(\cos\theta_L + 1) = 2 \cdot \sqrt{\gamma_x^{LW} \cdot \gamma_L^{LW}} + 2 \cdot \sqrt{\gamma_x^+ \cdot \gamma_L^-} + 2 \cdot \sqrt{\gamma_x^- \cdot \gamma_L^+} \quad (3)$$

where γ_L is the liquid−vapor surface free energies, θ_L is the probe liquid−solid equilibrium contact angle, the subscript x refers to the substrates probed (SAM surface or bacterial lawn), and the subscript L refers to the probe liquid. Reference values for the surface energies of the probe liquids (γ_L, γ_L^+, and γ_L^-) were taken from Good and van Oss (*34*) and they were confirmed with the supplier. Applying eq 3 and contact angle measurements for each of the three probe liquids, the three unknown surface energy components (γ_x^{LW}, γ_x^+, and γ_x^-) of each surface were calculated using eq 4:

$$\begin{bmatrix} \gamma_x^{LW} \\ \gamma_x^+ \\ \gamma_x^- \end{bmatrix} = \left\{ \left[2 \cdot \begin{pmatrix} \sqrt{\gamma_W^{LW}}\sqrt{\gamma_W^-} & \sqrt{\gamma_W^+} \\ \sqrt{\gamma_D^{LW}}\sqrt{\gamma_D^-} & \sqrt{\gamma_D^+} \\ \sqrt{\gamma_F^{LW}}\sqrt{\gamma_F^-} & \sqrt{\gamma_F^+} \end{pmatrix} \right]^{-1} \cdot \begin{pmatrix} \gamma_W.[\cos(\theta_W) + 1] \\ \gamma_D.[\cos(\theta_D) + 1] \\ \gamma_F.[\cos(\theta_F) + 1] \end{pmatrix} \right\}^2 \quad (4)$$

where the subscript W denotes water, D denotes diiodomethane, and F denotes formamide.

Results and Discussion

SAM Surface Properties. The contact angles for each of the SAM surfaces and bacterial strains, as well as the calculated surface energies and surface energy parameters, are shown in Table 1. As noted, the terminal SAM functional group determines the SAM surface chemistry and is known to have a large influence on bacterial attachment (*17, 32*). As the only nonpolar surface, the CH_3 SAM was the most hydrophilic with $\theta_w = 108 \pm 1°$, which was similar to previously reported values of 107° (*27*) and 111−114° (*25*). The CH_3 SAM total surface energy was the lowest of all surfaces ($\gamma^{total} = 16.10 \pm 0.62$ mJ/m^2), and it was mostly comprised of the Lifshitz-van der Waals component ($\gamma^{LW} = 15.60 \pm 0.83$ mJ/m^2).

The other SAM surfaces (NH_2, NMe_3, COOH, and OH) had polar terminal groups, and the acid−base surface energy (γ^{AB}) was a relatively large component of the total surface energy (γ^{tot}) for these surfaces compared to CH_3 (Table 1). The electron-donor (Lewis basic) components (γ^-) of their surface energies were much higher than the electron-acceptor (Lewis acidic) components (γ^+). The polar SAM surfaces had similar γ^{tot} values, although NH_2 and NMe_3^+ were more Lewis acidic and less Lewis basic than the others. The NH_2 surface demonstrated intermediate wettability ($\theta_w = 40 \pm 1°$), which was similar to a previous report ($\theta_w = 44 \pm 3°$) (*35*). This surface had the highest surface energy ($\gamma^{total} = 56.80 \pm 0.08$ mJ/m^2). The θ_w values of the NMe_3, COOH, and OH SAMs were similar to each other, and they were near the wettable range (<20°) (*25*). The θ_w of the OH SAM was 22 ± 1°, which was higher than some previous reports (<10°) (*36, 37*), but was similar to the value of 22° reported by others (*38, 39*).

Bacterial Surface Properties. Contact angle data and estimated surface energetic components for bacteria are also shown in Table 1. The *E. coli* surface θ_W value (67 ± 1°) was consistent with the values reported by Liu et al. (*20*) (56 to 68°) for several strains of *E. coli*. The θ_W values for the AOB were both less than that of *E. coli*. and their total surface energies were higher than that of *E. coli*. The Lewis basic components (γ^-) of the surface energy for all three bacteria were higher than the Lewis acidic components (γ^+), as was found for the SAM surfaces, which may indicate that these bacteria have either a strongly monopolar surface or that they favor Lewis base properties (*40*). van Oss and colleagues (*33, 40*) reported that monopolar surfaces had much higher electron donor properties than electron acceptor properties and showed strong interactions with bipolar materials (for example, water as a polar liquid). *E. coli* had the highest polar component (highest γ^{AB}), was the most Lewis acidic (highest γ^+), and had the lowest surface energy of the three bacteria. *N. europaea* was most Lewis basic (highest γ^-) and had the highest total surface energy (Table 1). The γ^{total} of the bacteria tested in this study followed the inverse trend of their respective θ_W values, but this was not strictly true for the SAM surfaces due to the inclusion of the nonpolar CH_3 SAM.

The Lifshitz-van der Waals (nonpolar) components of the surface energies (γ^{LW}) of biopolymers have been reported to be generally within 10% of 40 mJ/m^2 (*33*). Since the bacterial cell surfaces are composed of biopolymers such as peptidoglycan, phospholipids, and lipopolysaccharides, bacterial cells can be expected to have γ^{LW} values in this range (*41*). This was consistent with the γ^{LW} measured for the AOB in this study; however, the *E. coli* γ^{LW} value (27.00 ± 0.36 mJ/m^2) was somewhat below this range. Liu et al. (*31*) also reported a relatively low bacterial γ^{LW} value 31.9 ± 1.3 mJ/m^2 (*Staphylococcus epidermidis*). The reason for lower γ^{LW} values for *E. coli* relative to previous research (*41*) is not known. Little research has been performed on the effects of bacterial states and growth conditions on bacterial surface properties, and such factors may have contributed to the somewhat lower values found for *E. coli* in this study.

Bacterial Adhesion. Results from flow cell adhesion tests are shown in Figure 1 (for *N. europaea*) and in Figures S3 and S4 of the SI (for *N. multiformis* and *E. coli*). The numbers of attached cells consistently increased more or less linearly

TABLE 1. Contact Angles (θ) and Surface Free Energy (γ) Components of the Five SAMs and Three Bacteria Analyzed in This Work[a]

cells and SAMs	contact angle (degrees)			surface free energy components (mJ/m^2)				
	θ_W	θ_D	θ_F	γ^{LW}	γ^+	γ^-	γ^{AB}	γ^{total}
SAM surfaces								
NH_2	40 ±1	25 ±1	17 ±1	46.10 ±0.05	0.81 ±0.02	30.60 ±0.33	9.90 ±0.09	56.80 ±0.08
NMe_3	22 ±1	27 ±1	10 ±0	45.10 ±0.05	0.62 ±0.01	47.10 ±0.01	10.80 ±0.05	55.90 ±0.01
COOH	23 ±1	33 ±0	21 ±1	42.80 ±0.04	0.40 ±0.01	51.30 ±0.18	9.10 ±0.06	51.90 ±0.03
OH	22 ±1	27 ±1	24 ±1	45.30 ±0.32	0.11 ±0.02	53.30 ±0.37	4.80 ±0.38	50.20 ±0.14
CH_3	108 ±1	83 ±2	92 ±2	15.60 ±0.83	0.06 ±0.06	1.00 ±0.12	0.52 ±0.22	16.10 ±0.62
bacterial strains								
N. europaea	56 ±3	46 ±0	49 ±1	37.20 ±0.07	0.60 ±0.07	29.20 ±4.3	8.37 ±0.92	45.57 ±0.92
N. multiformis	61 ±3	45 ±2	47 ±2	36.60 ±0.83	0.37 ±0.24	19.40 ±3.90	5.40 ±1.30	42.00 ±1.20
E. coli	67 ±1	62 ±2	41 ±2	27.00 ±0.36	4.50 ±0.30	9.00 ±0.48	12.70 ±0.27	39.70 ±0.25

[a] The subscripts W, D, and F denote water, diiodomethane, and formamide, respectively. The error values represent ± one standard deviation calculated from at least five measurements on each of two surfaces.

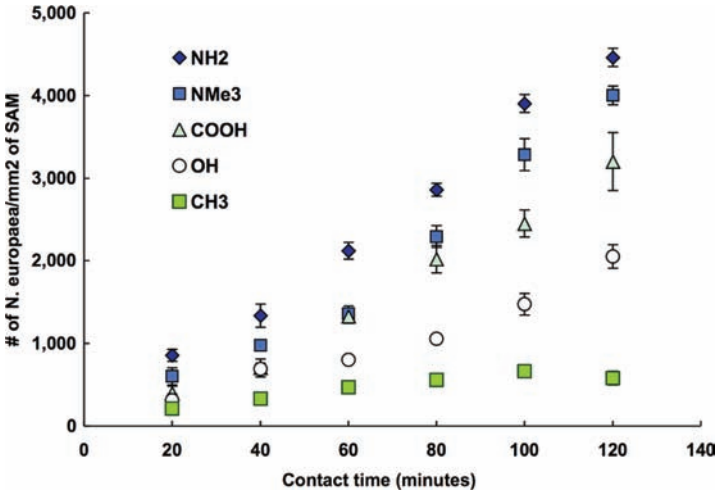

FIGURE 1. Example flow cell results. The numbers of attached *N. europaea* per square millimeter of five SAM surfaces during flow cell experiments. Each data point represents the average of at least four measurements. Error bars are ± one standard deviation in all figures. Some error bars are smaller than symbols.

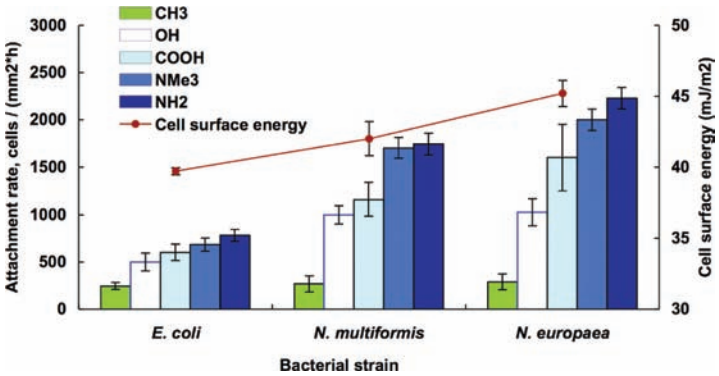

FIGURE 2. The bacterial surface energies and attachment rates over 2 h in fl o wcell tests on five SAM surfaces.

with time, except for the CH_3 surfaces, to which bacterial attachment plateaued after 80 to 100 min for *N. europaea* (Figure 1) and *N. multiformis* (Figure S3 of the SI). The mean attachment rates over 2 h were in the order NH_2 > NMe_3 > COOH > OH > CH_3 for all three strains (Figure 2). The differences in mean attachment rates between surfaces were significant ($p < 0.05$; all p values in this study were calculated using a two-tailed Students's t test) in all cases, except for the attachment rates of *N. multiformis* to the NMe_3 and NH_2 SAMs.

The attachment surface wettability (θ_w) was poorly correlated with attachment rates for all three bacteria (Figure 3A). Previous reports of the influence of wettability on attachment by bacteria have been variable. Tegoulia and Cooper (*42*) observed higher adhesion rates of *Staphylococcus aureus* on more hydrophobic SAM surfaces. Power et al. (*43*) reported that net adhesion of *Pseudomonas putida* was positively correlated with substrate hydrophobicity. Zhao et al. (*44*), however, found no systematic relationship between attachment and SAM surface properties. In our work, total surface energy (γ^{total}) appeared to be a better predictor of microbial attachment than was wettability, with increasing rates of attachment correlated with increasing surface energy (Figure 3B). All three bacterial strains exhibited the lowest rates of attachment on the CH_3 surface, which was also the least wettable ($\theta_W = 108 \pm 1°$; Figure 3A), and had the lowest surface energy (16.1 ± 0.62 mJ/m^2; Figure 3B). The NH_2 surface had the highest rate of attachment for all three strains, and it also had the highest surface energy (56.80 ± 0.08 mJ/m^2; Figure 3B), but it had intermediate wettability ($\theta_W = 40 \pm 1°$; Figure 3A). Furthermore, attachment rates for all three strains increased with increasing surface energy for the OH, COOH, and NMe_3 surfaces, while these surfaces had nearly the same θ_W values. These results indicated that not only was surface energy better correlated with attachment than was wettability, but also that relatively large increases in attachment rates occurred as surface energies increased above 50 mJ/m^2.

Attachment rates were previously reported to be correlated with θ_W (*22, 30, 45*). One difference between the data presented herein and these previous works is that these studies examined series of mixtures of functional groups (CH_3/OH and CH_3/COOH) to produce surfaces with ranges of θ_W values. Such mixtures would produce not only a gradient of θ_W values, but also they would also likely produce gradients of the polar (γ^{AB}) and nonpolar (γ^{LW}) components of the surface energy. This work examined 5 different SAM surfaces, which had contact angle and surface energy components that did not necessarily covary. Ista et al. (*27*) reported the attachment rates of *Staphylococcus epidermidis* and *Deleya marina* to SAMs with four different functional groups were not directly correlated with θ_w, with attachment rates of *S. epidermidis* higher on hydrophilic surfaces and those of *D. marina* higher on hydrophobic surfaces. They suggested other physicochemical factors than wettability may be involved in

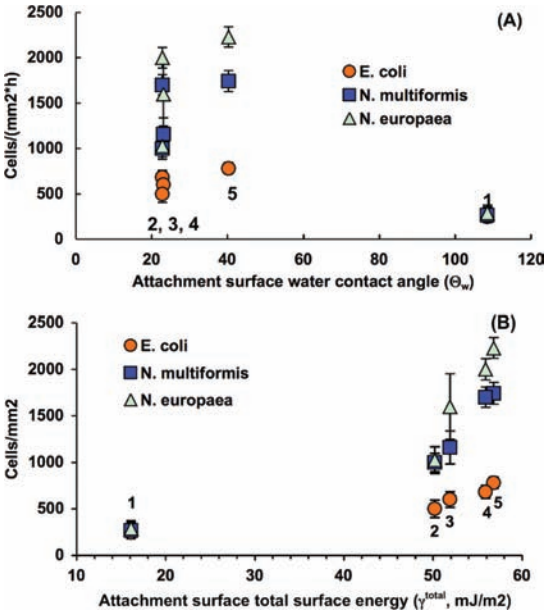

FIGURE 3. (A) The relationship between average cell attachment rate after 2 h and the water contact angle of SAM surfaces with (1) CH_3, (2) OH, (3) COOH, (4) NMe_3, and (5) NH_2 terminal groups. (B) The relationship between cell attachment rate and total surface energy for the same SAM surfaces. Some error bars are smaller than their corresponding symbols.

attachment, consistent with the results shown in Figure 3. In addition, Zhao et al. (*44*) suggested considering the inhomogeneity and specific interactions between bacteria and model surfaces during cell adhesion. The finding that attachment surface energy values were well correlated with attachment rates for the three strains studied suggests that surface energy measurements may be more useful in the determination of surface properties relevant to attachment than wettability alone.

The differences in attachment rates for the three strains included in this study may be related to their relative total surface energies. The rates of attachment were positively correlated with the bacterial surface energies, in agreement with the trends observed for the attachment surface total surface energies, with *N. europaea* exhibiting the highest rates of attachment overall (Figure 2) and the highest total surface energy (45.57 ± 0.92 mJ/m^2; Table 1), and *E. coli* exhibiting the lowest rates of attachment overall and the lowest total surface energy (39.7 ± 0.25 mJ/m^2).

One long-term goal of this research is the development of plastic surfaces which can be used as IFAS media for enhanced biofilm formation with improved functional behaviors, such as improved adhesion of nitrifiers on those suitable plastic surfaces for better nitrification rates in biological wastewater treatment. To this end, the rates of attachment of the two AOB included in this study were compared with those of *E. coli* (Figure 4). The rates of attachment for the AOB were nearly the same as *E. coli* on the lowest surface energy surface (CH_3), as indicated by the ratios to the *E. coli* attachment rates being nearly equal to 1, but for all other surfaces the AOB attachment rates were 190% to 290% those of *E. coli*. Cellular attachment of each AOB was significantly higher ($p < 0.05$) than that of *E. coli* for all surfaces except for CH_3 SAM (Figure 3). This suggests that higher surface energy surfaces may not only increase microbial attachment rates overall, but that there is also potential for their use in selectively attaching nitrifying bacteria.

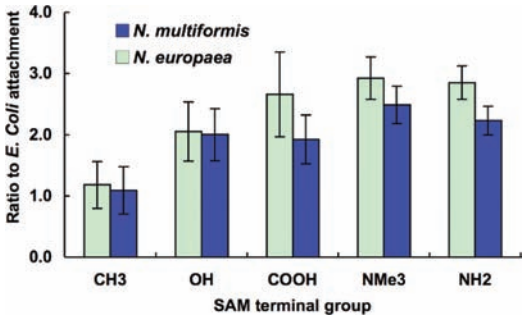

FIGURE 4. Ratio of *N. multiformis* and *N. europea* attachment rates to those of *E. coli* on five SAM surfaces.

These results are potentially useful for improving wastewater treatment system performance, because they provide fundamental information about the attachment preferences of nitrifying bacteria. Specifically, the finding that high surface energy surfaces may favor the attachment of nitrifiers suggests avenues for development and application of improved surfaces for use in hybrid systems, such as IFAS, and biofilm systems without a suspended biomass phase, such as MBBRs. For example, existing systems commonly use high density polyethylene (HDPE), which was measured in our laboratory to have a surface energy of 30 mJ/m^2, and therefore has a relatively low surface energy (Figure 3B).

This work focused on the attachment of pure cultures evaluated one at a time, in line with previous studies on bacterial attachment to SAMs under laboratory conditions (*13, 14, 16, 17, 20–23, 27, 31, 45*). In applied systems, the properties of the wastewater matrix, such as organic carbon, ammonia concentration, oxygen level, and pH, as well as cellular physiology and intercellular interactions, will affect microbial attachment rates and biofilm development. The results presented herein therefore provide promising but still preliminary and fundamental findings. Further research is needed, including studies of mixed populations of autotrophs and heterotrophs, with growth and competition in wastewater matrixes, to determine whether design of surface chemistry may be a useful strategy for improving wastewater treatment in attached growth or hybrid systems. Thermodynamic characterization and biofilm formation studies on different polymeric plastic media suitable for use in wastewater treatment systems are currently under investigation based on the results of this work.

Acknowledgments

This work was supported by the Water Environment Research Foundation (Paul L. Busch Award to A. Schuler), the National Science Foundation (Grant No. 0852469), and the Office of Naval Research (Grant No. N00014-08-0741). We thank Dr. Terri A. Camesano for her valuable advice on methods for deriving surface free energy parameters.

Supporting Information Available

An illustration of an alkanethiol SAM, a schematic of the flow cell, and temporal attachment data for *N. multiformis* and *E. coli*. This material is available free of charge via the Internet at http://pubs.acs.org.

Literature Cited

(1) Tchobanoglous, G.; Burton, F. L.; Stensel, H. D. *Wastewater Engineering: Treatment and Reuse*, 4th ed.; McGraw-Hill: New York, 2003.
(2) Prosser, J. I. Autotrophic nitrification in bacteria. *Adv. Microb. Physiol.* **1989**, *30*, 125–181.
(3) Rittmann, B. E.; McCarty, P. L. , *Environmental Biotechnology: Principles and Applications*. McGraw-Hill, NY: 2001.

(4) Limpiyakorn, T.; Shinohara, Y.; Kurisu, F.; Yagi, O. Communities of ammonia-oxidizing bacteria in activated sludge of various sewage treatment plants in Tokyo. *FEMS Microbiol. Ecol.* **2005**, *54*, 205–217.
(5) Geets, J.; Noon, N.; Verstraete, W. Strategies of aerobic ammonia-oxidizing bacteria for coping with nutrient and oxygen fluctuations. *FEMS Microbiol. Ecol.* **2006**, *58*, 1–13.
(6) Sen, D. ; Copithorn, R.; Randall, C.; Jones, R. ; Phago, D.; Rusten, B. *Investigation of Hybrid Systems for Enhanced Nutrient Control*; Water Environment Research Foundation: Alexandria VA, 2000; 96-CTS-4, 2000; p248.
(7) Randall, C. W.; Sen, D. Full-scale investigation of an integrated fixed-film activated sludge (IFAS) process for enhanced nitrogen removal. *Water Sci. Technol.* **1996**, *33* (12), 155–162.
(8) Batchelor, S. E.; Cooper, M.; Chhabra, S. R.; Glover, L. A.; Stewart, G. S. A. B.; Williams, P.; Prosser, J. I. Cell density-regulated recovery of starved biofilm populations of ammonia-oxidizing bacteria. *Appl. Environ. Microbiol.* **1997**, *63*, 2281–2286.
(9) Bollmann, A.; Schmidt, I.; Saunders, A. M.; Nicolaisen, M. H. Influence of starvation on potential ammonia-oxidizing activity and amoA mRNA levels of Nitrosospira briensis. *Appl. Environ. Microbiol.* **2005**, *71*, 1276–1282.
(10) Stoodley, P.; Sauer, K.; Davies, D. G.; Costerton, J. W. Biofilms as complex differentiated communities. *Annu. Rev. Microbiol.* **2002**, *56*, 187–209.
(11) Busscher, H. J.; Van der Mei, H. C. Initial microbial adhesion is a determinant for the strength of biofilm adhesion. *FEMS Microbiol. Lett.* **1995**, *128*, 229–234.
(12) Dalton, H.; Stein, J.; March, P. A biological assay for detection of heterogeneities in the surface hydrophobicity of polymer coatings exposed to the marine environment. *Biofouling* **2000**, *15*, 83–94.
(13) Absolom, D. R.; Lamberti, F. V.; Policova, Z.; Zingg, W.; van Oss, C. J.; Neumann, A. W. Surface thermodynamics of bacterial adhesion. *Appl. Environ. Microbiol.* **1983**, *46*, 90–97.
(14) Bellon-Fontaine, M.-N.; Rault, J.; van Oss, C. J. Microbial adhesion to solvents: a novel method to determine the electron-donor/electron-acceptor or Lewis acid-base properties of microbial cells. *Colloids Surf., B* **1996**, *7*, 47–53.
(15) Love, C. J.; Estroff, L. A.; Kriebel, J. K.; Nuzzo, R. G.; Whitesides, G. M. Self-assembled monolayers of thiolates on metals as a form of nanotechnology. *Chem. Rev.* **2005**, *105*, 1103–1169.
(16) Abu-Lail, L. I.; Liu, Y.; Atabek, A.; Camesano, T. A. Quantifying the adhesion and interaction forces between pseudomonas aeruginosa and natural organic matter. *Environ. Sci. Technol.* **2007**, *41*, 8031–8037.
(17) Hou, S.; Burton, E. A.; Simon, K. A.; Blodgett, D.; Luk, Y.-Y.; Ren, D. Inhibition of *Escherichia coli* biofilm formation by self-assembled monolayers of functional alkanethiols on gold. *Appl. Environ. Microbiol.* **2007**, *73*, 4300–4307.
(18) Kim, Y. H.; Cho, J. H.; Lee, Y. W.; Lee, W. K. Development of a carrier for adhesion of nitrifying bacteria using a thermodynamic approach. *Biotechnol. Tech.* **1997**, *11*, 773–776.
(19) van Oss, C. J.; Good, R. J.; Chaudhury, M. K. Additive and nonadditive surface-tension components and the interpretation of contact angles. *Langmuir* **1988**, *4* (4), 884–891.
(20) Liu, Y.; Gallardo-Moreno, A. M.; Pinzon-Arango, P. A.; Reynolds, Y.; Rodriguez, G.; Camesano, T. A. Cranberry changes the physicochemical surface properties of *E. coli* and adhesion with uroepithelial cells. *Colloids Surf., B* **2008**, *65* (1), 35–42.
(21) Weincek, K. M.; Fletcher, M. Effects of substratum wettability and molecular topography on the initial adhesion of bacteria to chemically defined substrata. *Biofouling* **1997**, *11*, 293–311.
(22) Ista, L. K.; Callow, M. E.; Finlay, J. A.; Coleman, S. E.; Nolasco, A. C.; Simons, R. H.; Callow, J. A.; Lopez, G. P. Effect of substratum surface chemistry and surface energy on attachment of marine bacteria and algal spores. *Appl. Environ. Microbiol.* **2004**, *70*, 4151–4157.
(23) Ista, L. K.; Mendez, S.; Lopez, G. P. Attachment and detachment of bacteria on surfaces with tunable and switchable wettability. *Biofouling* **2010**, *26*, 111–118.
(24) Bain, C. D.; Whitesides, G. M. Molecular-level control over surface order in self-assembled monolayer films of thiols on gold. *Science* **1988**, *240* (4848), 62–63.
(25) Bain, C. D.; Troughton, E. B.; Tao, Y.-T.; Evall, J.; Whitesides, G. M.; Nuzzo, R. G. Formation of monolayer films by the spontaneous assembly of organic thiols from solution onto gold. *J. Am. Chem. Soc.* **1989**, *111*, 321–335.
(26) McFeters, G. A.; Pyle, B. H.; Lisle, J. T.; Broadaway, S. C. Rapid direct methods for enumeration of specific, active bacteria in water and biofilms. *J. Appl. Microbiol.* **1999**, *85*, 193S–200S.
(27) Ista, L. K.; Fan, H. Y.; Baca, O.; Lopez, G. P. Attachment of bacteria to model solid surfaces: Oligo(ethylene glycol) surfaces inhibit bacterial attachment. *FEMS Microbiol. Lett.* **1996**, *142* (1), 59–63.
(28) Tien, J.; Terfort, A.; Whitesides, G. M. Microfabrication through electrostatic self-assembly. *Langmuir* **1997**, *13*, 5349–5355.
(29) Zhu, P.; Masuda, Y.; Koumoto, K. The effect of surface charge on hydroxyapatite nucleation. *Biomaterials* **2004**, *25*, 3915–3921.
(30) Khan, M. M. T.; Stewart, P. S.; Moll, D. J.; Mickols, W. E.; Burr, M. D.; Nelson, S. E.; Camper, A. K. Assessing biofouling on polyamide reverse osmosis (RO) membrane surfaces in a laboratory system. *J. Membr. Sci.* **2010**, *349*, 429–437.
(31) Liu, Y. T.; Strauss, J.; Camesano, T. A. Thermodynamic investigation of *Staphylococcus* epidermidis interactions with protein-coated substrata. *Langmuir* **2007**, *23* (13), 7134–7142.
(32) van Oss, C. J. Acid-Base Interfacial Interactions in Aqueous-Media. *Colloids Surf., A* **1993**, *78*, 1–49.
(33) van Oss, C. J. , *Interfacial Forces in Aqueous Media*; Marcel Dekker, Inc.: New York: 1994.
(34) Good, R. J.; van Oss, C. J. In *Modern Approaches to Wettability, Theory and Applications.*; Shrader, M. E., Loeb, G. I. , Eds.; Plenum Press: New York: 1992.
(35) Tan, J. L.; Tien, J.; Chen, C. S. Microcontact printing of proteins on mixed self-assembled monolayers. *Langmuir* **2002**, *18*, 519–523.
(36) Cho, E. C.; Kim, D.-H.; Cho, K. Contact angles of oils on solid substrates in aqueous media: Correlation with AFM data on protein adhesion. *Langmuir* **2008**, *24*, 9974–9978.
(37) Lestelius, M.; Liedberg, B.; Tengvall, P. In vitro plasma protein adsorption on w-functionalized alkanethiolate self-assembled monolayers. *Langmuir* **1997**, *13*, 5900–5908.
(38) Evans, S. D.; Sharma, R.; Ulman, A. Contact angle stability: Reorganization of monolayer surfaces. *Langmuir* **1991**, *7*, 156–161.
(39) Martins, M. C. L.; Ratner, B. D.; Barbosa, M. A. Protein adsorption on mixtures of hydroxyl- and methyl-terminated alkanethiols self-assembled monolayers. *J. Biomed. Mater. Res.* **2003**, *67*, 158–171.
(40) van Oss, C. J.; Chaudhury, M. K.; Good, R. J. Monopolar surfaces. *Adv. Colloid Interface Sci.* **1987**, *28* (1), 35–64.
(41) Sharma, P. K.; Rao, K. H. Analysis of different approaches for evaluation of surface energy of microbial cells by contact angle goniometry. *Adv. Colloid Interface Sci.* **2002**, *98*, 341–463.
(42) Tegoulia, V. A.; Cooper, S. L. *Staphylococcus aureus* adhesion to self-assembled monolayers: effect of surface chemistry and fibrinogen presence. *Colloids Surf., B* **2002**, *24*, 217–228.
(43) Power, L.; Itier, S.; Hawton, M.; Schraft, H. Time lapse confocal microscopy studies of bacterial adhesion to self-assembled monolayers and confirmation of a novel approach to the thermodynamic model. *Langmuir* **2007**, *23*, 5622–5629.
(44) Zhao, C.; Brinkhoff, T.; Burchardt, M.; Simon, M.; Wittstock, G. Surface selection, adhesion, and retention behavior of marine bacteria on synthetic organic surfaces using self-assembled monolayers and atomic force microscopy. *Ocean Dynam.* **2009**, *59*, 305–315.
(45) Wiencek, K. M.; Fletcher, M. Bacterial adhesion to hydroxyl- and methyl-terminated alkanethiol self-assembled monolayers. *J. Bacteriol.* **1995**, *177*, 1959–1966.

ES101389U

Chapter 5: Thermodynamic investigation of resistance of oligo(ethylene glycol)-terminate self assembled monolayers to bacterial attachment. *

* Manuscript in preparation to be submitted to Applied and Environmental Microbiology as Ista, L.K. and López, G.P. “Thermodynamic investigation of resistance of oligo(ethylene glycol)-terminate self assembled monolayers to bacterial attachment.”

Introduction

Oligo (ethylene glycol) (OEG) and poly(ethylene glycol) (PEG) surfaces are frequently used in applications that require a high degree of resistance to biomacromolecular and/or cellular adsorption (5, 31, 34).OEG modified self-assembled monolayers (OEG-SAMs) in particular are frequently employed to serve as a non-fouling background for patterning of proteins(8, 29, 30), nucleic acids(51), eukaryotic(28, 33) and prokaryotic(52) cells. OEG-SAMs have also been important in understanding the physicochemical and molecular processes involved in fouling resistance (32, 38).

The mechanism of fouling resistance to ethylene glycol (EG)-containing surfaces depends on the interaction between the EG backbone and water. Early analysis of a variety of fouling-resistant SAMs suggested that hose surfaces witha low water contact angles, i.e., hydrophilic, surfaces were the most resistant to non-specific protein and cellular accumulation (32); subsequent, systematic investigation of modifications of the terminal groups of normally non-fouling EG-SAMs n=6 to that increasing the water contact angle of the surface decreased its resistance to protein (15) and algal spores (39). Water surrounding the EG chains (internal water) is also known to be vital the fouling resistance of OEG- SAMs. When the lateral packing

density of EG-SAMs (n=6) is reduced by forming the SAMs on silver rather than gold, these surfaces lose their resistance to protein adsorption (14); since the surface contact angle of the EG-SAM is not largely different when formed on the two metals (33˚ on Au;36˚ on Ag), the difference must be due to penetration of water into the SAM interior(14).

The thermodynamics of fouling resistance take into account the interaction between EG and water. Hydration of PEG is associated with a large net enthalphic gain to the system (9, 11, 20)}; adsorption of a protein or cell compresses the PEG polymer, forcing water out of the system, and decreasing the enthalpy of the system. Additionally, when a macromolecule or cell attaches to PEG, it reduces the rotational degrees of freedom within the PEG chain, decreasing entropy (20). In OEG these thermodynamic principle are also operative, but to a lesser degree. Although hydration of the OEG is still enthalpically favored, and dehydration disfavoured, loss of entropy upon macromolecular adsorption is less pronounced do to the relatively fewer degrees of freedom (27 for EG n=3, ~200 for EG n=6) for OEG compared to PEG (~100,000,000 for PEG with a molecular weight of 2000 da) (14, 49).

The nonfouling nature OEG has been empirically determined to be dependent on hydrogen bonding between the ethylene EG moieties and water. Resistance of EG-containing SAMs was significantly decreased when terminal hydrogen bond accepting hydroxyl groups were replaced with hydrogen bond-donating amine groups (32). Nonfouling is also associated with a helical EG secondary structure, and *ab initio* calculations, suggested that water stabilized such structures (50). EG nonfouling conformations are proposed to be stabilized by the

formation of multiple hydrogen bonds between water and the lone electron pairs on the oxygen of the EG moiety as well as the formation of water bridges between the EG chains (15, 38, 49, 50). Furthermore, the number of hydrogen bonds an OEG molecule is capable of forming with water is now thought determine its degree of fouling resistance (49, 50).

The association between the number of hydrogen bonds between OEG and water and its degree of fouling has been made based on mathematical models only. Experimental and quantitative verification of the degree of hydrogen bonding and the fouling resistance of OEG may be obtained, however, by proper application of colloidal models of bacterial attachment. Of these models, the van der Waals-Lewis-Acid Base model proposed by van Oss, Chaudhury and Good (VCG) in the late1980s (48) was explicitly proposed to explain hydrogen bonding in aqueous interactions (45). It is, not coincidentally, the pre-eminent colloidal theory for modeling bacterial attachment. While developing their theory, VCG also proposed that monopolar interactions, i.e., those in which a molecule was only capable of electron donating or electron accepting behaviour) would be reflected in a negative interfacial tension (47) . Herein, we use VCG methods to examine the interfacial tension between OEG surfaces and water n to provide experimental evidence for the hydrogen bonding theory of OEG fouling resistance.

SAMs composed of alkanethiolates with ω-substitutions of varying lengths of oligo (ethylene glycol) (35) are a particularly attractive on for studying the relationship between bacterial attachment, surface tension and, ultimately, ΔG_{adh}. The number of ethylene glycol (EG) units (n=1-6) in a SAMs determines their

resistance to protein adsorption (37) and subsequently to mammalian cells (32), marine bacteria (3, 17) and algal zoospores (39). The difference between OEG SAMs that resist and permit cellular adsorption is one SAM moiety (40); if VCG accurately models bacterial attachment the ΔG_{adh} of the EG-SAMs that attach bacteria should be negative, whereas those that resist attachment should have a positive ΔG_{adh}. The OEG system is also unique in that the relatively low attachment to these surfaces means that over the course of our experiments (2 hr) it is extremely unlikely that an attachment maximum will be encountered, thus avoiding kinetic issues that may arise should this condition not be met (M. Grunze, personal communication). In this paper apply VCG analysis to OEG-SAMs of varying length to determine how well the calculated ΔG_{adh} matches attachment profiles of a marine bacterium.

Materials and Methods

Preparation and characterization of self-assembled monolayers

Self assembled monolayers (SAMs). of ω-subsituted alkanethiolates on gold were prepared as described previously (17); Briefly, glass coverslips were treated with 70:30 H_2SO_4/H_2O_2 for at least 20 minutes, rinsed in copious amounts of deionized water, and dried under liquid nitrogen. The samples were then loaded into a thermal evaporator. After evacuating the chamber to 10^{-6} millitorr, 15Å Cr were deposited followed by 300Å Au.

Contact angles of SAMs were measured using the Wilhelmy Plate method on a Krüss K100 tensiometer with Lab Desk 303 (Krüss) software. Measurements were made using water (18MΩ cm^{-1};Millipore Academic System; Millipore, Billerica),

diiodomethane (99% ReagentPlus; Sigma-Aldrich, St. Louis), formamide (Omipure; EMD; Gibbstown), glycerol (anhydrous; J.T. Baker, Phillipstown) and hexadecane(Sigma Aldrich, St. Louis). Samples were double-sided SAMs made on 22X40 mm coverslips (Fisher). For measurement, SAMs were immersed to a depth of 1 cm, with the force measured on the sample six times per mm beginning 1 mm from the end of the sample (a total of 54 data points per sample). Lab Desk 303 software computed the contact angle according to the equation:

$$\cos\theta = \frac{F - F_b}{L\gamma_{LV}} \quad \textbf{[1]}$$

where θ= the contact angle, F= the measured force F_b is the buoyant force (calculated from density of the probe liquid and the relevant parameters of the sample when not submersed), L= wetted length, and γ_{LV} the surface tension of the probe liquid. Data are reported as a plot of θ vs. position and in tabular form as the mean of the cumulative data ± standard deviation from the mean. For each SAM formulation, a minimum of three samples were measured per probe liquid.

Calculation of surface and interfacial tensions and ΔG_{adh}

The model of surface tension articulated by van Oss, Chaudhury and Good (48) was used both to calculate surface tensions (γ_{SV}) from contact angle data and

the interfacial tension (γ_{SL}) between SAMs and water. Surface tensions were estimated from contact angles using the following equation:

$$1+\cos\theta = \frac{2(\sqrt{\gamma_{SV}^{LW}\gamma_{LV}^{LW}} + \sqrt{\gamma_{SV}^{+}\gamma_{LV}^{-}} + \sqrt{\gamma_{SV}^{-}\gamma_{LV}^{+}}}{\gamma_{LV}} \quad \textbf{[2]}$$

where γ_{SV}^{LW}, γ_{SV}^{+}, and γ_{SV}^{-} are the Lifshitz-van der Waals, Lewis acid, and Lewis base components of surface tensions of the SAM and γ_{LV}^{LW}, γ_{LV}^{+}, and γ_{LV}^{-} are the corresponding value for the probe liquid. Because there are 3 unknowns within the equation (the components of probe liquid surface tension being established in the literature), contact angles must be taken with three different probe liquids and the unknowns γ_{SV}^{LW}, γ_{SV}^{-} and γ_{SV}^{+} calculated from simultaneously solving the three equations. Surface tension in the VCG model is defined as

$$\gamma_{SV} = \gamma_{SV}^{LW} + \gamma_{SV}^{AB} \quad \textbf{[3]}$$

where γ_{SV}^{AB} is the acid-base component of surface tension, calculated from γ_{SV}^{+} and γ_{SV}^{-} as follows:

$$\gamma_{SV}^{AB} = 2\sqrt{\gamma_{SV}^{+}\gamma_{SV}^{-}} \quad \textbf{[4]}$$

Calculation of the interfacial tension between the SAM and water can then be calculated using the geometric mean (45):

$$\gamma_{SL} = (\sqrt{\gamma_{SV}^{LW}} - \sqrt{\gamma_{LV}^{LW}}) + 2\left[(\sqrt{\gamma_{SV}^{+}} - \sqrt{\gamma_{LV}^{+}})(\sqrt{\gamma_{SV}^{-}} - \sqrt{\gamma_{LV}^{-}})\right] \quad \textbf{[5]}.$$

Measurement of bacterial contact angles.

A 150 mL aliquot of *C. marina* was collected from the chemostat and filtered through a 0.2μm cellulose acetate filter, resulting in a visible "pad" of bacteria on the filter. Three sample bacterial pads were dried in air and monitored by water contact angle on a Ramé-Hart contact angle goniometer until the contact angle stabilized, indicating that interstitial water was evaporated, but the cells themselves remained hydrated (27, 44), about 45 minutes. Pads for contact angle analysis were dried in ambient air for 50 minutes. Bacterial contactl angles were measured with the same solvents as used for SAMs (deionized water, diiodomethane, formamide, glycerol and hexadecane). The values obtained were then inserted in to Equation **[2]** and γ_{BV} calculated.

Calculations of ΔG_{adh}

Calculation of ΔG_{adh} was performed in two ways. All surface-energetic based models of bacterial attachment relate the free energy of adhesion, ΔG_{adh}, to the interfacial tensions between the attaching bacterium and the attachment substratum (γ_{BS}), the bacterium and the bulk liquid (γ_{BL}) and the attachment substratum and the bulk liquid (γ_{SL}):

$$\Delta G_{adh} = \gamma_{BS} - \gamma_{BL} - \gamma_{SL}$$ **[6]** (1, 48).

Once the values of γ_{BV} and γ_{SV} were calculated using equations **[2, 3** and **4**] the values of γ_{BS}, γ_{BL} and γ_{SL} (Equation **[5]**) were inserted into Equation **[6]** and ΔG_{adh} determined.

A second method, proposed by VCG, states that, in analogy to γ_{SV}, ΔG_{adh} can be divided into two components, an apolar Lifshitz-van der Waals component (ΔG_{adh}^{LW}) and a polar, Lewis acid base component (ΔG_{adh}^{AB}):

$$\Delta G_{adh} = \Delta G_{adh}^{LW} + \Delta G_{adh}^{AB} \quad \textbf{[7]}$$ (45, 46).

VCG asserts, however, that each individual interfacial tension is the sum of non-polar, van der Waals, interactions and polar, Lewis acid-base interactions. For example γ_{SL} is:

$$\gamma_{SL} = \gamma_{SL}^{LW} + \gamma_{SL}^{AB} \quad \textbf{[8]}$$

where γ_{SL}^{LW} and γ_{SL}^{AB} are the Lifshitz van der Waals and Lewis acid base components, respectively, of γ_{SL}. Applying equation **[8]** to each interfacial tension in equation **[6]**, the Dupré equation can be rewritten as:

$$\Delta G_{adh} = (\gamma_{BS}^{LW} + \gamma_{BS}^{AB}) - (\gamma_{BL}^{LW} + \gamma_{BL}^{AB}) - (\gamma_{SL}^{LW} + \gamma_{SL}^{AB}) \quad \textbf{[9]}$$

or

$$\Delta G_{adh} = \Delta G_{adh}^{LW} + \Delta G_{adh}^{AB} \quad \textbf{[10]}$$

where

$$\Delta G_{adh}^{LW} = \gamma_{BS}^{LW} - \gamma_{BL}^{LW} - \gamma_{SL}^{LW} \quad \textbf{[11]}$$

and

$$\Delta G_{adh}^{AB} = \gamma_{BS}^{AB} - \gamma_{BL}^{AB} - \gamma_{SL}^{AB} \quad \textbf{[12]}.$$

The values obtained by both methods should be equal, and cross checking the two will reveal possible errors in calculation of the individual surface and interfacial tension values.

Bacterial culture conditions

All media and buffers were prepared with de-ionized water (resistivity > 18MΩ cm^{-1}). Marine Broth 2216 (MB, Difco, Franklyn Lakes, NJ) was prepared according to manufacturer's instructions. Marine Agar (MA) was prepared by the addition of 1.5% Bacto agar (Difco) to MB. Artificial sea water (ASW) contained 400 mM NaCl, 100 mM $MgSO_4$, 20 mM KCl, 10 mM $CaCl_2$ (21). Modified basic marine medium plus glycerol (MBMMG) contained 0.5× ASW plus 19 mM NH_4Cl, 0.33 mM K_2HPO_4, 0.1 mM $FeSO_4 \cdot 7H_2O$, 5 mM Trishydroxyaminomethane hydrochloride pH 7, and 2 mM glycerol (18, 21). *Cobetia marina* (basonym, *Halomonas marina*) ATCC 25374, is stored in frozen stock aliquots, made from first generation cultures of the original ATCC lyophilate, in MB containing 20% glycerol at -70°C. Experimental stock preparations were maintained on marine agar slants and were stored at 4°C for up to 2 weeks. Prior to inoculation into a chemostat, a single colony from a MB slant was inoculated into 50 ml of MB and grown overnight with shaking at 25°C. A chemostat culture was established by inoculating 3 ml of the overnight culture into MBMMG. The chemostat was maintained at a flow rate of 1 ml min^{-1} (dilution rate, 0.16 h^{-1}) with constant stirring. The concentration of the subsequent culture was ~10^7 cells ml^{-1}.

Attachment studies. SAMs prepared on gold films coated on 60 x 24 mm coverslips were placed into a flow-cell apparatus (17) which was then mounted onto the stage of an optical microscope (Axioskop, Zeiss, Jena) and connected to the outflow of the chemostat. The C. marina culture was allowed to flow through the cell at a rate of 1 ml min^{-1} for two hours. Bacterial attachment was monitored through a CCD camera

attached to the microscope. The images were fed to a computer using Axiovision software (Zeiss, Jena). At the end of the attachment time, images of 10 fields of view within 10 mm of the horizontal midline of the slide were captured, the number of attached bacteria subsequently counted and the average for each sample determined. For each SAM, a minimum of 3 experiments were performed.

Results

The bacterial attachment profile of *C. marina* on EG-SAMs is shown in Figure 1. Data are shown as the average of at least 3 flow cell experiments ± one standard deviation. Fouling resistance (defined as attachment of ~1 or less cell mm^{-2}) is first observed at EG≥4. For PEG-SAM the attachment is effectively 0 (0.06±0.05 cells mm^{-2}).

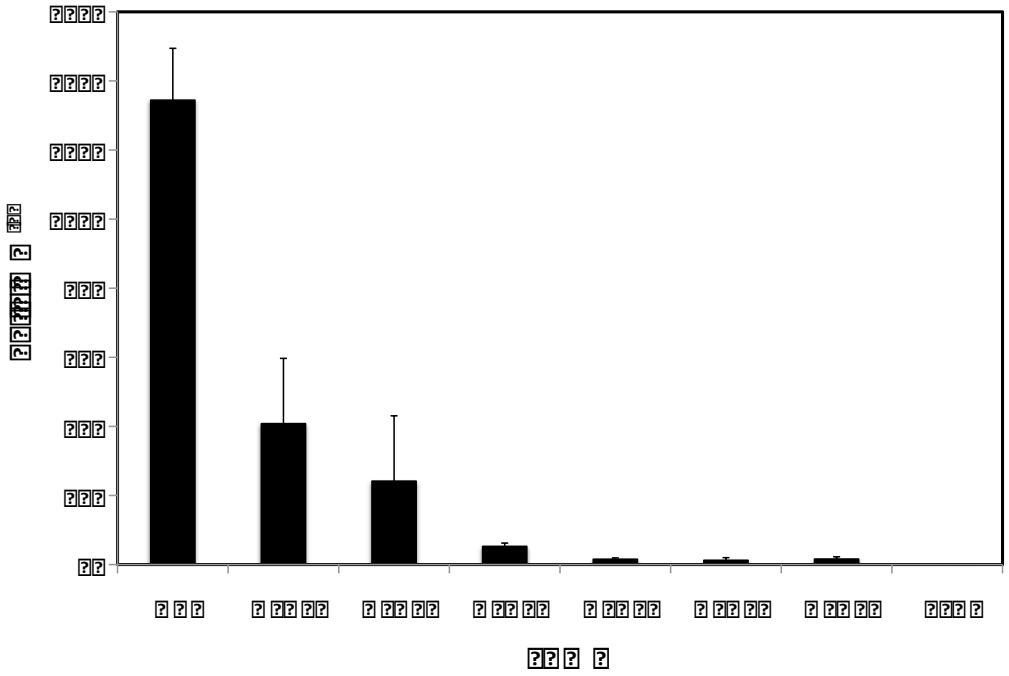

Figure 1: Two hour attachment of *Cobetia marina* to EG SAMs. Error bars are ± 1 standard deviation.

The contact angles of EG-SAMs are shown in Table 1. OEG 0 is the OH-terminated SAM (OH-SAM) and OEG-500 is the PEG-SAM (MW of PEG in thiol = 1964 Da; MW 1 EG unit=44 Da; Number of repeats =491). The advancing water contact angles (θ_{AW}) for all SAMs are similar to those reported previously (2, 16, 40). A one-way ANOVA of the data in Table 1 for each solvent grouping those SAMs that attached bacteria (EG n<4) and those that did not (EG n≥ 4) showed no statistical difference between the two groupings for diiodomethane (p=0.52) and formamide (p=0.1) but a statistically meaningful separation with glycerol (p=0.0002) and water (p=0.001), although in the final case, the water contact angles of EG n=2-6 were indistinguishable (p=0.33). Although statistically significant differences were observed among the advancing contact angles of hexadecane (θ_{AH}) between several

Table 2: Contact angles of study SAMs with different contact angle solvents

Liquid / EG n=	Diiodo-methane	Form-amide	Glycerol	Hexa-decane	Water
0	35 ± 1°	24 ± 1°	39 ± 2°	5 ± 3°	24 ± 2°
1	25 ±1°	29 ±2°	35 ± 2°	7± 2°	28 ± 2°
2	25 ±2°	29 ±1°	39 ±1°	15 ± 1°	32 ± 1°
3	27 ± 2°	23 ±2°	38 ± 3°	18 ± 1°	33 ± 1°
4	24 ± 3°	27 ±2°	42 ± 1°	1 ± 1°	33 ± 1°
5	32 ±2°	26 ±2°	44 ± 3°	11 ± 1°	34 ± 1°
6	27 ± 2°	24 ± 3°	47 ± 2°	11 ± 1°	33 ± 2°
500	29 ±1°	21 ±1°	60 ± 1°	3 ± 2°	37 ± 1°

of the EG-SAMs, all values of θ_{AH} were less than 20°, and thus, the differences where insignificant when $\cos\theta_{AH}$, the input into Equation **[2]** were not significant.

Surface tension and components calculated from θ_A values in Table 1 using VGC are summarized in Figure 2. Total surface tension is plotted as a function of EG length in Figure 2B. An increase in γ_{SV} is observed as EG chain length increases from 0-6 for γ_{SV} calculated using θ_A obtained for water, diiodomethane and formamide (WDF; closed circles) while a decreasing trend is observed for γ_{SV}

calculated using water, diiodomethane and glycerol (WDG; open circles). In both cases, γ_{SV} values for PEG (EG=500) SAMs did not follow the trend observed for SAMs of shorter length. The ability of the two groups of solvents to differentiate between fouling and non-fouling surfaces was quite different; whereas γ_{SV} calculated from neither WDF nor WDG showed statistically significant difference between all fouling and non-fouling SAMs (p_{WDF}=0.05, p_{WDG}=0.06) when considering the full data set, if the OH and PEG data were removed, γ_{SV} calculated from WDG differentiated well between fouling and non fouling surfaces (p=0.0004) whereas the data obtained using WDF did not (p=0.96).

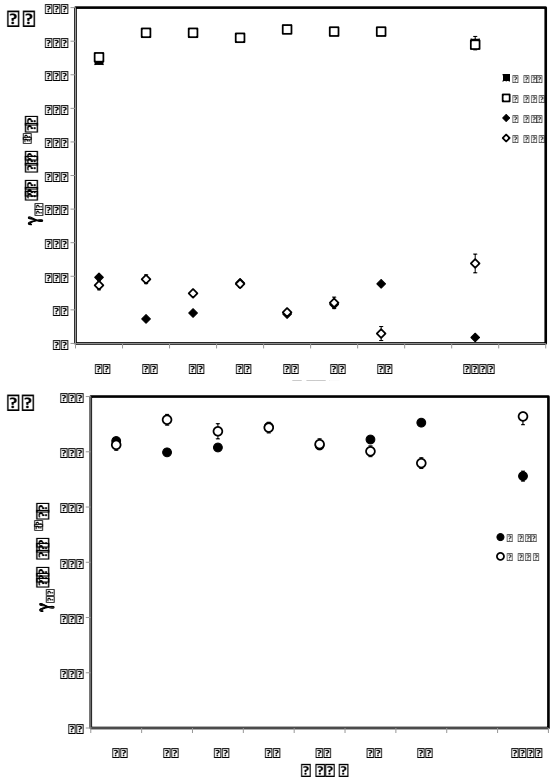

Figure 2: Additive components of (A) and total (B) γ_{SV} of EG-SAMs used in this study. A. Squares are the apolar γ_{SV}^{LW} component diamonds are the polar γ_{SV}^{AB} component. Solid symbols are values calculated from the contact angles of water, diiodomethane (WDF); open symbols are values calculated from the contact angles of water, diiodomethane and glycerol (WDG). Error bars indicate 95% confidence levels.

When the additive components of γ_{SV}, γ_{SV}^{LW} andγ_{SV}^{AB}, were analyzed, it was clear that although the non-polar γ_{SV}^{LW} component dominated the total value of γ_{SV}, it was uniform (~45 mJ m^{-2}) for each SAM; variation in γ_{SV} calculated for different

SAMs was largely the result of the relatively small γ_{SV}^{AB} component, which followed the same trends as total γ_{SV}. When the non-additive components γ_{SV}^{AB}, $\gamma_{SV}^{+}$and γ_{SV}^{-}, were plotted (Figure 8, below), it is clear that γ_{SV}^{AB} component is itself dominated by γ_{SV}^{-}, or the Lewis basic component of surface tension, as was expected given the electron-donating nature of the lone pair with increasing length of EG.

Table 3: Contact angles (θ) of pads of logarithmic phase *C. marina* supported on cellulose acetate filters.

Solvent	θ
Diiodomethane	34± 2˚
Formamide	53 ± 2˚
Glycerol	64 ± 2˚
Hexadecane	2 ± 1˚
Water	52 ± 3˚

Advancing contact angles of *C. marina* pads on cellulose acetate filters using the five probe liquids from this study are found in Table 2. An uncoated cellulose acetate filter was permeable to all solvents, rendering it effectively completely wettable (θ_A=0˚).

Bacterial surface tension (γ_{BV}) for *C. marina* as calculated from contact angle values in Table 2

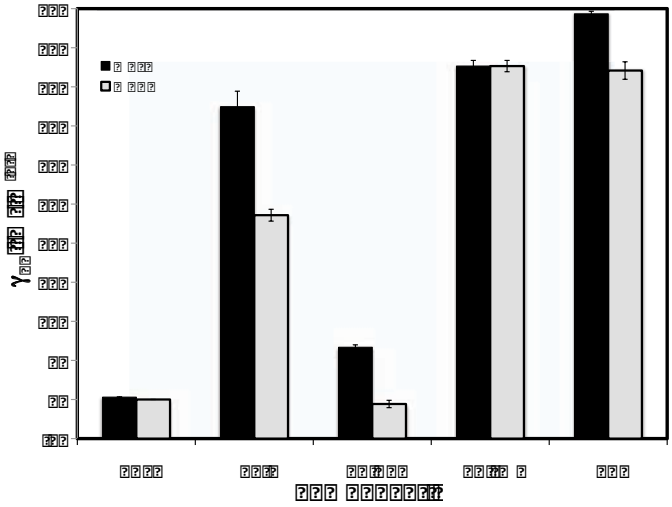

Figure 3: *C. marina* bacterial surface energy (γ_{BV}) and components as calculated from contact angles taken with solvent sets water, diiodomethane and formamide (WDF) or water, diiodomethane and glycerol (WDG). Error bars represent 95% confidence levels.

is shown in Figure 3. The total surface tension is dominated by the apolar component of surface tension, γ_{BV}^{LW}. When the polar component of bacterial surface tension, γ_{BV}^{AB} is separated into its non-additive Lewis acidic (γ_{BV}^{+}) and Lewis basic (γ_{BV}^{-}), it is predominantly Lewis basic. This observation is consistent with data that demonstrates that *C. marina* attaches preferentially to Lewis acidic amine- and trimethyl amine-terminated SAMs. Use of glycerol as a probe liquid resulted in a decrease in both γ_{BV}^{AB} and its γ_{BV}^{-} component.

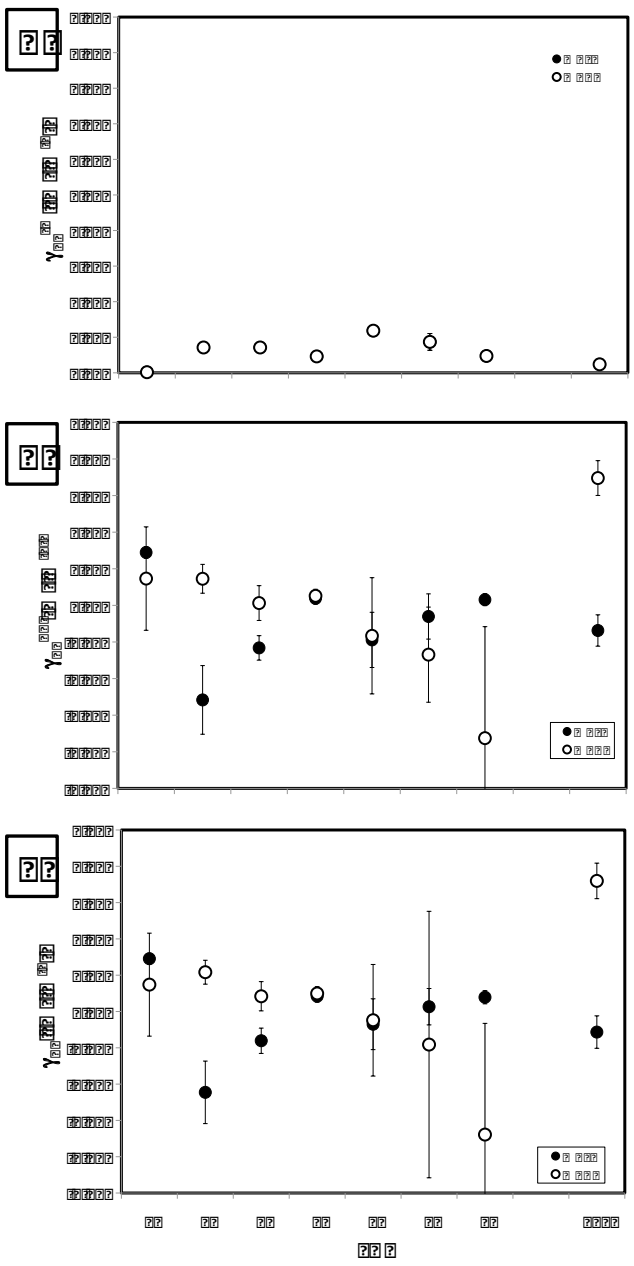

Figure 4: γ_{BS} (C) and additive components γ_{BS}^{LW} (A) andγ_{BS}^{AB}(B). Filled circles are values calculated from (θ_{AX}) using the solvent set water, diiodomethane and formamide (WDF); open circles from the solvent set water, diiodomethane and glycerol (WDG). Error bars represent 95% confidence intervals.

The interfacial tension between the bacterium and the substratum, γ_{BS} and its additive apolar and polar

components are shown in Figure 4. The value of γ_{BS} is quite small ($-1<\gamma_{BS}<1$ mJ m^{-2}). The apolar component of γ_{BS} is less than 0.01 mJ m^{-2}, suggesting that the apolar interactions between the bacterium and the surfaces are minimal. γ_{BS} is most influenced by the value of γ_{BS}^{AB} and when calculated from contact angles obtained with water, diiomethane and glycerol, becomes negative at the point where non-fouling sets in, although PEG surfaces (EG n=500) surfaces do not fall within this trend.

The second input into ΔG_{adh} in Equation **[6]** is the interfacial tension between the bacterium and the bulk liquid, which we are modeling as water. . No statistical difference was observed between γ_{BL} as calculated using solvent set WDF compared to that calculated solvent set WDG ; both solvent sets resulted in a value of γ_{BL}

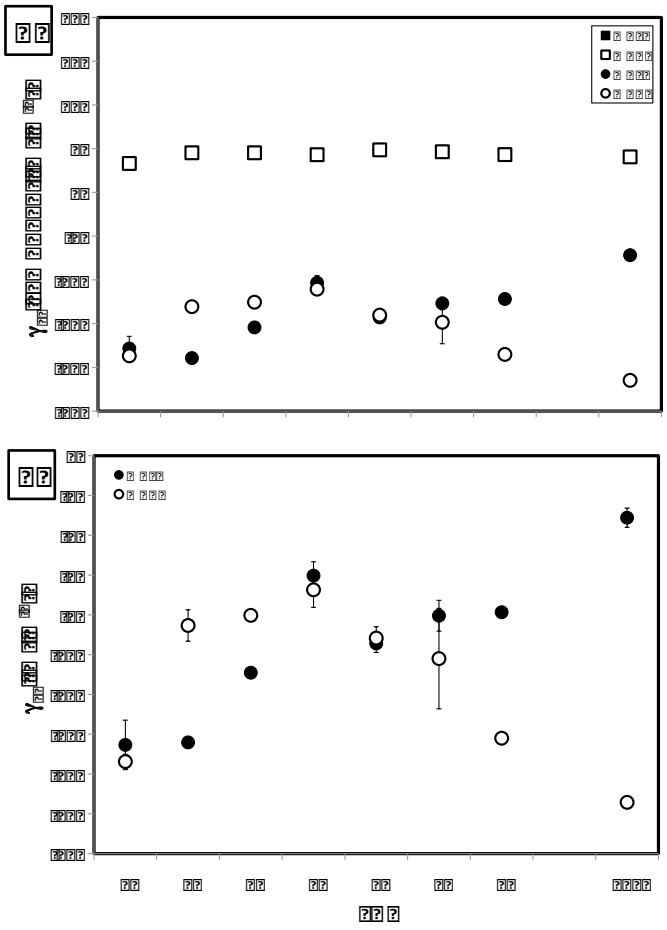

Figure 5:A. Additive components of and B. **total γ_{SL}** between EG-SAMs and water. A. Squares are the apolar γ_{SL}^{LW} component and circles are the polar γ_{SL}^{AB} component. Solid symbols are values calculated from the contact angles of water, diiodomethane (WDF); open symbols are values calculated from the contact angles of water, diiodomethane and glycerol (WDG). Error bars indicate 95% confidence levels.

~-6.2 mJ m^{-2}. This value suggests that the interaction between the bacterium and the water is monopolar (47).

The interfacial tension between EG-SAMs and water, γ_{SL} is summarized in Figure 5. For all EG-SAMs, this value is negative, suggesting a monopolar interaction with between the EG-SAMs and water. All EG-SAMs have statistically identical values (~5 mJ m^{-2}) for the apolar component of interfacial tension, γ_{SL}^{LW}. There is a profound difference in the profiles of γ_{SL}^{AB} and γ_{SL} as calculated from contact angles of EG-SAMs taken with water, diiodomethane and formamide and those taken with water, diiodomethane and glycerol. Although both show an inflection between EG n=3 and EG n=4, the transition between a fouling and non fouling regimes in Figure 1, the latter show increasing strength of monopolar interactions (47) with increasing EG content.

The interfacial tension γ_{BS}, γ_{BL} and γ_{SL} combine in Equation **[6]** to yield the free energy of attachment ΔG_{adh} (45). These data are shown in Figure 6. Both fouling (EG n<4) and nonfouling (EG n≥ 4) EG-SAMs

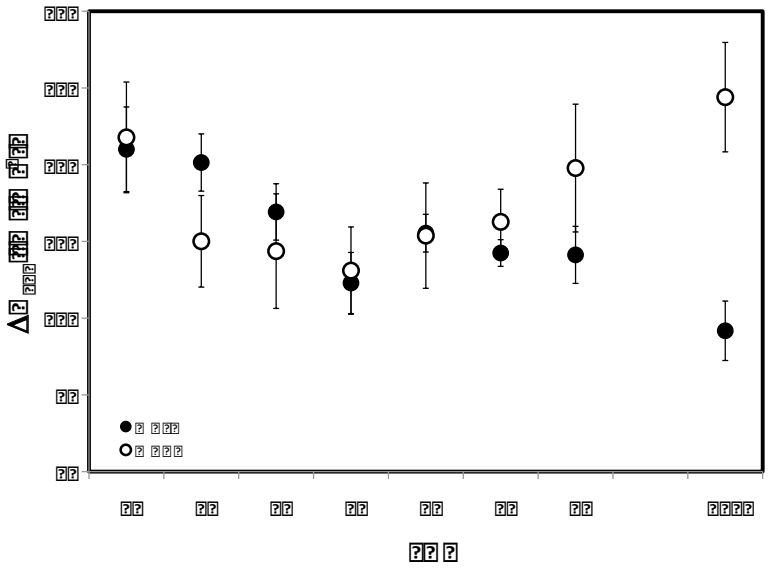

Figure 6: ΔG_{adh} of EG-SAMs as calculated from contact angles taken with water, diiodomethane, and formamide(WDF, closed circles) and water, diiodomethane and glycerol (WDG, open circles). Error bars represent 95% confidence levels.

were calculated to have a positive value. When ΔG_{adh} was ultimately calculated from contact angles taken with WDG, however, an inflection occurred at the change from the attaching to non-attaching regimes, and ΔG_{adh} increased with increasing number of EG moieties. No difference was observed between ΔG_{adh} calculated using the Dupre equation and that calculated by the VCG equation **[10]**.

Discussion

The interaction between ethylene glycol moieties and water is the key to fouling resistance for longer chained oligo(ethylene glycol) SAMs and poly(ethylene glycol) (14, 15, 20, 37, 40, 42, 49, 50, 53). Recent mathematical models of this interaction suggest that water stabilizes non-fouling configurations of OEG and PEG through hydrogen bonding with water, both directly and via hydrogen bond bridges between entrapped water molecules (38, 49, 50) . This interaction is, for the first time in this work, verified experimentally using contact angle analysis and the colloidal model of of Van Oss, Chaudhury and Good (VCG) (45, 48). The hydrogen bonding interaction between water and EG has been quantified and correlated with bacterial attachment data and has been shown to be significantly different between fouling and non-fouling EG-SAMs.

The model marine bacterium, *Cobetia marina*, attaches to EG-SAMs differently depending on the length of the EG chain (Figure 1). When EG n=0-3, cells will attach to these surfaces, albeit in decreasing numbers as n increases; above n=4, cellular attachment is less than 1 cell mm^{-2}. When we examined the physicochemistry of the EG-SAMs, a difference was observed between the interfacial tension between the SAM and water for EG-SAMs EG n<4 and EG n≥4

(Figure 5), with γ_{SL} decreasing significantly after EG n=3. This decrease in γ_{SL} is indicative of a stronger interaction between the EG-SAMs and water. The negative value of γ_{SL} suggests that this interaction is monopolar (47), as would be expected from a primarily hydrogen bond accepting EG-containing molecule. That the interaction with water is hydrogen bond – accepting is further supported by examining the Lewis acid-base components of surface tension of EG-SAMs (Figure 7). When γ_{SV}^-, the Lewis basic component of surface tension, is calculated using contact angles from the solvent set water, diiodomethane and glycerol (WDG), this value sharply increases when EG n=4-6; a small, but statistically significant, decrease in the Lewis acidic component, γ_{SV}^+, is also observed that is consistent with models of non-fouling EG conformations in which the terminal –OH moiety is lost from the surface of the SAM as the end of the molecule bends toward the interior (50).

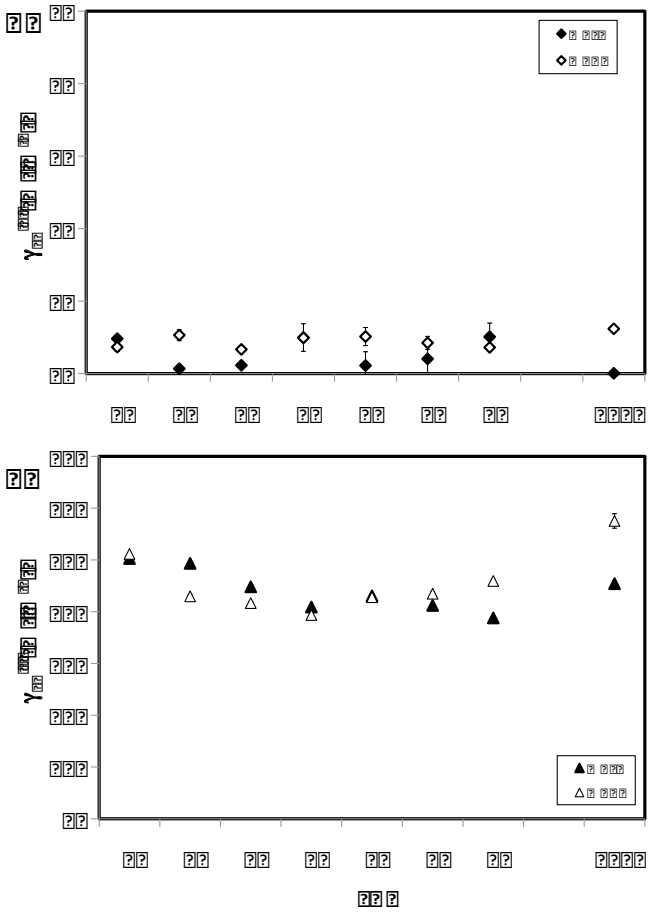

Figure 7: Non additive components of γ_{SV}^{AB}; A . The Lewis acidic component (γ_{SV}^+); B. The Lewis acidic component (γ_{SV}^-). Solid symbols are values calculated from the contact angles of water, diiodomethane and formamide(WDF); open symbols are values calculated from the contact angles of water, diiodomethane and glycerol (WDG). Error bars represent 95% confidence levels.

Lateral packing density of the EG-molecules is also known to play a role in the fouling resistance of EG-SAMs (15) and were also able to investigate this parameter using experiments and calculations based on VCG models. Figure 8 shows γ_{SL} as a function of lateral packing density for EG n=1-6 as extrapolated from the literature (15) . When contact angles obtained from the solvent set WDG are used, γ_{SL} decreases dramatically as lateral packing density decreases on EG-SAMs with larger n. The inflection point is at packing density 3.8 molecules/nm^{-2}, with the number of molecules per nm^2 and the γ_{SL} decreasing thereafter. This observation confirms that γ_{SL} calculated from the contact angle data collected using solvent set WDG more accurately reflects the hydrogen bonding activity of EG-SAMs than does contact angle data collected using water, diiodomethane and formamide, the most commonly used set of contact angle solvents.

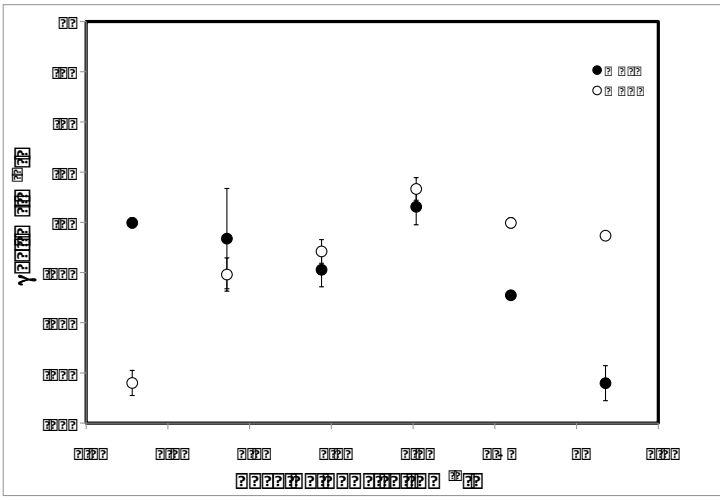

Figure 8: γ_{SL} as a function of lateral packing density. The latter is extrapolated for study SAMs using a linear regression of the values found in reference (15). Lateral packing density decreases as the number of EGs increases, thus a lateral packing density of 3.45 nm^{-1} corresponds to EG n=6 and 4.3 corresponds to EG n=1. Error bars represent 95% confidence levels.

While it is clear that the VCG model captures all the information needed to accurately describe the hydrogen bonding interactions responsible for the resistance and non-resistance of EG-SAMs to attachment, the same cannot be said when the results of ΔG_{adh} are analyzed. ΔG_{adh} is positive for *all* EG-SAMs, whereas, given the attachment data in Figure 1, one would expect it to be negative for EG-SAMs n=0-3. When we examined ΔG_{adh} for a variety of different SAMs known to support attachment of *C. marina* , only one, a methyl (CH_3-) terminated SAM, yielded a negative ΔG_{adh} when calculated using the VCG model.

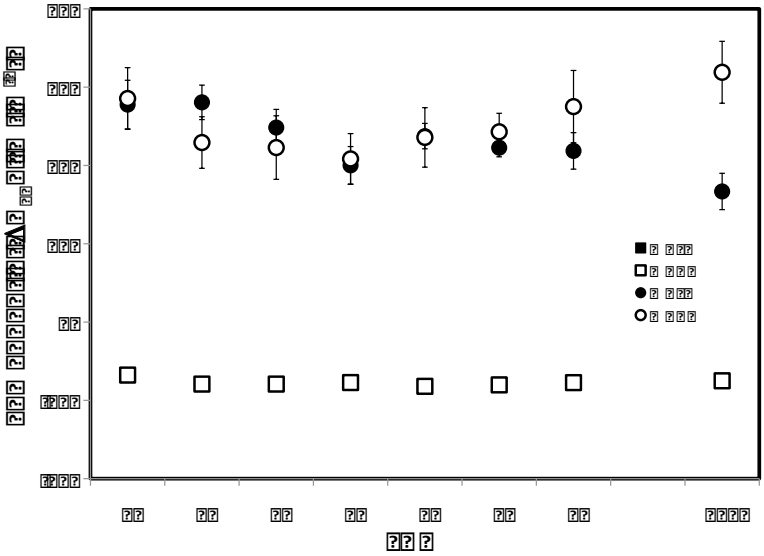

Figure 9: Additive components of ΔG_{adh}. Squares are the apolar γ_{SL}^{LW} component and circles are the polar γ_{SL}^{AB} component. Solid symbols are values calculated from the contact angles of water, diiodomethane (WDF); open symbols are values calculated from the contact angles of water, diiodomethane and glycerol (WDG). Error bars indicate 95% confidence levels.

That a completely apolar was the only one for which a ΔG_{adh} corresponding evening qualitatively to attachment data suggests that certain information is lacking with regard to the polar interactions contributing to ΔG_{adh} . If we divide ΔG_{adh} into its additive components (Figure 9), the apolar component ΔG_{adh}^{LW} and the polar component, ΔG_{adh}^{AB}, we see that the apolar component is

constant between the samples and has negative value; in contrast, ΔG_{adh}^{AB} is large, positive and is responsible for the differences between data points. Examination of the interfacial tensions comprising ΔG_{adh}^{AB} should reveal which interactions are being accurately captured and which are not.

ΔG_{adh}^{AB} is calculated from the nonadditive, Lewis acidic and basic components of γ_{SV}, γ_{BV} and γ_{LV} according to :

$$\Delta G_{adh}^{AB} = 2[\sqrt{\gamma_{LV}^{+}}(\sqrt{\gamma_{BV}^{-}} + \sqrt{\gamma_{SV}^{-}} - \sqrt{\gamma_{SV}^{-}}) + \sqrt{\gamma_{LV}^{-}}(\sqrt{\gamma_{BV}^{+}} + \sqrt{\gamma_{SV}^{+}} - \sqrt{\gamma_{LV}^{+}}) - \sqrt{\gamma_{BV}^{+}\gamma_{SV}^{-}} - \sqrt{\gamma_{BV}^{-}\gamma_{SV}^{+}}]$$ (15, 45, 48). An examination, therefore of these components would seem worthwhile. For water, γ_{LV}^{+} is assumed, in analogy, to proton acids, to be equal to γ_{LV}^{-}, i.e. 25.5 mJ m^{-2}. Examination of Figures 3 and 7 reveals that both γ_{SV} and γ_{BV} are dominated by their Lewis basic component. This would lead one to believe that the bacterium and substrata would repel one another and that the major interaction would be a monopolar interaction with water. As we have seen above, the interaction between the SAMs and water is monopolar; the γ_{BL} is -6.7, and is, thus also monopolar. While the data are internally consistent, they still do not make qualitative sense.

One criticism of the VCG model, acknowledged by VCG themselves, is that all polar surfaces calculate to have an overwhelmingly Lewis basic component (45, 48); this observation they attribute to most biological surfaces being dominated by oxygen containing groups and being, therefore inherently Lewis basic(45). Alternatively, they suggest that the lack of sufficiently Lewis acidic apolar solvents results in an underestimation of Lewis acidity (48). Thus, it seems that the choice of solvent may exert a large influence on calculated surface tension components of all

three participants in the interaction: the bacterium, the water and the SAM. Throughout this chapter, data have been presented as calculated from contact angle of water, diiodomethane and formamide (WDF) and water, diiodomethane and glycerol (WDG). It has been noted, several times, that the values calculated from the latter are more consistent with current models of water interactions with EG-SAMs. Thus choice of polar solvent does make a difference to calculated values, even if it does not lead to a qualitatively acceptable calculation of ΔG_{adh}.

Both glycerol and formamide are overwhelmingly Lewis basic (γ_{LV}^-: γ_{LV}^+ = 14.6 and 17.3, respectively) and while we have found that contact angles of EG-SAMs with the former, combined with contact angle data from dioodomethane and water, yield calculations of γ_{SL} that accurately reflect the interaction between EG-SAMs and water. Perhaps, then, using a solvent with a smaller ratio of γ_{LV}^- to γ_{LV}^+ will result in more accurate renderings of ΔG_{adh} as well? Although our choices of solvents are somewhat limited, it was noted several years ago that the assumption that the Lewis acid and basic components of water are not equal, except at 0°C (25), but are, rather γ_{LV}^-:γ_{LV}^+ =0.55 at room temperature. Since the Lewis acidic and basic components of surface tension of all other solvents are calculated relative to water, they are similarly skewed toward being more Lewis basic than their hydrogen bonding suggests. When we used the corrected values of γ_{LV}^+ and γ_{LV}^- in our calculations of surface tensions of *C. marina* and SAMs, we did see a significant shift in the values of γ_{SV}^+, γ_{SV}^-, γ_{BV}^+ and γ_{BV}^-; when inserted into the calculations for γ_{SV}, γ_{BV} and all the interfacial tensions dependent on them, there was no significant change in any of these values and ΔG_{adh} showed the same patterns as in Figure…

We did observe one final effect that solvent choice had on predicting surface tension and its dependent values: the choice of apolar solvent. Although it is frequently described as being exclusively apolar (7, 25, 27), diiodomethane has been found to have a small (0.72 mJ m^{-2}) acidic monopole(12). In order to determine what effect this monopole has on ΔG_{adh}, we compared ΔG_{adh} when calculated using diiodomethane assuming no monopole ($\gamma_{LV}^{+}=0$), including the monopole ($\gamma_{LV}^{+}=0.72$ mJ m^{-2}) and with the apolar solvent hexadecane ($\gamma_{LV}=\gamma_{LV}^{LW}=27.4$ mJ mm^{-2}). The effect of apolar solvent on the additive components of ΔG_{adh}, ΔG_{adh}^{LW} and ΔG_{adh}^{AB} is shown in Figure 10. For the polar SAMs (*i.e.,* those which are not CH_3–SAMs), ΔG_{adh}^{LW} changes from ~7 mJ m^{-2} when ΔG_{adh}^{LW} is calculated omitting the Lewis acidic monopole (D) between -2-3 mJ m^{-2} when the Lewis acidic monopole is included (Da). ΔG_{adh}^{LW} is ~-0.6 mJ m^{-2} when hexadecane is used as the apolar solvent (H). While a statistically significant reduction in ΔG_{adh}^{AB} is observed when the acidic monopole of dioodomethane is included in its calculation (WDaF, WDaG),

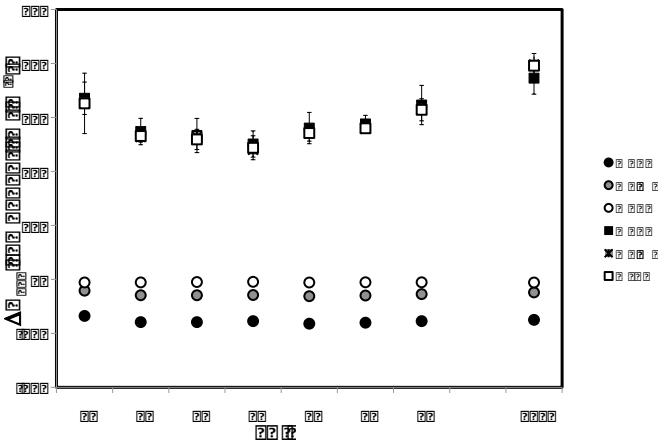

Figure 10: Additive components of ΔG_{adh} for *C. marina* adhering to SAMs. Circles represent ΔG_{adh}^{LW} calculated using θ of diiodomethane (D), diiodomethane including the acidic monopole (Da) and hexadecane (H). Squares represent ΔG_{adh}^{AB} using water and glycerol θ in combination with the apolar contact angles. Error bars represent 95% confidence levels.

there is no difference between ΔG_{adh}^{AB} calculated with hexadecane and dioodomethane without the monopole considered (WHF= WDF, WHG=WDG).

The differences in γ_{SV}^{LW} of polar SAMs as measured with hexadecane and diiodomethane is profound, whether or not the acidic monopole of the latter is considered; γ_{SV}^{LW} calculated from diiodomethane is ~45 mJ m^{-2}, if the acid monopole is included that value drops to ~35 mJ m^{-2}, whereas that using hexadecane is ~27 mJ m^{-2}, similar to that for the CH_3-SAM. The inclusion of the acid monopole calculation of γ_{SV}^{LW}, thus, has a profound effect on γ_{SV}^{LW}. These results indicate that either the supposition that either Keesom or Debye interactions is insignificant may be revealed by these measurements to be false (as they seem to account for nearly 10 mJ m^{-2} when the acid monopole is not measured on its own) or the assumption that acid or base components <1.0 mJ m^{-2} is insignificant (45, 48) is unwarranted; in either case, re-examination of these assumptions is suggested by these results.

The value of γ_{SV}^{LW} for organic polymers and biopolymers is claimed by van Oss to be universally ~45 mJ m^{-2} (45, 48), but we wonder if this is an artifact based on the use of diiodomethane as an apolar solvent that seems to always results in this value (see also the value of γ_{BV}^{LW} in Figure 4) . Examination of the γ_{SV}^{LW} of SAMs as calculated with diiodomethane and hexadecane seems to indicate that that this value may be an artifact. γ_{SV}^{LW} of an OH-SAM, is , for example about 20 mJ m^{-2} higher than γ_{SV}^{LW} of an CH_3-SAM using contact angles of diiodomethane and ignoring the acid component If we compare γ_{LV}^{LW} for n-decane (23.8 mJ m^{-2}) and 1-

decanol (22 mJ m^{-2}) we see no such increase (24). More to the point, the total surface tension for dodecane (similar to CH_3-SAM) is 25.6 mJ m^{-2}, whereas that for dodecanol is 28.6. Taking into account that γ_{LV}^{AB} for most alcohols (24) is 3-6 mJ m^{-2}, it seems very unlikely to us that a similar change on a SAM surface would suddenly nearly double γ_{SV}^{LW}. We propose, therefore, that hexadecane or some other completely apolar solvent is the most relevant when analyzing SAMs.

In addition to the abotic factors that may be missed when using VCG to model interactions between *C. marina* and EG-SAMs, certain biological information may not be entirely captured as the model is currently employed. The first consideration is that the interactions between EG-SAMs and *C. marina* may not, in fact, be non-specific, as VCG has found to not model specific interactions accurately (26, 27). Conditioning films resulting from exopolymeric substance (EPS) secreted by planktonic *C. marina* might present specific ligands for attachment. The EPS of oral streptococci attached to teeth contains ligands for lectins present on cariogenic *Streptococcus mutans* , leading to specific attachment (4). Although less well studied, marine bacteria are known to produce exopolymeric substances (EPS) while growing planktonically (6) and to attach to conditioning films formed on surfaces (13). It was not hard, therefore to envision a scenario in which *C. marina* could produce EPS, even while in carbon-limited chemostat conditions, that could form conditioning films on SAMs, to which *C. marina* could bind specifically.

We tested for the presence of EPS deposited onto SAMs from filtered (0.45 μm) chemostat effluent and for carbohydrate, DNA and protein in the filtered effluent.

The lectin concavalin A (ConA) binds specifically to α-D-mannosyl and α-D-glucosyl groups in carbohydrates and glycoproteins. These residues are frequently found in the EPS of *Pseudomonas aeruginosa* (43) and more specifically in that of marine pseudomonads (6). Alexa-dye-conjugated ConA staining of SAMs exposed for 2 hours to filtered chemostat effluent showed no discernable deposits, whereas the same SAMs exposed to 1μg ml^{-1} dextran stained easily. The amount of dissolved carbohydrate in filtered chemostat effluent was estimated using the phenol-sulfuric acid method as modified by Jain for use in salt water (19) and no detectable (i.e.< 1μg/mL) carbohydrate was found when compared with a glucose standard. Bradford assays for protein of the filtered effluent were similarly negative and no peak was found at 260nm indicating the presence of nucleic acid. As much as conditioning films would have been a very satisfactory answer to the non-correlation between ΔG_{adh} and attachment profiles, we have to conclude that, at least under our experimental conditions, conditioning films do not play a role in attachment of *C. marina* to SAMs.

Cell heterogeneity may also affect the ability of VCG to accurately model attachment. In VCG, and all colloidal models, is the assumption that the average surface tension of a pad of bacteria accurately represents the part of the cell that is, in fact, interacting with the surface. We and others have proposed that bacteria have different attachment mechanisms on different surfaces (10, 18, 36); the role of extracellular appendages such as flagella and pili are well known (22, 23), and even though we deliberately chose *C. marina* as a model organism partly due to the lack of observable extracellular structures (41), years of observation have led us to

conclude that the surface is very likely not uniform. The relevant γ_{BV} and components to include in a free-energy calculation are, therefore, less likely to be those of the whole bacterium, but rather that of the part of the cell which is interacting with the SAM. Ascertaining which part of the cell surface is relevant on which each SAM (or other model surface) is, at first, perhaps, daunting; we are currently investigating the interactions between SAMs and bacteria at the sub-cellular scale.

Conclusions

We have demonstrated experimentally, using the van Oss Chaudhury Good model of non-specific attachment, that the fouling resistance of oligo(ethylene glycol) –containing SAMs is mediated through increased hydrogen bonding between the EG moieties and water, in accordance with mathematical models of this interaction. The VCG model as used in current practice, however, does not accurately capture all the information necessary for calculation of ΔG_{adh} that is either qualitatively or quantitatively reflected in attachment data. Both abiotic and biotic factors may be under or misrepresented by VCG. The most prominent of the abiotic factors is the inability to accurately determine hydrogen bond donating potential of bacteria and SAMs. The most prominent biological factor is the assumption that the cell surface is uniform and that all parts of the cell contribute equally to attachment.

Literature cited

1. **Absolom, D. R., F. V. Lamberti, Z. Policova, W. Zingg, C. J. van Oss, and A. W. Neumann.** 1983. Surface thermodynamics of bacterial adhesion. Appl. Environ. Microbiol. **46:**90-97.
2. **Bain, C. D., E. B. Troughton, Y.-T. Tao, J. Evall, and G. M. Whitesides.** 1989. Formation of monolayer films by the spontaneous assembly of organic thiols from solution onto gold. J Am Chem Soc **111:**321-335.
3. **Balamurugan, S., L. K. Ista, J. Yan, G. P. Lopez, J. Fick, M. Himmelhaus, and M. Grunze.** 2005. Reversible protein adsorption and bioadhesion on

monolayers terminated with mixtures of oligo(ethylene glycol) and methyl groups J Am Chem Soc **127:**14548-14549.

4. **Banas, J. A., and M. M. Vicermann.** 2003. Glucan-binding proteins of the oral Streptococci. Crit Rev Oral Biol Med **14:**89-99.
5. **Banerjee, I., R. C. Pangule, and R. S. Kane.** 2011. Antifouling Coatings: Recent Developments in the Design of Surfaces That Prevent Fouling by Proteins, Bacteria, and Marine Organisms. Advanced Materials **23:**690-718.
6. **Beech, I. B., R. Gubner, V. Zinkevich, L. Hanjangsit, and R. Avci.** 2000. Characterisation of conditioning layers formed by exopolymeric substances of Pseudomonas NCIMB 2021 on surfaces of AISI 316 stainless steel. Biofouling **16:**93-104.
7. **Bellon-Fontaine, M.-N., J. Rault, and C. J. van Oss.** 1996. Microbial adhesion to solvents: a novel method to determine the electron-donor/electron-acceptor or Lewis acid-base properties of microbial cells. Colloid Surface B **7:**47-53.
8. **Bi, X. Y., H. Xu, S. L. Lai, and K. L. Yang.** 2009. Bifunctional oligo(ethylene glycol) decorated surfaces which permit covalent protein immobilization and resist protein adsorption. Biofouling **25:**435-444.
9. **Blainey, B. L., and K. C. Marshall.** 1991. The use of block copolymers to inhibit bacterial adhesion and biofilm formation on hydrophobic surfaces in marine habitats. Biofouling **4:**309-318.
10. **Dalton, H., J. Stein, and P. March.** 2000. A biological assay for detection of heterogeneities in the surface hydrophobicity of polymer coatings exposed to the marine environment. Biofouling **15:**83-94.
11. **Desai, N. P., S. F. A. Hossainy, and J. A. Hubbell.** 1992. Surface-immobilized polyethylene oxide for bacterial repellence. Biomaterials **13:**417-420.
12. **Gonzalez-Martin, M. L., B. Janczuk, L. Labajos-Broncano, and J. M. Bruque.** 1997. Determination of the carbon black surface free energy components from the heat of immersion measurements. Langmuir **13:**5991-5994.
13. **Gubner, R., and I. B. Beech.** 2000. Characterisation of conditioning layers formed by exopolymeric substances of *Pseudomonas* NCIMB 2021 on surfaces of AISI 316 stainless steel. Biofouling **16:**93-104.
14. **Harder, P., M. Grunze, R. Dahint, G. M. Whitesides, and P. E. Laibinis.** 1998. Molecular conformation in oligo(ethylene glycol)-terminated self-assembled monolayers on gold and silver surfaces determines their ability to resist protein adsorption. J Phys Chem B **102:**426-436.
15. **Herrwerth, S., W. Eck, S. Reinhardt, and M. Grunze.** 2003. Factors that determine the protein resistance of oligoether self-assembled monolayers - Internal hydrophilicity, terminal hydrophilicity, and lateral packing density. J Am Chem Soc **125:**9359-9366.
16. **Ista, L. K., M. E. Callow, J. A. Finlay, S. E. Coleman, A. C. Nolasco, J. A. Callow, and G. P. Lopez.** 2004. Effect of substratum surface chemistry and surface energy on attachment of marine bacteria and algal spores. Appl Environ Microbiol **70:**4151-4158.

17. **Ista, L. K., H. Fan, O. Baca, and G. P. López.** 1996. Attachment of bacteria to model solid surfaces: oligo(ethylene glycol) surfaces inhibit bacterial attachment. FEMS Microb. Lett. **142:**59-63.
18. **Ista, L. K., V. H. Perez-Luna, and G. P. Lopez.** 1999. Surface-grafted, environmentally sensitive polymers for biofilm release. . Appl Environ Microbiol **65:**1603-1609.
19. **Jain, A., and N. Bhosle.** 2009. Biochemical composition of the marine conditioning film: implications for bacterial adhesion. Biofouling **25:**13-19.
20. **Jeon, S. I., J. H. Lee, J. D. Andrade, and P. G. Degennes.** 1991. Protein surface interactions in the presence of polyethylene oxide .1. simplified theory. J Colloid Interf Sci **142:**149-158.
21. **Kersters, K.** 1992. The genus *Deleya*, p. 3189-3197. *In* A. Balows, H. G. Trüper, M. Dworkin, W. Harder, and K. H. Schliefer (ed.), The Prokaryotes, 2 ed, vol. 4. Springer-Verlag, New York.
22. **Klausen, M., A. Aaes-Jorgensen, S. Molin, and T. Tolker-Nielsen.** 2003. Involvement of bacterial migration in the development of complex multicellular structures in *Pseudomonas aeruginosa* biofilms. . Molec Microbiol **50:**61-68.
23. **Klausen, M., A. Heydorn, P. Ragas, L. Lambertsen, A. Aaes-Jorgensen, S. Molin, and T. Tolker-Nielsen.** 2003. Biofilm formation by *Pseudomonas aeruginosa* wild type, flagella and type IV pili mutants. Molec Microbiol **48:**1511-1524.
24. **Krüss Corporation, G.** 2003, posting date. Surface tensions of solids and liquids. [Online.]
25. **Lee, L. H.** 1996. Correlation between Lewis acid-base surface interaction components and linear solvation relationship solvatochromic alpha and beta parameters (vol 12, pg 1681, 1996). Langmuir **12:**5972-5972.
26. **Liu, Y., A. M. Gallardo-Moreno, P. A. Pinzon-Arango, Y. Reynolds, G. Rodriguez, and T. A. Camesano.** 2008. Cranberry changes the physicochemical surface properties of *E. coli* and adhesion with uroepithelial cells. Colloid Surface B **65:**35-42.
27. **Liu, Y. T., J. Strauss, and T. A. Camesano.** 2007. Thermodynamic investigation of *Staphylococcus epidermidis* interactions with protein-coated substrata. Langmuir **23:**7134-7142.
28. **Lopez, G. P., M. W. Albers, S. L. Schreiber, R. Carroll, E. Peralta, and G. M. Whitesides.** 1993. Convenient methods for patterning the adhesion of mammalian cells to surfaces using self-assembled monolayers of alkanethiolates on gold. J Am Chem Soc **115:**5877-5878.
29. **Lopez, G. P., H. A. Biebuyck, R. Harter, A. Kumar, and G. M. Whitesides.** 1993. Fabrication and imaging of 2-dimensional patterns of proteins adsorbed on self-assembled monolayers by scanning electron-microscopy. J Am Chem Soc **115:**10774-10781.
30. **Lopez, G. P., H. A. Biebuyck, and G. Whitesides.** 1993. Scanning electron-microscopy can form images of patterns in self-assembled monolayers. Langmuir **9:**1513-1516.
31. **Magin, C. M., S. P. Cooper, and A. B. Brennan.** 2010. Non-toxic antifouling strategies. Materials Today **13:**36-44.

32. **Ostuni, E., R. G. Chapman, R. E. Holmlin, S. Takayama, and G. M. Whitesides.** 2001. A survey of structure-property relationships of surfaces that resist the adsorption of protein. Langmuir **17:**5605-5620.
33. **Otsuka, H.** 2010. Nanofabrication of Nonfouling Surfaces for Micropatterning of Cell and Microtissue. Molecules **15:**5525-5546.
34. **Otsuka, H., Y. Nagasaki, and K. Kataoka.** 2001. Self-assembly of poly(ethylene glycol)-based block copolymers for biomedical applications. Curr Opin Colloid Interface Sci **6:**3-10.
35. **Pale-Grosdemange, C., E. S. Simon, K. L. Prime, and G. M. Whitesides.** 1991. Formation of self-assembled monolayers by chemisorption of derivatives of oligo(ethylene Glycol) of Structure HS(CH2)11(OCH2CH2)meta-OH on gold. J Am Chem Soc **113:**12-20.
36. **Paul, J. H., and W. H. Jeffrey.** 1985. Evidence for separate adhesion mechanisms for hydrophilic and hydrophobic surfaces in *Vibrio proteolytica*. Appl Environ Microbiol **50:**431–437.
37. **Prime, K. L., and G. M. Whitesides.** 1993. Adsorption of proteins onto surfaces containing end-attached oligo(ethylene oxide): a model system using self-assembled monolayers. J Am Chem Soc **115:**10714-10721.
38. **Rosenhahn, A., S. Schilp, H. J. Kreuzer, and M. Grunze.** 2010. The role of "inert" surface chemistry in marine biofouling prevention. Phys Chem Chem Phys **12:**4275-4286.
39. **Schilp, S., A. Kueller, A. Rosenhahn, M. Grunze, M. E. Pettitt, M. E. Callow, and J. A. Callow.** 2007. Settlement and adhesion of algal cells to hexa (ethylene glycol)-containing self-assembled monolayers with systematically changed wetting properties. Biointerphases **2:**143-150.
40. **Schilp, S., A. Rosenhahn, M. E. Pettitt, J. Bowen, M. E. Callow, J. A. Callow, and M. Grunze.** 2009. Physicochemical properties of (ethylene glycol)-containing self-assembled monolayers relevant for protein and algal cell resistance. Langmuir **25:**10077-10082.
41. **Shea, C., L. J. Lovelace, and H. E. Smith-Somerville.** 1995. *Deleya marina* as a model organism for studies of bacterial colonization and biofilm formation. J Indust Microbiol **15:**290-296.
42. **Stevens, M. J., and G. S. Grest.** 2008. Simulations of water at the interface with hydrophilic self-assembled monolayers. Biointerphases **3:**Fc13-Fc22.
43. **Tolker-Neilsen, T., U. C. Brinch, P. C. Ragas, J. B. Anderson, C. S. Jacobson, and S. Molin.** 2000. Development and dynamics of *Pseudomonas* sp. biofilms. J Bacteriol **182:**6482-6489.
44. **Ubbink, J., and P. Schar-Zammaretti.** 2007. Colloidal properties and specific interactions of bacterial surfaces. Curr Opin Colloid Interface Sci **12:**263-270.
45. **van Oss, C. J.** 2006. Interfacial Forces in Aqueous Media, 2nd ed. Taylor and Francis, Boca Raton.
46. **van Oss, C. J.** 2002. Use of the combined Lifshitz-van der Waals and Lewis acid-base approaches in determining apolar and polar contributions to surface and interfacial tensions. J Adhes Sci Technol **16:**669-677.

47. **van Oss, C. J., M. K. Chaudhury, and R. J. Good.** 1987. Monopolar surfaces. Adv Colloid Interfac **23:**35-64.
48. **van Oss, C. J., R. J. Good, and M. K. Chaudhury.** 1988. Additive and nonadditive surface-tension components and the interpretation of contact angles. Langmuir **4:**884-891.
49. **Wang, R. L. C., H. J. Kreuzer, and M. Grunze.** 1997. Molecular conformation and solvation of oligo(ethylene glycol)-terminated self-assembled monolayers and their resistance to protein adsorption. J Phys Chem B **101:**9767-9773.
50. **Wang, R. L. C., H. J. Kreuzer, and M. Grunze.** 2000. The interaction of oligo(ethylene oxide) with water: a quantum mechanical study. Phys Chem Chem Phys **2:**3613-3622.
51. **Zhang, X. J., and V. K. Yadavalli.** 2011. Surface immobilization of DNA aptamers for biosensing and protein interaction analysis. Biosensors & Bioelectronics **26:**3142-3147.
52. **Zhao, C., M. Burchardt, T. Brinkhoff, C. Beardsley, M. Simon, and G. Wittstock.** 2010. Microfabrication of Patterns of Adherent Marine Bacterium Phaeobacter inhibens Using Soft Lithography and Scanning Probe Lithography. Langmuir **26:**8641-8647.
53. **Zwahlen, M., S. Herrwerth, W. Eck, M. Grunze, and G. Hahner.** 2003. Conformational order in oligo(ethylene glycol)-terminated self assembled monolayers on gold determined by soft X-ray absorption. Langmuir **19:**9305-9310.

Chapter 6: Conclusions and future directions

Conclusions

Attachment of bacteria to surfaces is the foundational event in the transformation of bacteria from their free-living, planktonic forms to surface-attached biofilms. Because specific attachment mechanisms that result in attachment are not well understood for all but the most well-studied human pathogens and commensal organisms, colloidal models are frequently employed to gain insights into non-specific attachment mechanisms likely to predominate in attachment of bacteria to abiotic surfaces.

We have conducted a systematic investigation of surface tension properties thought to influence attachment of bacteria to abiotic substrata. Wettability is the most frequently used representation of total substratum surface tension and our initial studies demonstrated that attachment of both the marine bacterium, *Cobetia marina* and zoospores of the fouling alga, *Ulva linza* correlate linearly to $\cos\theta_{AW}$, where θ_{AW} is the advancing contact angle formed as a drop of water spreads over the attachment substratum (Chapter 2 and (8)).

The importance of substratum wettability is was further supported by the observation that attachment substrata that are able to change their wettability are, under the right conditions, able to detach both recently attached bacteria and fully formed biofilms (11). Furthermore, alterations in the overall wettability of such switchable substrata can reduce or enhance both initial attachment of bacteria and their eventual removal (Chapter 2 and (10)).

Subsequent studies (Chapter 3 and (13)) revealed that attachment substrata with the same water contact angle but different surface chemistries attach different numbers of bacteria, leading us to investigate more complex models of bacterial attachment, specifically that of Van Oss, Chaudhury and Good (VCG), that take into account both apolar and polar, specifically hydrogen bonding, interactions likely to be active at the interface between the attaching bacterium and the attachment substratum(13, 27, 28). It became clear, however, that even these more complex models failed to accurately capture all the molecular events leading to attachment (Chapter 3 and (13)).

The very first study I conducted with regard to bacterial attachment indicated that bacteria do not attach to substrata containing oligo(ethylene glycol) (OEG) (9). The molecular nature of the resistance of OEG to adsorption of proteins and attachment of cells has been the subject of investigation for many years (1-3, 5-7, 12, 16-18, 21, 23-25, 29, 30). OEG resistance is now known to be the result of resistant molecular conformations stabilized by water; the nature of the stabilization has been hypothesized, based on mathematical calculations, to be the result of the formation of multiple hydrogen bonds between the OEG backbone and water molecules (23, 29, 30).

The VCG model was specifically articulated to illuminate hydrogen bonding interactions, but, surprisingly, has not been applied to the question of OEG fouling resistance until the present work. When a series of OEG-terminated self assembled monolayer (SAMs) that vary in their ability to attach bacteria were examined, we were able to differentiate between those SAMs that attached bacteria and those that

did not based on their ability to hydrogen bond with water, thus providing experimental verification of the mathematical models. The VCG model was originally meant, however, to address the thermodynamics of attachment, specifically the free energy of attachment, ΔG_{adh}. Under our experimental conditions, however, ΔG_{adh} as calculated using VCG neither qualitatively nor quantitatively correlated with attachment of *C. marina*, suggesting that the VCG model as routinely used fails to capture all the molecular events associated with attachment of bacteria to surfaces.

I examined a number of experimental parameters associated with standard application of the VCG theory and found that the choice of solvent used to measure contact angles with surfaces, the experimental input into the VCG model, profoundly affected the resulting calculations of surface and interfacial tensions, and, ultimately ΔG_{adh}. The single most important failure of the use of VCG seems to be that there is no solvent that can adequately measure the hydrogen-bond donating capacity of either the attachment substratum or the bacteria, leading to this process being underrepresented in subsequent calculations.

There may be biological facets of attachment that are not adequately addressed using VCG. The first consideration is that the interactions between EG-SAMs and *C. marina* may not, in fact, be non-specific, as VCG has found to not model specific interactions accurately (19, 20). Conditioning films resulting from exopolymeric substance (EPS) secreted by planktonic *C. marina* might present specific ligands for attachment. We found no indication of conditioning film

production in our logarithmic chemostat cultures, so under our experimental conditions, specific attachment was likely not a factor.

Cell heterogeneity may also affect the ability of VCG to accurately model attachment. In VCG, and all colloidal models, is the assumption that the average surface tension of a pad of bacteria accurately represents the part of the cell that is, in fact, interacting with the surface. We and others have proposed that bacteria have different attachment mechanisms on different surfaces (4, 11, 22); the role of extracellular appendages such as flagella and pili are well known (14, 15), and even though we deliberately chose *C. marina* as a model organism partly due to the lack of observable extracellular structures (26), years of observation have led us to conclude that the surface is very likely not uniform. The relevant γ_{BV} and components to include in a free-energy calculation are, therefore, less likely to be those of the whole bacterium, but rather that of the part of the cell which is interacting with the SAM. This, I feel, is the single most important issue in application of VCG, or, indeed, any colloidal model to bacterial attachment.

Future directions

The most intriguing aspect of this work has been the possible role of bacterial surface heterogeneity in attachment. We are currently probing the cell surface of *Cobetia marina* with SAMs made on gold nanoparticles. Because the chemistries on the nanoparticle SAMs are the same as those on the planar SAMs to which we have been attaching bacteria, the nanoparticles will provide specific information on which part of the bacterial cell is the most relevant for each SAM. Eventually such

an approach could lead to probing the specific thermodynamic interactions leading to attachment, and a modification of the VCG model.

A second important question arising from this work is whether the bacteria attaching to SAMs of different chemistry have the same phenotypes. Are the cells which attach to a hydroxyl terminated-SAM the same subpopulation of cells that would to a methyl-terminated SAM? Experiments in which the bacteria attached to one SAM are removed, regrown and exposed to another SAM are currently being planned.

Thirdly is the question of growth phase. With the exception of the ammonia oxidizing bacteria in Chapter 4, all of the bacteria used in these studies were in logarithmic phase when exposed to surfaces. It is extremely unlikely that even carbon limited log phase cells establish biofilms in the wild. Examining the attachment of bacteria grown in stationary phase and under different nutrients conditions may reveal much about attachment. Furthermore, bacteria fed differently may produce different amounts and kinds of exopolymers that could profoundly affect their attachment.

Finally, a long-term goal of this research should be to combine the precise control over attachment substratum chemistry enabled by SAMs with genomic technologies to assess the precise molecular interactions involved in attachment. Specifically, development of a GFP expression library in *C. marina* would allow investigation of which genes are turned on and off when a bacterium encounters the

surface and whether substratum chemistry affects biological molecular events involved in attachment.

Literature cited

1. **Banerjee, I., R. C. Pangule, and R. S. Kane.** 2011. Antifouling coatings: recent developments in the design of surfaces that prevent fouling by proteins, bacteria, and marine organisms. Advanced Materials **23:**690-718.
2. **Blainey, B. L., and K. C. Marshall.** 1991. The use of block copolymers to inhibit bacterial adhesion and biofilm formation on hydrophobic surfaces in marine habitats. Biofouling **4:**309-318.
3. **Clare, A. S.** 1998. Towards nontoxic antifouling. J Mar Biotechnol **6:**3-6.
4. **Dalton, H., J. Stein, and P. March.** 2000. A biological assay for detection of heterogeneities in the surface hydrophobicity of polymer coatings exposed to the marine environment. Biofouling **15:**83-94.
5. **Desai, N. P., S. F. A. Hossainy, and J. A. Hubbell.** 1992. Surface-immobilized polyethylene oxide for bacterial repellence. Biomaterials **13:**417-420.
6. **Ekblad, T., G. Bergstroem, T. Ederth, S. L. Conlan, R. Mutton, A. S. Clare, S. Wang, Y. L. Liu, Q. Zhao, F. D'Souza, G. T. Donnelly, P. R. Willemsen, M. E. Pettitt, M. E. Callow, J. A. Callow, and B. Liedberg.** 2008. Poly(ethylene glycol)-Containing Hydrogel Surfaces for Antifouling Applications in Marine and Freshwater Environments. Biomacromolecules **9:**2775-2783.
7. **Herrwerth, S., W. Eck, S. Reinhardt, and M. Grunze.** 2003. Factors that determine the protein resistance of oligoether self-assembled monolayers - Internal hydrophilicity, terminal hydrophilicity, and lateral packing density. J Am Chem Soc **125:**9359-9366.
8. **Ista, L. K., M. E. Callow, J. A. Finlay, S. E. Coleman, A. C. Nolasco, J. A. Callow, and G. P. Lopez.** 2004. Effect of substratum surface chemistry and surface energy on attachment of marine bacteria and algal spores. Appl Environ Microbiol **70:**4151-4158.
9. **Ista, L. K., H. Fan, O. Baca, and G. P. López.** 1996. Attachment of bacteria to model solid surfaces: oligo(ethylene glycol) surfaces inhibit bacterial attachment. FEMS Microb. Lett. **142:**59-63.
10. **Ista, L. K., S. Mendez, and G. P. Lopez.** 2010. Attachment and detachment of bacteria on surfaces with tunable and switchable wettability. Biofouling **26:**111-118.
11. **Ista, L. K., V. H. Perez-Luna, and G. P. Lopez.** 1999. Surface-grafted, environmentally sensitive polymers for biofilm release. . Appl Environ Microbiol **65:**1603-1609.
12. **Jeon, S. I., J. H. Lee, J. D. Andrade, and P. G. Degennes.** 1991. Protein surface interactions in the presence of polyethylene oxide .1. simplified theory. J Colloid Interf Sci **142:**149-158.
13. **Khan, M. M. T., L. K. Ista, G. P. Lopez, and A. J. Schuler.** 2011. Experimental and theoretical examination of surface energy and adhesion of

nitrifying and heterotrophic bacteria determined using self-assembled monolayers. . Environmental Sci Technol **45:**1055-1060.

14. **Klausen, M., A. Aaes-Jorgensen, S. Molin, and T. Tolker-Nielsen.** 2003. Involvement of bacterial migration in the development of complex multicellular structures in *Pseudomonas aeruginosa* biofilms. . Molec Microbiol **50:**61-68.
15. **Klausen, M., A. Heydorn, P. Ragas, L. Lambertsen, A. Aaes-Jorgensen, S. Molin, and T. Tolker-Nielsen.** 2003. Biofilm formation by *Pseudomonas aeruginosa* wild type, flagella and type IV pili mutants. Molec Microbiol **48:**1511-1524.
16. **Latour, R. A.** 2006. Thermodynamic perspectives on the molecular mechanisms providing protein adsorption resistance that include protein-surface interactions. J Biomed Mater Res A **78A:**843-854.
17. **Lee, J. H., J. Kopecek, and J. D. Andrade.** 1989. Protein-resistant surfaces prepared by PEO-containing block copolymer surfactants. J Biomed Mater Res **23:**351-368.
18. **Li, L., S. Chen, J. Zheng, B. D. Rattner, and S. Y. Jiang.** 2005. Protein adsorption on olgp(ethylene glycol)-terminated self-assembled monolyars: the molecular basis for nonfouling behavior . J Phys Chem B **109:**2934-2941.
19. **Liu, Y., A. M. Gallardo-Moreno, P. A. Pinzon-Arango, Y. Reynolds, G. Rodriguez, and T. A. Camesano.** 2008. Cranberry changes the physicochemical surface properties of *E. coli* and adhesion with uroepithelial cells. Colloid Surface B **65:**35-42.
20. **Liu, Y. T., J. Strauss, and T. A. Camesano.** 2007. Thermodynamic investigation of *Staphylococcus epidermidis* interactions with protein-coated substrata. Langmuir **23:**7134-7142.
21. **Ostuni, E., R. G. Chapman, R. E. Holmlin, S. Takayama, and G. M. Whitesides.** 2001. A survey of structure-property relationships of surfaces that resist the adsorption of protein. Langmuir **17:**5605-5620.
22. **Paul, J. H., and W. H. Jeffrey.** 1985. Evidence for separate adhesion mechanisms for hydrophilic and hydrophobic surfaces in *Vibrio proteolytica*. Appl Environ Microbiol **50:**431–437.
23. **Rosenhahn, A., S. Schilp, H. J. Kreuzer, and M. Grunze.** 2010. The role of "inert" surface chemistry in marine biofouling prevention. Phys Chem Chem Phys **12:**4275-4286.
24. **Schilp, S., A. Kueller, A. Rosenhahn, M. Grunze, M. E. Pettitt, M. E. Callow, and J. A. Callow.** 2007. Settlement and adhesion of algal cells to hexa (ethylene glycol)-containing self-assembled monolayers with systematically changed wetting properties. Biointerphases **2:**143-150.
25. **Schilp, S., A. Rosenhahn, M. E. Pettitt, J. Bowen, M. E. Callow, J. A. Callow, and M. Grunze.** 2009. Physicochemical properties of (ethylene glycol)-containing self-assembled monolayers relevant for protein and algal cell resistance. Langmuir **25:**10077-10082.
26. **Shea, C., L. J. Lovelace, and H. E. Smith-Somerville.** 1995. *Deleya marina* as a model organism for studies of bacterial colonization and biofilm formation. J Indust Microbiol **15:**290-296.

27. **van Oss, C. J.** 2006. Interfacial Forces in Aqueous Media, 2nd ed. Taylor and Francis, Boca Raton.
28. **van Oss, C. J., R. J. Good, and M. K. Chaudhury.** 1988. Additive and nonadditive surface-tension components and the interpretation of contact angles. Langmuir **4:**884-891.
29. **Wang, R. L. C., H. J. Kreuzer, and M. Grunze.** 1997. Molecular conformation and solvation of oligo(ethylene glycol)-terminated self-assembled monolayers and their resistance to protein adsorption. J Phys Chem B **101:**9767-9773.
30. **Wang, R. L. C., H. J. Kreuzer, and M. Grunze.** 2000. The interaction of oligo(ethylene oxide) with water: a quantum mechanical study. Phys Chem Chem Phys **2:**3613-3622.